Role of epithelial cells in detection and response to sensory stimuli in *Drosophila*

Kory Luedke

A dissertation
submitted in partial fulfillment of the
requirements for the degree of

Doctor of Philosophy

University of Washington
2020

Reading Committee:
Jay Parrish, Chair
Martha Bosma
Ajay Dhaka

Program Authorized to Offer Degree:
Biology

University of Washington

Abstract

Role of epithelial cells in detection and response to sensory stimuli in *Drosophila*

Kory Luedke

Chair of the Supervisory Committee:
Associate Professor Jay Z. Parrish
Department of Biology

Interactions between cell types plays an important role in shaping the morphology and function of those cells. One powerful example is in the peripheral nervous system, where sensory neurons coordinate with epidermal structures to help us sense the environment around us. However, there are many aspects of this sensory system that have only recently been investigated. First, this thesis reviews the current understanding of the mechanisms that guide, shape, and regulate the response to external stimuli in the epidermis. It describes our changing historical perspective on epithelial cells from simple physical support structures to active participants in the sensory apparatus. Second, we use the *Drosophila* peripheral nervous system as a model to identify novel regulators of neuron-epithelial interactions. We found that the microRNA *miR-14* is required in the epithelium, where it likely regulates the expression of gap junctions, which ensure tight coupling between adjacent epithelial cells. This prevents precocious innervation of the neuron into the cell junction. Changes in dendrite morphology and innervation of the junction are highly correlated with changes in sensitivity of the nociceptive neuron.

Table of Contents

Role of epithelial cells in detection and response to sensory stimuli

Abstract

Skin acts as a barrier and interface with the environment. Sensory neurons present in the skin allow us to detect a wide range of environmental cues that surround us. Specializations in the skin allow it to act with the sensory neurons to tune and shape the response of sensory neurons. These specializations appear to be somewhat conserved across the animal kingdom. This review describes the cells and circuits present in the epidermis that sense touch and pain. It highlights the recent advances in our understanding of the development of neuron-dendrite interactions, and the signals between non-neuronal cells and sensory neurons that convey sensory response.

Introduction

Sensation of external stimuli is critical to interacting with the world and protecting us from injury. Epithelial cells, and the neurons that innervate them, provide a critical barrier against the external environment and are the first point of contact for sensation. Despite the critical role that sensation plays in our lives, research into the molecules and mechanisms that underlie this process is still in early stages. Recent work has shown a greater diversity and importance of epithelial cells in actively participating in the sensory function than was previously believed.

In this review we look at recent advances in our understanding of the cellular and molecular relationships between epithelial cells and sensory neurons. Traditional dogma focused our understanding of sensory neurons as the primary or sole sensor,

with several well established examples of sensory epithelial cells, such as hair cells and olfactory epithelia. Recent research has found that epithelial cells contribute strongly to somatosensation in a rich and highly regulated way. Evidence of the molecular machinery regulating epithelium-neuron interaction suggests that it is also highly conserved across the animal kingdom.

Broadly, the contribution of non-neuronal cells falls in to three categories: (1) Physical support and tuning, (2) broad inflammation response to surrounding cells, and (3) active, paired signaling to the sensory neuron. Increasing our understanding of the molecules and circuits that contribute to touch response can help us address chronic or pathological pain, which affects up to hundreds of millions of Americans.

Role of epidermal targets in sensation

Canonical view

The role of sensory epithelial cells have been extensively studied in a small number of specialized cases. These include hearing/pressure sensing, taste, and olfaction. Hair cells of the vertebrate ear are specialized epithelial cells that have mechanically gated ion channels on stereocilia that lead to depolarization (B. Fritzsch et al., 2002; Wan, Corfas, & Stone, 2013). Analogous hair cells present in the fish lateral line system provide information about movement and pressure gradients of water (Atkinson, Huarcaya Najarro, Sayyid, & Cheng, 2015; Bleckmann & Zelick, 2009). In olfaction, epithelial stem cells differentiate into olfactory receptor neurons (ORNs). ORNs express a single or small number of olfactory receptor types, which inhibit expression of other receptors (Serizawa, Miyamichi, & Sakano, 2004).

Traditional dogma has believed that mechanosensory neurons were sufficient for sensing stimuli. In this view, the sensory neuron alone expressed the machinery necessary for mechanotransduction. Interestingly, this is in spite of the fact that there are four well identified epithelial sensory specializations: Ruffini endings, Pacinian corpuscles, Meissner's corpuscles, and Merkel's disks.

Structural support of mechanoreceptors

There are several canonical specializations in the in the vertebrate epidermis that are believed to physically tune the transduction of the force to the mechanoreceptor. Ruffini endings (or bulbous corpuscles) are composed of a complex dendrite ending embedded in an elongated capsule of connective tissue and a core of Schwann cells (Chambers, Andres, Duering, & Iggo, 1972). It is located deep in the dermis and senses stretch. Collagen fibers extend from the inner core into the surrounding tissue, which is proposed to mechanically link the sensory structure with the surrounding tissue and transmit force (Z Halata, 1977). Ruffini endings bear a strong resemblance to muscle spindle stretch receptors that provide force and position information via muscle stretching for proprioception.

Meissner's (or tactile) corpuscles convey vibration and textural information. Pacinian (or lamellar) corpuscles sense vibration and deep pressure. Both of these structures are have a lamellar structure of flattened cells, separated by extracellular matrix (ECM). These tend to be distributed in smooth skin of high touch sensitivity, such

as the finger pads. Computer modeling of Pacinian corpuscle structure suggests that the depth and shape of the lamellar disc contribute to its specificity of response to touch stimuli(Quindlen, Lai, & Barocas, 2015). Research implicates GABAergic and glutamatergic signaling from Schwann-like cells in the core of the corpuscle contribute to accommodation of the receptor, so these may also actively contribute to the sensory apparatus (Pawson, Pack, & Bolanowski, 2007; Pawson et al., 2009).

Active signaling to neurons- Merkel cells

Merkel Cells are specialized domed epithelial cells that primarily sense deep pressure and touch, and contribute to two-point discrimination. They make up a small percentage of the epithelial cell population (3-6%), but are enriched in areas of high touch sensitivity, such as the mouth and fingertips (Fradette et al., 2003; Moll, Moll, & Franke, 1986; Moll, Paus, & Moll, 1996). Merkel cells are also associated with hair follicles and detect deflections of the hair. Merkel cells also lie in close apposition to free nerve endings projecting into the dermis.

Merkel cells highly express the touch sensitive channel Piezo2 (Ikeda et al., 2014; Maksimovic et al., 2014; Woo, Lumpkin, & Patapoutian, 2015). Merkel cells exhibit a slow adapting (SA1) response to stimuli. When Piezo2 is specifically removed from epithelial cells, however, the action potential in the afferent nerve is truncated. Experiments show that both the Merkel and neurite may both mechanotranduce (Zdenek Halata, Grim, & Baumann, 2010; Ikeda et al., 2014). This suggests that both the Merkel cell and afferent nerve contribute to distinct phases of the receptor potential. Further work also suggests that Piezo2 may be required in Merkel cells to modulate the

conversion from light touch to itch sensation (Feng et al., 2018). Mice deficient in Merkel cell Piezo2 show increased scratching behavior. However, recent modeling of the firing properties pf the neuron suggests that a source of ultra-slow adapting current not presently accounted for is required (Gerling, Wan, Hoffman, Wang, & Lumpkin, 2018).

In addition to expression of mechanosensitive channels, Merkel cells also express a large complement of active synaptic release machinery, such as synaptotagmin and voltage-gated Ca2+ channels (Haeberle 2004). Electron microscopy descriptions have identified dense-core vesicles are enriched near the associated nerve ending (Winkelmann & Breathnach, 1973). Recent work has implicated serotonin release from the synapse-like structure between Merkel cell and neuron to transmit tactile stimulus (Chang et al., 2016). However, another work has found that norepinephrine, and not serotonin, is responsible for transmission from Merkel cell to neuron (Hoffman et al., 2018). Signaling to the sensory afferent is not entirely resolved.

Keratinocytes and keratinocyte-like epithelial cells

Recent work in mammals has sought to increase our understanding of the role of keratinocytes in nociceptive touch. Keratinocytes make up ~95% of the total epithelial composition, and are associated with free nerve endings, the unmyelinated sensory endings that terminate in the epidermis and mediate response to noxious stimuli. Canonically, researchers assumed that free nerve endings present epidermis were only physically supported by keratinocytes, because there are no apparent specialized structures linking the neuron and keratinocytes. Recent advances have identified

sensory capacity and neuromodulator release present within the keratinocyte that influence nerve response.

Keratinocytes express a number of ion channels that allow for depolarization of the cells following stimulus. For example, keratinocytes express the sensory channels from the TRPC (Cai, Fatherazi, Presland, Belton, & Izutsu, 2005) and TRPV (Lee & Caterina, 2005) families. Keratinocytes also express voltage gated sodium channels that are active during nociceptive stimuli (Zhao et al., 2008). Physiological evidence suggests that voltage-gated potassium channels present in keratinocytes may also respond to mechanical force (Gu et al., 2001; Hao et al., 2013; Laitko et al., 2006).

Several lines of experimentation have shown that altering the activity of the keratinocyte affects neuron output. Expressing dominant negative form of the Potassium channel Kv1.1 reduces mechanical sensitivity (Hao et al., 2013). Direct activation of keratinocytes using a transgenic channelrhodopsin (ChR2) is sufficient to produce action potentials in afferent nerves. This stimulation is also able to produce nocifensive behaviors in intact animals. Further, optogenetic inhibition of keratinocytes using Archaerhodopsin-3 (Arch) reduces sensitivity to innocuous and noxious mechanical stimuli in mice (Moehring et al., 2018).

Recent work suggests that signaling from keratinocytes occurs through several mechanisms. Short term response to inputs appear to primarily be mediated by ATP-P2X signaling. After keratinocytes are depolarized, they release ATP into the extracellular space, which is sensed by afferent P2X family receptors (Moehring et al., 2018). Mutations that reduce touch sensitivity also show diminished release of ATP compared to control animals (Zappia et al., 2016). P2X receptors have been shown to

modulate the activity of additional channels (Burnstock, 2016; Khakh & North, 2012), so it is proposed that ATP acts as a potentiator to modulate the response to stimuli, rather than directly initiating action potentials (Moehring et al., 2018).

Keratinocytes can also mediate chronic changes in response following chemical or cellular damage via the inflammation response. We are familiar with a painful sunburn caused by UV exposure, or the dull pain of a wound infection. Sunburn is caused by UVB radiation of keratinocytes, which activate TRPV4 and leads to endothelin-1 signaling (Moore et al., 2013). Inflammation response is implicated in pathological skin irritation, such as psoriasis (Talagas & Misery, 2019). These responses to a broad variety of inputs in barrier cells allow for protection from environmental hazards.

In *Drosophila*, the somatosensory neurons of the larval body wall grow sandwiched between a monolayer of keratinocyte-like epithelial cells and ECM. Portions of the nociceptive C4da neuron become ensheathed within the epithelial cells. This ensheathment is regulated developmentally and occurs in a class specific fashion. Further, altering ensheathment rates (Jiang et al., 2019) or distribution of dendrite epithelial interactions (Chapter 2) affects sensitivity to noxious touch, suggesting that the epithelial cells modulate activity or directly signal to the neuron. As in keratinocytes, directly activating the epithelial cell is sufficient to depolarize the nociceptive neuron and elicit pain avoidance response (unpublished data).

These findings together suggest that keratinocytes, the most numerous cells in the skin barrier, are well positioned to act as sensory components and contribute to light

and noxious touch response, and can act to integrate a number of signal types to modulate mechanosensitivity.

Development of neuron-epithelial interactions

In vertebrates, somatosensory neurons arise from neural crest, delaminate and migrate to their peripheral targets (Weston, 1971). The neurons then innervate both the spinal cord and their epithelial target. Mechanisms for the targeting regions of the spinal cord are somewhat well studied (reviewed in Olson, Dong, Fleming, & Luo, 2016). However, the signals that target and recruit the neuron to the skin are less well understood. Merkel cell innervation provides an instructive example for the formation of neuron-epithelial coupling. Merkel cells are targets of Aβ – Low threshold mechanoreceptor afferents during embryonic development. Interestingly, the Merkel cell also appears to alter afferent morphology. NTF and NGF signaling are required in cell-neurite maintenance, where innervated Merkel cell numbers rapidly decline 3 weeks after birth in mice (Niu, Vysochan, & Luo, 2014). Blocking Merkel cell formation through removal of the neurogenic gene Atoh1 leads to an overbranched morphology, in addition to a reduction in response to touch stimuli (Maksimovic et al., 2014; Maricich et al., 2009). Further research suggests that BDNF signaling from the Merkel cell helps shape the development and gene expression of the innervating afferent (Reed-Geaghan et al., 2016). The long range guidance cues that direct growing neurites to their targets have not yet been identified. Signaling that controls targeting of the other sensory endings (Pacinian, Meissner, and Ruffini) are more poorly elucidated.

Invertebrate systems, with powerful genetic tools, have elucidated some of the mechanisms of targeting of touch receptors to the epithelial cells. There are features present in the epidermis that are conserved (Figure 1), suggesting that the molecular mechanisms that form the interactions between neuron and epidermis may be conserved across groups.

The nematode *C. elegans* is a useful model for identifying genes that pattern the branching structure of sensory endings. Expression menorin (MNR-1) and SAX-7 in the muscle and epithelia target the PVD nociceptors to form a complex branched menorah structure that covers the body wall (Figure 1A). Gene expression in epithelial cells can also alter the mechanical sensitivity of the touch receptor. Epithelial mec-5 (collagen type I alpha 2 chain) and mec-9 (human SPINT2 (serine peptidase inhibitor, Kunitz type 2) ortholog) regulate organization and gating of mechanosensitive channel complexes in the neuron that mediate light touch sensation (Du, Gu, & William, 1996; Emtage, Gu, Hartwieg, & Chalfie, 2004). These show that non-neuronal tissues contribute to both the structure and function of mechanosensory neurons.

Recent work in *Drosophila* and the zebrafish *Danio rerio* have sought to understand the molecular mechanisms that regulate the interaction between sensory neuron and keratinocyte-like cells. Early anatomical studies found that mammalian somatosensory neurons sometimes insert into the keratinocyte (Cauna, 1973). A number of studies have identified ensheathment structures in invertebrate and vertebrate species, whereby the free ending of a sensory neuron becomes ensheathed by their epithelial substrate. In the zebrafish, Rohon-Beard mechanosensory neurons in the developing fish become ensheathed (O'Brien et al., 2012). Likewise, extensive

portions of the Class IV dendritic arborization neuron wrapped by the epithelial cells (Han et al., 2012; Jiang, Soba, Parker, Kim, & Parrish, 2014; Kim, Shrestha, Blazeski, Mason, & Grueber, 2012).

Recent work has demonstrated that a number of conserved molecular components that compose and regulate the ensheathment are conserved between *Drosophila* and zebrafish (Jiang et al., 2019). First, the modified lipid PIP2 in the epithelial membrane accumulates in apposition to the sensory neuron dendrite. Regulators of the cytoskeleton such as the GTPases Rho and Arf6 are recruited to the site of ensheathment, leading to enrichment of F-actin. As the sheath matures, components of the epithelial junction are recruited, including coracle (*Drosophila* Protein 4.1 homolog) and E-cadherin. This leads to a stable physical coupling of the neuron and epithelial cell. The sheath structures alter the local stability and branching structure of the nociceptor (Jiang et al., 2019; Kim et al., 2012; Tenenbaum, Misra, Alizzi, & Gavis, 2017). The signal that initiates the formation of ensheathment is still unknown, but it appears to be derived from the sensory neuron.

Together, research suggest roles for long range and contact mediated signals in targeting and coupling mechanosensitive and nociceptive neurons and their epithelial partners. The epithelial partners can regulate the morphology and gene expression of the neuron. They can also alter the excitability of the neuron through structure, neuromodulation, or active signaling through neurotransmitters.

Discussion

The developmental origin of epithelium and neuron

Development of the somatosensory system requires the coordinated regulation and activation of many transcription factors (TFs) to define precursor stem cells and initiate differentiation into the cell types of the nervous and sensory system (Bernd Fritzsch, Jahan, Pan, & Elliott, 2015; Imayoshi & Kageyama, 2014). The sensory neuron and some of its epidermal targets arise from the ectoderm of the early embryo. The neurons and Schwann cells originate from neural crest precursors that migrate from the dorsal ectoderm of the neural crest to their innervation targets (George, Chaverra, Todd, Lansford, & Lefcort, 2007; Raible & Ungos, 2006). Epidermal cells are specialized from ectoderm *in situ* (Eckert, Crish, & Robinson, 1997; Van Keymeulen et al., 2009).

This common origin may make expression of transcriptionally regulated networks of sensory genes in epidermal cells more readily available. Regulatory networks that are controlled by common early TFs may make expression of neuronal sensory genes in epithelium more likely. For example, the TF Atonal (Atoh1) is required for specification of a number of sensory cell types. It is required for neurogenesis inner ear hair cells, and sensory neurons in the gut (Atkinson et al., 2015; Mulvaney & Dabdoub, 2012). It is also required to specify Merkel cells in vertebrates (Maricich et al., 2009; Van Keymeulen et al., 2009). In *Drosophila*, atonal specifies the R8 photoreceptor cell in the eye and chordotonal sensory organs in the bodywall and cuticle (Jarman, Sun, Jan, & Jan, 1995; Melicharek et al., 2008; Sun et al., 1998). The TF Neurog1 is also required for differentiation of hair cells and neurons in the ear (B. Fritzsch et al., 2002; Bernd Fritzsch, Eberl, & Beisel, 2010; Ma, Anderson, & Fritzsch, 2000), fate of olfactory

sensory neurons (Shaker, Dennis, Kurrasch, & Schuurmans, 2012), and acts to specify neuronal fate in the developing cortex (Dixit et al., 2014).

Epidermal cells like keratinocytes and Merkel cells express a variety of mechanosensitive ion channels canonically associated with neurons. It is possible that these cells types co-opt the expression profile of sensory neurons, and contribute to the sensory apparatus of the animal. It is less likely that these specializations arise from specialization of another neuronal type with reduced axon, given that they originate from the epidermis (Van Keymeulen et al., 2009).

Epithelia-neuron interactions are conserved between distantly related groups

Somatosensation is required at all times to allow for locomotion, feeding, and protection against injury. Because of this, there is likely very high selective pressure to maintain functional sensory structures. This pressure is likely to maintain the genes that underlie the development of the somatosensory organs. Our recent work in *Drosophila* and zebrafish have identified a strongly conserved developmental mechanism that regulates epidermal ensheathment of sensory neurites (Jiang et al., 2019).

One area where we see diversification is in the sensory ion channels themselves. There is a small number of identified mechanosensitive and mechanosensitive-like channels present in plants and microbes (Haswell, Phillips, & Rees, 2011; Wilson, Maksaev, & Haswell, 2013). These are believed to have originated to regulate osmotic pressure, regulating ion flow in response to stretch on the cell membrane caused by increased water volume. In the animal kingdom, there is are a number of gene

duplications and radiations that allow for a finer sense of temperature, chemical, and touch stimuli (Martinac, 2004; Saito & Tominaga, 2017).

Diversity of sensory components allow for complex signal integration

Because the sensory neuron must depolarize and repolarize rapidly to send action potentials to the CNS, neurons are somewhat limited in the properties they can possess to respond to sensory input. By having an additional sensory cell in the epithelium, the circuit can maintain depolarization for a greater period of time. These differential responses allow for more complex neural coding and permit distinction between a greater variety of touch types. Further, the epithelial cell can integrate more types of stimuli, such as injury, infection, heat. Finally, by utilizing the barrier cell as a sensor, the neuron is more protected from environments that could damage or kill the neuron, which would disrupt the sensory circuit.

Conclusion

Touch sensation is very important to everyday life and ensures that we can safely navigate a dangerous world. Despite our improving knowledge of the molecules and cells that regulate somatosensation, we still don't know many of signals that regulate the targeting/ regulation of the interactions. However, because of the diversity and specialized nature of the sensory structures, patterning and signaling must be tightly regulated to precisely by a number of molecular mechanisms. And given their apparent conservation across the animal kingdom, research in model organisms can bring powerful genetic and transgenic tools to elucidate the role epithelial cells perform

in sensation. Improved tools to identify cell types and signaling pathways will increase our understanding of touch and pain. These improvements may increase our ability to treat pain disorders without resorting to opioid painkillers.

Bibliography

Atkinson, P. J., Huarcaya Najarro, E., Sayyid, Z. N., & Cheng, A. G. (2015). Sensory hair cell development and regeneration: similarities and differences. *Development (Cambridge, England)*, *142*(9), 1561–1571. https://doi.org/10.1242/dev.114926

Bleckmann, H., & Zelick, R. (2009). Lateral line system of fish. *Integrative Zoology*, *4*(1), 13–25. https://doi.org/10.1111/j.1749-4877.2008.00131.x

Burnstock, G. (2016). Purinergic Mechanisms and Pain. *Advances in Pharmacology*, *75*, 91–137. https://doi.org/10.1016/BS.APHA.2015.09.001

Cai, S., Fatherazi, S., Presland, R. B., Belton, C. M., & Izutsu, K. T. (2005). TRPC channel expression during calcium-induced differentiation of human gingival keratinocytes. *Journal of Dermatological Science*, *40*(1), 21–28. https://doi.org/10.1016/j.jdermsci.2005.06.005

Cauna, N. (1973). The free penicillate nerve endings of the human hairy skin. *Journal of Anatomy*, *115*(Pt 2), 277–288. Retrieved from http://www.ncbi.nlm.nih.gov/pubmed/4756249

Chambers, M. R., Andres, K. H., Duering, M. v., & Iggo, A. (1972). THE STRUCTURE AND FUNCTION OF THE SLOWLY ADAPTING TYPE II MECHANORECEPTOR

IN HAIRY SKIN. *Quarterly Journal of Experimental Physiology and Cognate Medical Sciences*, *57*(4), 417–445. https://doi.org/10.1113/expphysiol.1972.sp002177

Chang, W., Kanda, H., Ikeda, R., Ling, J., DeBerry, J. J., & Gu, J. G. (2016). Merkel disc is a serotonergic synapse in the epidermis for transmitting tactile signals in mammals. *Proceedings of the National Academy of Sciences of the United States of America*, *113*(37), E5491-500. https://doi.org/10.1073/pnas.1610176113

Dixit, R., Wilkinson, G., Cancino, G. I., Shaker, T., Adnani, L., Li, S., … Schuurmans, C. (2014). Neurog1 and Neurog2 control two waves of neuronal differentiation in the piriform cortex. *Journal of Neuroscience*, *34*(2), 539–553. https://doi.org/10.1523/JNEUROSCI.0614-13.2014

Du, H., Gu, G., & William, C. M. (1996). *Extracellular Proteins Needed for C. elegans Mechanosensation*. *Neuron* (Vol. 16).

Eckert, R. L., Crish, J. F., & Robinson, N. A. (1997). The epidermal keratinocyte as a model for the study of gene regulation and cell differentiation. *Physiological Reviews*, *77*(2), 397–424. https://doi.org/10.1152/physrev.1997.77.2.397

Emtage, L., Gu, G., Hartwieg, E., & Chalfie, M. (2004). Extracellular proteins organize the mechanosensory channel complex in C. elegans touch receptor neurons. *Neuron*, *44*(5), 795–807. https://doi.org/10.1016/j.neuron.2004.11.010

Feng, J., Luo, J., Yang, P., Du, J., Kim, B. S., & Hu, H. (2018). Piezo2 channel-Merkel cell signaling modulates the conversion of touch to itch. *Science (New York, N.Y.)*, *360*(6388), 530–533. https://doi.org/10.1126/science.aar5703

Fradette, J., Larouche, D., Fugère, C., Guignard, R., Beauparlant, A., Couture, V., … Germain, L. (2003). Normal human Merkel cells are present in epidermal cell populations isolated and cultured from glabrous and hairy skin sites. *Journal of Investigative Dermatology*, *120*(2), 313–317. https://doi.org/10.1046/j.1523-1747.2003.12024.x

Fritzsch, B., Beisel, K. W., Jones, K., Fariñas, I., Maklad, A., Lee, J., & Reichardt, L. F. (2002). Development and evolution of inner ear sensory epithelia and their innervation. *Journal of Neurobiology*, *53*(2), 143–156. https://doi.org/10.1002/neu.10098

Fritzsch, Bernd, Eberl, D. F., & Beisel, K. W. (2010, September). The role of bHLH genes in ear development and evolution: Revisiting a 10-year-old hypothesis. *Cellular and Molecular Life Sciences*. https://doi.org/10.1007/s00018-010-0403-x

Fritzsch, Bernd, Jahan, I., Pan, N., & Elliott, K. L. (2015, January 1). Evolving gene regulatory networks into cellular networks guiding adaptive behavior: an outline how single cells could have evolved into a centralized neurosensory system. *Cell and Tissue Research*. Springer Verlag. https://doi.org/10.1007/s00441-014-2043-1

George, L., Chaverra, M., Todd, V., Lansford, R., & Lefcort, F. (2007). Nociceptive sensory neurons derive from contralaterally migrating, fate-restricted neural crest cells. *Nature Neuroscience*, *10*(10), 1287–1293. https://doi.org/10.1038/nn1962

Gerling, G. J., Wan, L., Hoffman, B. U., Wang, Y., & Lumpkin, E. A. (2018). Computation predicts rapidly adapting mechanotransduction currents cannot account for tactile encoding in Merkel cell-neurite complexes. *PLOS Computational*

Biology, *14*(6), e1006264. https://doi.org/10.1371/journal.pcbi.1006264

Halata, Z. (1977). The ultrastructure of the sensory nerve endings in the articular capsule of the knee joint of the domestic cat (Ruffini corpuscles and Pacinian corpuscles). *Journal of Anatomy*, *124*(Pt 3), 717–729. Retrieved from http://www.ncbi.nlm.nih.gov/pubmed/604339

Halata, Zdenek, Grim, M., & Baumann, K. I. (2010). Current understanding of Merkel cells, touch reception and the skin. *Expert Review of Dermatology*, *5*(1), 109–116. https://doi.org/10.1586/edm.09.70

Han, C., Wang, D., Soba, P., Zhu, S., Lin, X., Jan, L. Y., & Jan, Y.-N. (2012). Integrins Regulate Repulsion-Mediated Dendritic Patterning of Drosophila Sensory Neurons by Restricting Dendrites in a 2D Space. *Neuron*, *73*(1), 64–78. https://doi.org/10.1016/J.NEURON.2011.10.036

Haswell, E. S., Phillips, R., & Rees, D. C. (2011, October 12). Mechanosensitive channels: What can they do and how do they do it? *Structure*. https://doi.org/10.1016/j.str.2011.09.005

Hoffman, B. U., Baba, Y., Griffith, T. N., Mosharov, E. V., Woo, S. H., Roybal, D. D., … Lumpkin, E. A. (2018). Merkel Cells Activate Sensory Neural Pathways through Adrenergic Synapses. *Neuron*, *100*(6), 1401-1413.e6. https://doi.org/10.1016/j.neuron.2018.10.034

Ikeda, R., Cha, M., Ling, J., Jia, Z., Coyle, D., & Gu, J. G. (2014). Merkel Cells Transduce and Encode Tactile Stimuli to Drive Aβ-Afferent Impulses. *Cell*, *157*(3), 664–675. https://doi.org/10.1016/J.CELL.2014.02.026

Imayoshi, I., & Kageyama, R. (2014, April 2). bHLH factors in self-renewal, multipotency, and fate choice of neural progenitor cells. *Neuron*. Cell Press. https://doi.org/10.1016/j.neuron.2014.03.018

Jarman, A. P., Sun, Y., Jan, L. Y., & Jan, Y. N. (1995). Role of the proneural gene, atonal, in formation of Drosophila chordotonal organs and photoreceptors. *Development*, *121*(7), 2019–2030.

Jiang, N., Rasmussen, J. P., Clanton, J. A., Rosenberg, M. F., Luedke, K. P., Cronan, M. R., … Parrish, J. Z. (2019). A conserved morphogenetic mechanism for epidermal ensheathment of nociceptive sensory neurites. *ELife*, *8*. https://doi.org/10.7554/eLife.42455

Jiang, N., Soba, P., Parker, E., Kim, C. C., & Parrish, J. Z. (2014). The microRNA bantam regulates a developmental transition in epithelial cells that restricts sensory dendrite growth. *Development (Cambridge, England)*, *141*(13), 2657–2668. https://doi.org/10.1242/dev.107573

Khakh, B. S., & North, R. A. (2012). Neuromodulation by Extracellular ATP and P2X Receptors in the CNS. *Neuron*, *76*(1), 51–69. https://doi.org/10.1016/j.neuron.2012.09.024

Kim, M. E., Shrestha, B. R., Blazeski, R., Mason, C. A., & Grueber, W. B. (2012). Integrins Establish Dendrite-Substrate Relationships that Promote Dendritic Self-Avoidance and Patterning in Drosophila Sensory Neurons. *Neuron*, *73*(1), 79–91. https://doi.org/10.1016/J.NEURON.2011.10.033

Lee, H., & Caterina, M. J. (2005). TRPV channels as thermosensory receptors in

epithelial cells. *Pflügers Archiv - European Journal of Physiology*, *451*(1), 160–167. https://doi.org/10.1007/s00424-005-1438-y

Ma, Q., Anderson, D. J., & Fritzsch, B. (2000). Neurogenin 1 null mutant ears develop fewer, morphologically normal hair cells in smaller sensory epithelia devoid of innervation. *JARO - Journal of the Association for Research in Otolaryngology*, *1*(2), 129–143. https://doi.org/10.1007/s101620010017

Maksimovic, S., Nakatani, M., Baba, Y., Nelson, A. M., Marshall, K. L., Wellnitz, S. A., … Lumpkin, E. A. (2014). Epidermal Merkel cells are mechanosensory cells that tune mammalian touch receptors. *Nature*, *509*(7502), 617–621. https://doi.org/10.1038/nature13250

Maricich, S. M., Wellnitz, S. A., Nelson, A. M., Lesniak, D. R., Gerling, G. J., Lumpkin, E. A., & Zoghbi, H. Y. (2009). Merkel cells are essential for light-touch responses. *Science (New York, N.Y.)*, *324*(5934), 1580–1582. https://doi.org/10.1126/science.1172890

Martinac, B. (2004). Mechanosensitive ion channels: Molecules of mechanotransduction. *Journal of Cell Science*, *117*(12), 2449–2460. https://doi.org/10.1242/jcs.01232

Melicharek, D., Shah, A., DiStefano, G., Gangemi, A. J., Orapallo, A., Vrailas-Mortimer, A. D., & Marenda, D. R. (2008). Identification of novel regulators of atonal expression in the developing Drosophila retina. *Genetics*, *180*(4), 2095–2110. https://doi.org/10.1534/genetics.108.093302

Moehring, F., Cowie, A. M., Menzel, A. D., Weyer, A. D., Grzybowski, M., Arzua, T., …

Stucky, C. L. (2018). Keratinocytes mediate innocuous and noxious touch via ATP-P2X4 signaling. *ELife*, *7*. https://doi.org/10.7554/eLife.31684

Moll, I., Moll, R., & Franke, W. W. (1986). Formation of epidermal and dermal merkel cells during human fetal skin development. *Journal of Investigative Dermatology*, *87*(6), 779–787. https://doi.org/10.1111/1523-1747.ep12458993

Moll, I., Paus, R., & Moll, R. (1996). Merkel Cells in Mouse Skin: Intermediate Filament Pattern, Localization, and Hair Cycle-Dependent Density. *Journal of Investigative Dermatology*, *106*(2), 281–286. https://doi.org/10.1111/1523-1747.EP12340714

Moore, C., Cevikbas, F., Pasolli, H. A., Chen, Y., Kong, W., Kempkes, C., … Liedtke, W. B. (2013). UVB radiation generates sunburn pain and affects skin by activating epidermal TRPV4 ion channels and triggering endothelin-1 signaling. *Proceedings of the National Academy of Sciences of the United States of America*, *110*(34), E3225-34. https://doi.org/10.1073/pnas.1312933110

Mulvaney, J., & Dabdoub, A. (2012). Atoh1, an essential transcription factor in neurogenesis and intestinal and inner ear development: Function, regulation, and context dependency. *JARO - Journal of the Association for Research in Otolaryngology*, *13*(3), 281–293. https://doi.org/10.1007/s10162-012-0317-4

Niu, J., Vysochan, A., & Luo, W. (2014). Dual Innervation of Neonatal Merkel Cells in Mouse Touch Domes. *PLoS ONE*, *9*(3), e92027. https://doi.org/10.1371/journal.pone.0092027

O'Brien, G. S., Rieger, S., Wang, F., Smolen, G. A., Gonzalez, R. E., Buchanan, J., & Sagasti, A. (2012). Coordinate development of skin cells and cutaneous sensory

axons in zebrafish. *The Journal of Comparative Neurology*, *520*(4), 816–831. https://doi.org/10.1002/cne.22791

Olson, W., Dong, P., Fleming, M., & Luo, W. (2016). The specification and wiring of mammalian cutaneous low-threshold mechanoreceptors. *Wiley Interdisciplinary Reviews: Developmental Biology*, *5*(3), 389–404. https://doi.org/10.1002/wdev.229

Pawson, L., Pack, A. K., & Bolanowski, S. J. (2007). Possible glutaminergic interaction between the capsule and neurite of Pacinian corpuscles. *Somatosensory & Motor Research*, *24*(1–2), 85–95. https://doi.org/10.1080/08990220701388364

Pawson, L., Prestia, L. T., Mahoney, G. K., Güçlü, B., Cox, P. J., & Pack, A. K. (2009). GABAergic/glutamatergic-glial/neuronal interaction contributes to rapid adaptation in pacinian corpuscles. *The Journal of Neuroscience : The Official Journal of the Society for Neuroscience*, *29*(9), 2695–2705. https://doi.org/10.1523/JNEUROSCI.5974-08.2009

Quindlen, J. C., Lai, V. K., & Barocas, V. H. (2015). Multiscale Mechanical Model of the Pacinian Corpuscle Shows Depth and Anisotropy Contribute to the Receptor's Characteristic Response to Indentation. *PLOS Computational Biology*, *11*(9), e1004370. https://doi.org/10.1371/journal.pcbi.1004370

Raible, D. W., & Ungos, J. M. (2006). Specification of sensory neuron cell fate from the neural crest. *Advances in Experimental Medicine and Biology*. Springer New York. https://doi.org/10.1007/978-0-387-46954-6_10

Reed-Geaghan, E. G., Wright, M. C., See, L. A., Adelman, P. C., Lee, K. H., Koerber, H. R., & Maricich, S. M. (2016). Merkel cell-driven BDNF signaling specifies SAI

neuron molecular and electrophysiological phenotypes. *Journal of Neuroscience*, *36*(15), 4362–4376. https://doi.org/10.1523/JNEUROSCI.3781-15.2016

Saito, S., & Tominaga, M. (2017, April 3). Evolutionary tuning of TRPA1 and TRPV1 thermal and chemical sensitivity in vertebrates. *Temperature*. Routledge. https://doi.org/10.1080/23328940.2017.1315478

Serizawa, S., Miyamichi, K., & Sakano, H. (2004, December). One neuron-one receptor rule in the mouse olfactory system. *Trends in Genetics*. https://doi.org/10.1016/j.tig.2004.09.006

Shaker, T., Dennis, D., Kurrasch, D. M., & Schuurmans, C. (2012). Neurog1 and Neurog2 coordinately regulate development of the olfactory system. *Neural Development*, *7*(1). https://doi.org/10.1186/1749-8104-7-28

Sun, Y., Jan, L. Y., Jan, Y. N., Tucker, P. K., Gemza, D. L., Glaser, T., … Zoghbi, H. Y. (1998). Transcriptional regulation of atonal during development of the Drosophila peripheral nervous system. *Development (Cambridge, England)*, *125*(18), 3731–3740. https://doi.org/9806930

Talagas, M., & Misery, L. (2019). Role of Keratinocytes in Sensitive Skin. *Frontiers in Medicine*, *6*. https://doi.org/10.3389/fmed.2019.00108

Tenenbaum, C. M., Misra, M., Alizzi, R. A., & Gavis, E. R. (2017). Enclosure of Dendrites by Epidermal Cells Restricts Branching and Permits Coordinated Development of Spatially Overlapping Sensory Neurons. *Cell Reports*, *20*(13), 3043–3056. https://doi.org/10.1016/J.CELREP.2017.09.001

Van Keymeulen, A., Mascre, G., Youseff, K. K., Harel, I., Michaux, C., De Geest, N., …

Blanpain, C. (2009). Epidermal progenitors give rise to Merkel cells during embryonic development and adult homeostasis. *The Journal of Cell Biology*, *187*(1), 91–100. https://doi.org/10.1083/jcb.200907080

Wan, G., Corfas, G., & Stone, J. S. (2013). Inner ear supporting cells: Rethinking the silent majority. *Seminars in Cell & Developmental Biology*, *24*(5), 448–459. https://doi.org/10.1016/J.SEMCDB.2013.03.009

Weston, J. A. (1971). Neural crest cell migration and differentiation. *Advances in Morphogenesis*. https://doi.org/10.1016/b978-0-12-028608-9.50006-5

Wilson, M. E., Maksaev, G., & Haswell, E. S. (2013). MscS-like mechanosensitive channels in plants and microbes. *Biochemistry*, *52*(34), 5708–5722. https://doi.org/10.1021/bi400804z

Winkelmann, R. K., & Breathnach, A. S. (1973). The Merkel Cell. *Journal of Investigative Dermatology*, *60*(1), 2–15. https://doi.org/10.1111/1523-1747.EP13069480

Woo, S.-H., Lumpkin, E. A., & Patapoutian, A. (2015). Merkel cells and neurons keep in touch. *Trends in Cell Biology*, *25*(2), 74–81. https://doi.org/10.1016/J.TCB.2014.10.003

Zappia, K. J., Garrison, S. R., Palygin, O., Weyer, A. D., Barabas, M. E., Lawlor, M. W., … Stucky, C. L. (2016). Mechanosensory and ATP Release Deficits following Keratin14-Cre-Mediated TRPA1 Deletion Despite Absence of TRPA1 in Murine Keratinocytes. *PLOS ONE*, *11*(3), e0151602. https://doi.org/10.1371/journal.pone.0151602

Zhao, P., Barr, T. P., Hou, Q., Dib-Hajj, S. D., Black, J. A., Albrecht, P. J., … Waxman, S. G. (2008). Voltage-gated sodium channel expression in rat and human epidermal keratinocytes: evidence for a role in pain. *Pain*, *139*(1), 90–105. https://doi.org/10.1016/j.pain.2008.03.016

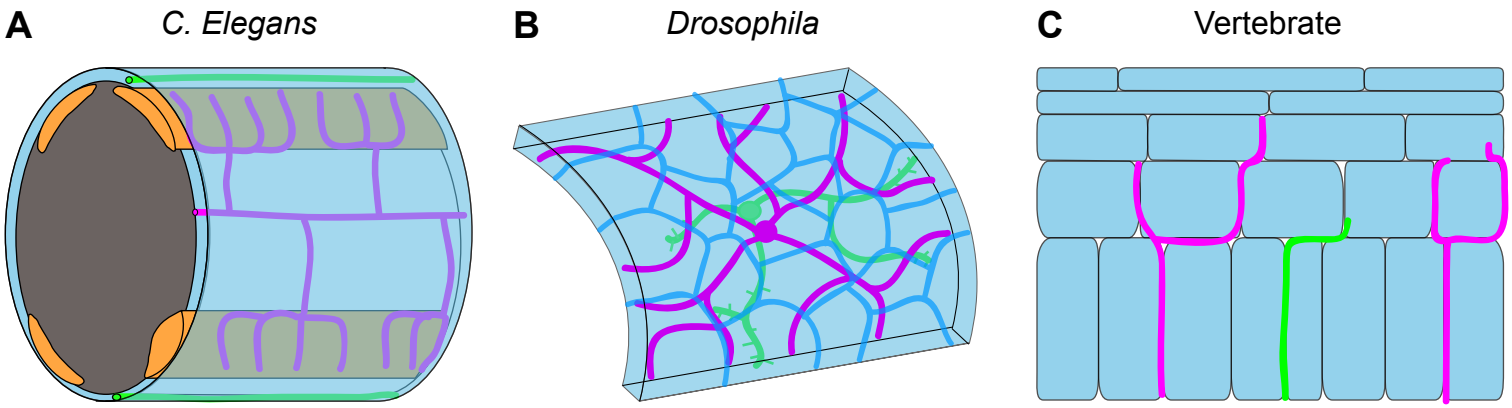

	Epithelium			
Neuron	Touch	PVM and PLM	C3da	Low threshold mechanoreceptors
	Pain	PVD	C4da	C- fiber pencillate

Figure 1. Epidermal Circuits for mechanical and nociceptive sensation in laboratory models. Low threshold (green) and high threshold (magenta) neurons innervate the epidermis in (A) C. elegans, (B) Drosophila, and (C) representative vertebrate skin, from mouse.

The microRNA *miR-14* regulates dendrite axial positioning and nociceptive sensitivity through control of epidermal gap junctions

Abstract

Interaction between epithelial cells and neurons are important for shaping our responses to wide variety of sense. The interactions between these cell types can influence the structure and function of the sensory neuron, although much remains unknown about the molecular underpinnings. Here, we describe the link between dendrite morphology and neuron sensitivity in the *Drosophila* PNS by identifying novel regulators through a genetic screen. We characterize the novel role of the microRNA *miR-14* to regulate the development of peripheral nociceptors. *miR-14* regulates the interaction of C4da neurons with the epithelium by preventing precocious innervation of the epithelial junctions of the epidermis. These mutants are significantly more sensitive to noxious mechanical stimulus. *miR-14* appears to regulate expression of epithelial expression of gap junction proteins, which tightly seal the basal domain of the cell junction. These results suggests a direct link between the dendrite pattern and interaction with epithelial cells and excitability of the nociceptor.

Introduction

A number of patterning cues in epidermis are known to regulate the position and morphology of somatosensory neurons. In zebrafish, the neuronal receptor LAR and its ligands Heparan sulfate proteoglycans (HSPGs) (Fox & Zinn, 2005) play a role in targeting Rohon-Beard neurons. Mutants or treatments deficient in HSPG production produce fail to properly target and branch in their target tissue (Lee et al., 2004; Wang, Wolfson, Gharib, & Sagasti, 2012). In *C. elegans*, epidermal MNR-1 acts via neuronal receptors to target the sensory neuron and regulate its branching structure (Salzberg et al., 2013; Zou et al., 2016). Negative cues can also regulate patterning of sensory neurons. In mouse, loss of Sema3A show increased branching in axons of peripheral sensory neurons (Taniguchi et al., 1997).

The structure of the dendrite can impact the activity and output of the neurons. The excitability of vertebrate CA1 and CA3 hippocampal neurons are determined by the dendrite structure and distribution of input synapses (Makara & Magee, 2013; Takahashi & Magee, 2009). The structure of inputs into the dendrite of direction-selective retinal ganglion cells confer specificity of response to visual input (Hoon, Okawa, Della Santina, & Wong, 2014; Komendantov & Ascoli, 2009).

In the peripheral nervous system (PNS), cutaneous sensory neuron dendrites innervate epidermal structures that can also influence the sensitivity of the neuron. The lamellar epithelial structures that form Meissner and Pacinian corpuscles tune response to gentle touch and vibration (Fleming & Luo, 2013). Aβ low-threshold mechanoreceptors innervate Merkel cells, which mediate response to deep touch (Halata, Grim, & Baumann, 2010), and ablation of the Merkel cell severely reduces the

response of the receptor (Maksimovic et al., 2014). Noxious response is mediated by free nerve endings, which associate with keratinocytes of the epidermis (Moehring et al., 2018).

In the *Drosophila* PNS, the dendrite morphology of peripheral neurons is partially shaped by its interaction with the epithelium. the dendrite arbor of sensory neurons, such as the Class IV dendritic arborization (C4da) neuron is largely restricted to a two dimensional plane, in contact with the Extracellular matrix (ECM)basement membrane and growing over the monolayer of epithelial cells that form the body wall. The neuron interacts with both the ECM and the epidermis to shape the sensory dendrites. In wild-type neurons, small portions of these neurons detach from the basement membrane and become embedded within epithelial cells in a developmentally regulated fashion, called ensheathment (Jiang et al., 2019). Embedding of neurons in epithelia has been observed in other systems, such as *C. elegans* (Goodman, 2006; Krieg, Dunn, & Goodman, 2015) and developing zebrafish larvae (O'Brien et al., 2012). This ensheathment rate is affected in a number of mutant paradigms (Han et al., 2012; Jiang et al., 2019). When there are higher levels of embedding, the neurons cannot contact one another to produce a repulsive signal, so the branches appear to cross in two dimensional space. Reducing ensheathment of the neurons reduces sensitivity to noxious mechanical stimuli.

We sought to understand the link between dendrite morphology and neuron sensitivity in the *Drosophila* PNS through a genetic screen. Here, we characterize the novel role of the microRNA *miR-14* to regulate the development of peripheral nociceptors. *miR-14* regulates the interaction of C4da neurons with the epithelium by

preventing precocious innervation of the epithelial junctions of the epidermis. These mutants are significantly more sensitive to noxious mechanical stimulus. *miR-14* appears to regulate expression of epithelial expression of gap junction proteins, which tightly seal the basal domain of the cell junction. These results suggests a direct link between the dendrite pattern and interaction with epithelial cells and excitability of the nociceptor.

Results

To identify genes that function at the interface of dendrite structure and somatosensory neuron function, we performed a forward genetic screen of EMS-induced mutations, using c4da neuron coverage index and dendrite-dendrite crossing points as proxies for effects on spatial distribution and axial positioning of dendrites, respectively. In wild-type controls, c4da neurons establish nearly coverage, non-redundant coverage of the body wall by 48 h AEL (Fig 1A), with the highly branched arbor of individual c4da neurons covering an average of 88% of the territory in which they reside. Larvae grow extensively during development, and dendrite arbors of c4da neurons likewise exhibit sustained growth while maintaining their complete, non-redundant body wall coverage until larvae leave their food source to pupate. Homotypic repulsive interactions shape dendrite territories in c4da dendrites, therefore dendrite-dendrite crossing events are rarely observed in wild-type control dendrites.

From our screen we identified a single mutant allele, *dg29 (dendrite growth 29)*, which exhibited specific and progressive effects on dendrite crossing and coverage.

C4da axon and dendrite morphogenesis in *dg29* mutants was indistinguishable from wild-type controls until 48 h AEL (Figure 1F). Subsequently, *dg29* mutants exhibited progressive defects in dendrite but not axon morphogenesis (Figure 1G-J). First, although *dg29* mutant c4da neurons grew at rates comparable to controls, the dendrite arbors covered progressively smaller proportions of the body wall as a result in changes in terminal dendrite distribution (Figure 1S). In late-stage larvae, this resulted in gaps in c4da coverage over large portions of the body wall. Second, *dg29* displays increased dendrite-dendrite crossing (Figure 1T).

To determine the genetic basis for these defects, we identified the molecular nature of the *dg29* allele using genetic complementation analysis. We identified dg29 as a mutation in the RNAse III gene Dicer1 (Dcr1). Dcr1 is required for canonical processing of all pre-miRNAs into mature miRNAs (Bernstein, Caudy, Hammond, & Hannon, 2001; Knight & Bass, 2001). Dcr^{dg29} carries single amino acid substitution in the location directly next to the catalytic amino acid required to cleave dsRNA, resulting in a hypomorphic allele that is late larval lethal (data not shown).

Next, we wanted to identify which miRNA(s) produced by Dcr1 are required for proper dendrite morphogenesis. We screened from a large collection of miRNA deficiencies that cover over 80% of miRNA genes and 99% of miRNA sequence reads in *Drosophila* (Chen et al., 2014) to identify single miRNA deletions that most closely phenocopy the C4da dendrite defects seen in $Dcr1^{dg29}$. We found that loss of the miRNA *miR-14* through a deletion ($MiR\text{-}14^{\Delta1}$) is sufficient to cause defects in coverage and dendrite-dendrite crossing that we observed in Dcr^{dg29}. As with dg29, $miR\text{-}14^{\Delta1}$is

indistinguishable from wild-type, with growing defects through larval development (Figure 1K-O).

Having noted the increase in homotypic crossings of dendrite branches, we noticed that many of the dendrites that show homotypic crossing follow a hexagonal pattern (Figure 1), which resemble the size and shape of individual epithelial cells. We investigated the dendrite-epithelial architecture using PLCδ PH-GFP (Figure 2A-D'. This marker carries the pleckstrin homology domain of phospholipase C fused to a green fluorescent reporter (Várnai & Balla, 1998). This domain binds to the modified lipid Phosphatidylinositol 4,5-bisphosphate (PIP2). We have previously shown that this marker is enriched in epithelial cells at sites of dendritic ensheathment, as well as cell-cell junctions (Jiang et al., 2019). Using this, we can see that terminal branches are aligned along the cell borders of epithelial cells, and are apically displaced. In third instar larvae, we see a modest decrease in the total arbor that is ensheathed on the basal surface (Figure 2D). However, a greatly increased proportion of the arbor is aligned along cell-cell junctions, and are thus unavailable for ensheathment (Figure 2E). The distribution of ensheathed dendrites along main branches is similar to wild-type animals, suggesting that there is defect that is independent of the previously identified regulators of ensheathment. These results suggest that terminal branches are able to align along epithelial cell-cell junctions and enter the junctional space.

To assay whether these dendrite crossings are due to a loss of repulsive signaling or a disruption in ECM attachment, we used several assays to investigate the displacement of dendrites apically into the epithelial cell layer. First, we utilized the ECM component *trol*, the *Drosophila* perlecan homolog, that is tagged with green fluorescent

protein via exon-trapping (Morin, Daneman, Zavortink, & Chia, 2001). This allows for dual-labelling of the ECM and dendrite, and allows us to measure colocalization of the neuron and ECM as previously published (Jiang, Soba, Parker, Kim, & Parrish, 2014). We find that portions of the dendrite are highly apically displaced away from the ECM into the epithelial layer in *miR-14* mutants, primarily effecting terminal dendrite branches (Figure 3).

We observed the morphology of some of the other SSNs to determine if these mutants regulate dendritic arborization neurons in a class specific manner. C1da neurons form small, simple dendrites that project primarily anteriorly (ddaE) or posteriorly (ddaD) (Figure 4A). The dendrite structure and length are unaffected in *miR-14* mutant animals (Figure 4B). C3da neurons form a moderately complex dendrite arbor with distinctive, short spike terminals (Figure 4C). We found that the branch structure of these neurons are unaffected by *miR-14* (Figure 4E). We also checked for alignment with the epithelial cell junction using an RFP labelled *Drosophila* E-cadherin (*shg*). In wild-type and *miR-14* animals, very little of the dendrite arbor aligns with junction domains in either class (Figure 4F).

The miRNA *miR-14* is required for proper larval nociception

We next sought to understand the relationship between C4da dendrite morphogenesis and larval responses to noxious stimuli. We tested third instar larvae by applying a noxious mechanical stimuli using calibrated von Frey filaments and monitoring corkscrew-like nocifensive escape responses. We first established force

thresholds using wild-type animals. 25 mN von Frey filaments as the lowest force that resulted in nociceptive rolls, and trials could be easily carried out. Lower force filaments often deflect off the animal, making trials non- reproducible. Compared to wild-type controls, dg29 mutants exhibited significant increases in the response frequency (% of larvae that rolled) and magnitude (number of rolls in responders in response to mildly noxious (25 mN and 35 mN) stimulus. *miR-14* animals likewise show a particularly highly increased escape response probability to low threshold noxious stimulus, when wild-type animals rarely respond (Figure 5A). They are also more likely to perform a larger number of nocifensive rolls following a single stimulus (Figure 5B). To test that the increased response is due to activity of the nociceptor, we silenced neuron activity by expressing the tetanus toxin light chain (TNT) specifically in C4da neurons. TNT eliminates synaptic transmission from the neuron by specifically cleaving neuronal synaptobrevin, preventing vesicle docking and evoked release. TNT expression in C4da neurons blocks the evoked escape rolling in response to noxious touch. This confirms that the roll response, and the nociceptive hyperalgesia of *miR-14*, are mediated by activation of the C4da neuron.

To identify the specificity of sensory hypersensitivity, we then assayed additional sensory behaviors that are mediated by the C4da neuron, which acts as a polymodal nociceptor in the larval body wall. These nociceptive neurons are polymodal, mediating avoidance to a number of other aversive stimuli, such as noxious chemicals, noxious heat, and blue light (Im & Galko, 2012; Xiang et al., 2010). Stimulation with a noxious chemical allyl isothiocyanate (AITC), the active chemical in mustard and wasabi, has been used to test noxious chemical sensitivity in *Drosophila* and vertebrates (Lehto et

al., 2016; Mandel, Shoaf, Braco, Silver, & Johnson, 2018). To measure sensitivity, larva were immersed in a 25 mM solution of AITC in mineral oil and were tested for the latency from application of AITC until the start of nocifensive rolling (Figure 6A). Wild-type animals tested have a median latency of 22 seconds, with 50% of the animals not showing nociceptive rolling within 30 seconds of application. *miR-14* animals showed a significant reduction in latency to the stimulation, with a median response time of 8 seconds. Only 10% of animals tested did not respond within 30 seconds. *miR-14* animals produce a low level of nociceptive response to mineral oil vehicle alone (5 of 25 tested), whereas no wild-type animals were observed (Figure 6B).

C4da neurons also mediate the nocifensive escape response to noxious thermal stimuli (Terada et al., 2016), and requires a number of TRP family channels to mediate the response, such as painless (Sokabe, Tsujiuchi, Kadowaki, & Tominaga, 2008; Tracey, Wilson, Laurent, & Benzer, 2003) and TRPA1 (Boiko et al., 2017; Neely et al., 2011). We tested sensitivity using a heated probe applied to the side of the thoracic segments (Figure 7A). Interestingly, *miR-14* mutants showed no change in response latency either to high noxious heat (Figure 7B) or sub-threshold (Figure 7C), showing that the increased sensitivity is specific to C4da sensory modality.

MiR-14 loss of function specifically affects C4da mediated behaviors

To test if the increase in sensitivity is restricted to the C4da neuron, we tested a number of additional behaviors mediated by the other classes of da neurons and other neurons of the PNS. C3da neurons are sensory neurons that mediate gentle touch via

the TRP family channel, NOMPC (Yan et al., 2013). To test their sensitivity, we performed a light touch assay, where locomoting larvae are stroked with the tip of an eyelash, which evokes a limited number of behavioral responses, such as pausing, turning, and backward locomotion (Kernan, Cowan, & Zuker, 1994) (Figure 8A). Mutant animals that are hypersensitive to noxious touch do not exhibit increased response rates to low threshold gentle touch (Figure 8B). This suggests that activity of the C3da neurons is not altered by loss of *miR-14*.

C1da neurons are the least elaborate of the da neurons, and function as proprioceptive neurons important for body posture and locomotion (Cheng, Song, Looger, Jan, & Jan, 2010), and are required for coordinating rhythmic locomotion (Song, Onishi, Jan, & Jan, 2007). We measured locomotion of free larvae crawling, and observed a small decrease in locomotor speed (Figure 9A) and a small but not significant decrease in forward locomotion percentage (Figure 9B). During animal handling, no observable gross locomotor defects were observed (data not shown). Previous observations have shown that reducing C4da output also impacts locomotion, resulting in a different distribution of random searching and forward walking (Ainsley et al., 2003; Gorczyca et al., 2014). These results are consistent are consistent with effecting C4da, but not C1da function.

Drosophila larvae are capable of detecting sound stimuli, such as the sound of predatory wasps or pure tones of similar frequency (Zhang, Yan, Jan, & Jan, 2013). These stimuli are detected by chordotonal (cho) neurons in the PNS, and animals respond with a startle-freeze response. Animals were placed in an agar dish positioned

above a speaker playing 500 hz pure tones capable of eliciting the startle response. *miR-14* animals show no defect in the startle freeze response (Figure 10).

Larval chemotaxis is important for larvae to find additional food sources. *Drosophila melanogaster* primarily feed in ripe or decomposing fruit, and as such, are attracted to olfactory cues such as alcohol and acetic acid, products of fermentation. Here, we used dilute ethyl acetate as a chemoattractant (Figure 11A). Both wild-type and *miR-14* flies show similarly strong preferences for the attractive cue (Figure 11B). To validate our findings, we tested animals lacking the gene ORCO (Olfactory receptor co-receptor), an obligate co-receptor required to form all functional olfactory receptors in *Drosophila* (Larsson et al., 2004). As expected, *ORCO* mutants completely lose preference for the attractive odorant.

These results together suggest that the function of class 4 neurons is affected in a modality and class specific fashion. First, no behaviors mediated by other dendritic arborization neurons other than C4da suggest altered activity or behavioral output. Likewise is true for other behaviors mediated by sensory organs from other lineages. This suggests that *miR-14* is regulating the excitability of a very narrow nociceptive circuit, rather than broadly regulating neuronal excitability. Interestingly, the impact on C4da sensitivity appears to be modality specific, as we did not detect significantly different responses to thermal stimulation.

miR-14 hypersensitivity is independent of known mechanisms of nociceptive sensitization

Several paradigms for altering sensitivity to mechanical or thermal stimuli have been identified. One example is UV exposure, such as the sensitivity following a sunburn. A number of mechanosensitive ion channels have been identified that are required for proper UV induced hypersensitivity, such as TRPV4 in mouse (Bishop et al., 2007; Moore et al., 2013) and TRPA1 in *Drosophila* (Babcock, Landry, & Galko, 2009; Babcock et al., 2011; Im et al., 2015). Drugs can also activate these channels directly. We tested these two known mechanisms that are known to increase sensitivity to nocifensive stimuli; exposure to ultraviolet (UV) light and chemotherapeutic Vinca alkaloids.

Drosophila, exhibit increased sensitivity to mechanical or thermal stimuli following UV exposure (Babcock et al., 2009; Moore et al., 2013). UV exposure can result in painful response to normally benign stimuli (allodynia) and increased pain response to noxious stimuli (hyperalgesia). The UV exposure elicits an inflammatory response in a number of animal models, and in *Drosophila* it activates tachykinin signaling in the epithelium to increase activity of sensory channels. To test the epistatic relationship between cytokine signaling and *miR-14* hypersensitivity, we exposed wild-type and *miR-14* mutant larvae to UV irradiation. After recovering for 24 hours, we subjected them to either mechanical stimulation via Von Frey (Figure 12A) or thermal probe at a sub-noxious temperature to test for allodynia (Figure 7D). We observe increases in response in both genotypes. *miR-14* and UV exposure show an additive effect on sensitivity in mechanical trials. This increase is mirrored in thermal sensitivity (Figure 7D). We tested the role of cytokine signaling by reducing expression of the *Drosophila* tumor necrotic factor, *Eiger*, which is required for hyperalgesia following UV exposure.

Eiger is released from the epidermis and signals the TNF receptor expressed on the nociceptor (Babcock et al., 2009). We used RNAi to reduce Eiger expression using an epidermal Gal4 driver. Expression of the Eiger-RNAi did not impact mechanonociception in the absence of UV exposure (Figure 12B). *miR-14* mutants showed no change in hyperalgesia to noxious mechanical stimulus relative to the mutant alone. Eiger-RNAi did reduce the hyperalgesia in response to UV stimulation in both wild-type and *miR-14* backgrounds. These results suggest that inflammation response is not the driver of increased sensitivity in *miR-14* mutants.

Likewise, vinca alkaloids, used to treat some forms of cancer, can induce hypersensitivity or nerve pain, called chemotherapy induced peripheral neuropathy (CIPN). This pain syndrome causes pain, burning, or numbness, and often limits the dose of chemotherapeutic drugs that can be administered to a patient(Boyette-Davis, Walters, & Dougherty, 2015; Zajączkowska et al., 2019). Though it may differ for the various classes of chemotherapeutic agents, recent work in *Drosophila* suggests that the vinca alkaloid vinblastine increases nociceptor firing by directly activating TRPA1 channels(Boiko et al., 2017). Following feeding of vinblastine, both genotypes show increased sensitivity of similar magnitude (Figure 12C), suggesting that increased TRPA1 activation is not epistatic to *miR-14* hypersensitivity.

We further tested the requirement of mechanosensitive channels for mediating the mechanosensation in *miR-14*. We created stocks that were double mutants for previously identified mechanosensitive channels and *miR-14*, and tested the response to low threshold Von Frey stimulation(Gorczyca et al., 2014; S. E. Kim, Coste, Chadha, Cook, & Patapoutian, 2012; Neely et al., 2011; Tracey et al., 2003). We found a drop in

sensitivity at low noxious forces with all channel mutants, except for TRPA1 (Figure 13A). Piezo, pickpocket (ppk), and painless double mutants all show reduced sensitivity. However, single mutant sensitivity is also reduced as previously reported, so the effect may be additive. We also sought to further investigate mechanosensory channel contribution by feeding animals Ruthenium Red (RR). RR is an inorganic dye that functions as a channel blocker that effects RyR, TRPA, TRPM, and TRPV channels(Tapia & Velasco, 1997). RR fed animals show a reduction in nociceptive sensitivity in a dose dependent fashion (Figure 13B). Because oral feeding of RR had not previously been reported, we carried out a dose and force response curve to determine efficacy (Figure 14).

Time-lapse analysis

We sought to understand the growth dynamics that lead to a progressive disruption of the dendrite (Figure 15). We sequentially imaged individuals as early third instar larvae (72h after egg lay (AEL)) or as late thirds (120h AEL), and imaged them every 12 hours. We then compared extent of junctional alignment and dynamics of dendrite terminals. We compared rates of growing, stable, and retracting terminals in the arbor, both for aligned and basal terminals. The distribution of dynamics between wild-type and *miR-14* mutant dendrites are similar, suggesting that the intrinsic growth control is not strongly impacted. However, *miR-14* terminals appear to be far more likely to maintain their alignment with the junction than WT neurons. This is likely due to the neuron being displaced into the epithelial junction and sequestered there. Over

development, this leads to a progressive shift toward neurons that are junctionally inserted.

miR-14 expression is required in the Epithelium for proper dendrite morphogenesis

The epithelium provides several guidance and growth cues that direct dendrite morphology. We sought to know whether *miR-14* was required in the neuron or epithelium. We also tested the sufficiency of *miR-14* expression to rescue the mutant phenotype in a tissue specific manner. Under UAS control, we can express a Luciferase transgene that carry functional *miR-14* stem loops in the 3' UTR, that are cleaved following transcription(Bejarano et al., 2012). Ubiquitous expression using actin- Gal4 rescues the dendrite crossing phenotype seen in *miR-14* mutants (Figure 16A-B). When we resupply *miR-14* in epithelial cells, we see a partial rescue of the dendrite morphology (Figure 16C), with negligible rescue when expressed in the neuron (Figure 16D). Rescue of the mechanonociception hypersensitivity mirrors the morphological rescue (Figure 16F). This demonstrates that *miR-14* expression is sufficient in the epithelial cells, and appears dispensable for regulating morphology and sensitivity in the neuron.

To test requirement, we used a transgenic miRNA sponge to reduce the bio-available pool of *miR-14*. These transgenes encode a DsRed fluorescent protein, with a transgenic 3' UTR that carries synthetic miRNA binding sites, under the control of the UAS/Gal4 binary expression system(Fulga et al., 2015). These sites act as competitive inhibitors, binding the miRNA and prevents its regulation of its normal target genes. A

sponge carrying scrambled miRNA binding sites with no known miRNA complementarity are used for control (Figure 16 G-H). Ubiquitous or epithelial expression of the *miR-14* sponge causes both a disruption of dendrite morphology (Figure 16J-K). Interestingly, neuronal expression appears to have no meaningful effect on either measure (Figure 16L). Dendrite crossings were monitored as a proxy for the mutant phenotype (Figure 16M). The morphology defects seen in the ubiquitous or epidermal *miR-14* sponge expression are reflected in the mechanical nociceptive sensitivity (Figure 16N), showing that *miR-14* expression is required in the epidermis for regulating the morphology and nociceptive sensitivity of C4da neurons.

These findings are corroborated by single cell mosaic mutants produced through MARCM. Positively labelled homozygous mutant neurons are produced through recombination of sister chromosomes at FRT sites. In a heterozygous background, mutant neurons of the RNA processing enzyme *Drosha* (Figure 17B) and *miR-14* (Figure 17C) do not significantly differ from the wild-type mosaic control (Figure 17D-E).

We also interrogated whether the requirement was a contact/short range or a long range diffusible signal. We expressed transgenes reducing miRNA processing (Figure 18A-B) or *miR-14* levels directly (Figure18C-D) using an engrailed (en) Gal4, which is expressed in epithelial cells in the posterior-most domain of each larval segment. We then measured dendrite branch crossings in between regions of expression (Figure 18G-I). When *miR-14* signaling is reduced, we find that in en+ areas show significant crossing defects, as we saw in whole epithelial experiments, and en- regions showing low crossing rates. This suggests that *miR-14* is regulating a contact mediated or short range cue. To differentiate between these, we measured crossing

rates in the en- areas 1 or 2 average epithelial cell diameters away from the en+ area. If it is a diffusible cue, you would expect a gradient of crossings across the segment. However, we do not observe increased rates in these areas, suggesting that the restriction of precocious growth into epithelial junctions is mediated by direct contact with the epithelial cell. We see no effect on dendrite crossing when *miR-14* is overexpressed in the en+ stripe (Figure 18E-F).

Because *miR-14* appears to regulate a contact mediated cue that regulates insertion into the epithelial junction, we sought to find if modifying neuronal adhesive properties could modify the precocious junctional insertion. Integrin is a cell-surface adhesion molecule that regulates binding to ECM. In C4da neurons, integrin binding to the ECM affects the ensheathment rate of the dendrite by the epithelial cell. Using a transgene carrying all necessary integrin subunits, we drove overexpression in the neuron and monitored junctional alignment using RFP-tagged E-cadherin (Figure 19A-D). We hypothesized that increasing adhesion to the ECM would decrease the ability of *miR-14* dendrites to detach from the ECM and insert in to the epithelial cell junction. In *miR-14* mutants, integrin overexpression partially rescues alignment with the epithelial cell junction (Figure 19E), and the homotypic dendrite crossing phenotype (Figure 19F). Integrin overexpression reduces the coverage area of the dendrite in both wild-type and *miR-14*, likely due to increased adhesion that reduces dynamics required for growth, as previously reported. We hypothesize that increased adhesion to the ECM shifts the balance of adhesion away from binding to the epithelial cells, and makes it less likely that they will enter the epithelial junction and become trapped. Integrin overexpression also modifies the nociceptive hypersensitivity, reducing, but not completely rescuing, the

response rate to noxious touch (Figure 19G), which suggests that this redistribution of sensory innervation is functionally relevant to nociception.

Expression data

To determine what genes may be regulating changes dendrite morphology, we profiled the gene expression using RNA sequencing. We dissociated larval body walls and picked positively labeled 10-cell samples using a mouth pipet. We identified genes that were >2 fold difference and a q-value <0.05. In neurons, we identified only 42 genes that were significantly dysregulated between wild-type and *miR-14*$^{\Delta 1}$ neurons. In epithelial cells, we identified 800 genes that are differentially expressed in *miR-14*$^{\Delta 1}$ (Figure). Because our mosaic analysis suggests that the site of action for regulating dendrite morphology is in the epithelial cells, and a dispensable role in the neuron, we the subsequent analysis on the epithelial cells.

We carried out gene ontology (GO) enrichment analysis to identify pathways biological pathways that are overrepresented in the differentially expressed genes relative to the frequency they appear in the genome. We identified dysregulation of some metabolism components, which is consistent with *miR-14*'s previously identified role in regulating insulin production and fat metabolism(Varghese, Lim, & Cohen, 2010; Xu, Vernooy, Guo, & Hay, 2003). Interestingly, the GO analysis highlighted genes related to the development and adhesion of epithelial sheets (Figure 20). A number of epithelial adhesion molecules were dysregulated, including the downregulation of all three epithelially-expressed innexin genes. In *Drosophila*, 8 total innexin proteins are the components that form gap junctions, tightly packed membrane channels that connect the cytoplasm of adjacent cells. Gap junctions form the basal-most adhesive

domain in the *Drosophila* epithelial sheet. Loss of these gap junction adhesions may lead to reduced integrity in the epithelial cell-cell junctions, allowing dendrites to invade and grow within the junction.

Tests of epithelial integrity

We propose that the adhesive gap junctions between adjacent cells act to tightly seal the junctional domain, greatly limiting the ability of neurons to become inserted into the epithelial cell junction. A reduction in the expression of gap junction proteins in *miR-14* mutants allows the neurons to enter. There, the neurons have increased contact and adhesion with the epithelial cells, increasing their stability (Figure 22). C4da neurons are more likely to become inserted for 2 likely reasons. First, their large, elaborate dendrites grow throughout development, providing greater opportunity for insertion into the junction. Second, C4da neurons are preferentially ensheathed by epithelial cells, so the milieu of adhesive molecules or ensheathment initiation signal may push adhesion of the neuron toward the epithelium, making it more likely for the dendrite branch to lose adhesive contact with the ECM.

To test this model, we will seek to measure the openness of epithelial junctions by monitoring dye uptake. Using a dextran dye applied to a fileted larval body wall, we can monitor the extent of dye penetration into epithelial cell junctions. If gap junctions expression is reduced in *miR-14*, we expect that the basal portion of the epithelial cell-cell junction will be less tightly closed, allowing for greater penetration of the hydrophilic dye into the junctional space.

We will also investigate whether gap junctions are required to prevent junctional insertion of wild-type neurons. We sought to test the requirement of the gap junctions in maintaining epithelial integrity and dendrite patterning. To test this, we first attempted single innexin knock-downs for the 3 epithelially-expressed genes (Ogre (Inx1), Inx2, and Inx3) in the epithelium. For single gene knock-outs, Inx3 RNAi had little effect on the dendrite patterning. Inx2 had a moderate phenotype. Ogre RNAi animals were embryonic lethal. Because of issues with lethality when reduced in the whole epithelium, we will knock-down Ogre or Inx2 in smaller subsets of the epithelium. We will monitor rates of insertion into the junction within the epithelial patches.

Discussion

The interaction of many somatosensory neurons with their innervation targets profoundly shapes both the morphology and function of the neuron. While specialized structures are more well-known, the interaction of nociceptors with keratinocytes are only recently being studied in depth. Recent work in *Drosophila* has sought to investigate the molecular basis of interaction with keratinocyte-like epidermal cells. Here, we identify *miR-14* as a novel regulator of this interaction that results in reorientation of dendrite terminals along epithelial cell-cell junctions.

Functional effect on nociception

Our studies find a large increase in the behavioral response to nociceptive mechanosensation. Our results show that the sensitization is independent of other previously demonstrated mechanisms of sensitization, such as TNF signaling or CIPN.

The mechanism of changes in sensitivity remain unclear. Changes to ensheathment by epithelial cells have been shown by our lab to have a positive correlation with sensitivity. It is possible that insertion into the epithelial cell junctions is functionally similar to the regulated epidermal ensheathment of the dendrite. Many of the components that form epidermal sheaths are also cell junction components. Experimentally targeting otherwise wild-type neurons to cell junctions through ectopic adhesion may demonstrate whether insertion in the cell junction is functionally similar to ensheathment or sufficient to increase behavioral sensitivity.

Precisely why neuron ensheathment effects sensitivity is not yet clear. Another possibility is that the epithelial cells form part of the sensory apparatus. Recent studies in vertebrate suggest that keratinocytes respond to external stimulus and modulate neuron activity, acting as part of the sensory apparatus (Baumbauer et al., 2015; Moehring et al., 2018). Ensheathment and junctional insertion may form stable synapse-like sites that allow for signal transmission between the epidermis and neuron. Merkel cells are epithelial and display a number of hallmarks of active neurotransmitters. Keratinocyte and Drosophila epidermal cell neurotransmitter apparatuses have not been well established.

There are several possibilities for the modality specificity seen in the nociceptive sensitivity. First, mechanosensitive channel activity may be increased by altering the environment they reside in. Another possibility is that the increased sensitivity to the noxious AITC is due to increased apical displacement into the junction, where the neuron is more readily in contact with the chemicals invading the body wall.

Epidermal changes regulate morphology of neurons in a class-specific fashion

We find a number of interesting First, *miR-14* is regulating gene expression within the epidermis, and appears completely dispensable in the neuron. This loss results in a novel dendrite phenotype. In *Drosophila*, ensheathment by epidermal cells tends to form on primary dendrites, whereas *miR-14* mutants show a large increase in detachment from the ECM in terminal dendrites. The primary dendrites are established before we see the onset of junctional insertion in *miR-14* mutants. Therefore, they are not dynamic during the developmental phase that is effected by mutant so cannot become junctionally inserted. This junctional insertion into cell junctions is specific to the C4da nociceptor. While the mechanism for this specificity is unclear, we have previously showed that C4da neurons become ensheathed on the basal surface of the epidermis at a dramatically higher rate than other neuron types. So it is possible that the same factor that initiates ensheathment also increases the permissivity of growth in the junctional insertion. The sensory neurons express a large complement of cell-adhesion molecules, and a balance between adhesion to the ECM and to the epidermal cells may regulate the probability of detachment from the ECM.

Alternatively, it is possible that C1da and C3da neurons are less dynamic late in development. These neurons do not completely tile the body wall as C4da neurons do, so they require less growth to accommodate the expansion in larval body size. This difference in growth programming could result in a largely patterned dendrite arbor prior to start of the mutant phenotype between 48 and 72 hours AEL (sites for this). This would produce less junctional alignment and insertion. Experiments where growth properties or class identity are altered may help elucidate if there is a class-specific

signal allowing junctional insertion. Overexpression of *knot* or *collier* in C1da neurons produces larger more elaborate arbors (Jinushi-Nakao et al., 2007). The bHLH TF *spineless* mutants fail to properly diversify dendritic arborization neurons, producing a neurons with cytoskeletal and morphological properties intermediate between classes (M. D. Kim, Lily, & Yuh, 2006). Using these to tools to alter the growth properties of other classes may help identify if the alignment is caused by differences in adhesion molecules or differences in growth timing.

Overall, these results suggest that *miR-14* controls a system that regulates neuron morphology by restricting growth into the epithelial sheet. This prevents precocious innervation, and limits the excitability of the C4da neuron in response to noxious stimuli.

Materials and Methods

Drosophila lines

Flies stocks were maintained at RT. Experimental crosses were reared at 25°C with 12 hour light-dark cycle on standard cornmeal-molasses-agar media.

Noxious Touch

Animals are rinsed, and placed in a plastic bottom dish with water to prevent dehydration. Von Frey filaments were made from monofilament line and affixed to a glass capillary handle with cyanoacrylate glue. The tip of the monofilament is pressed

into segments A3 through A6 once per animal to deliver force. The number of nocifensive rolls following stimulus were recorded.

Drug Feeding

Animals were rinsed in DI water and transferred to dishes containing standard cornmeal-molasses-agar food with drug and green food dye. Only animals with significant food uptake, scored by presence of food dye in the intestinal tract, were tested. For 25 mN force, Ruthenium Red was fed to animals 96 to 120h AEL at 50 µM for 4-6 hours. Vinblastine was fed to animals 96h AEL for 24 hours. Animals were rinsed in DI water before transferring for behavior.

Allyl isothiocyanate

Animals were removed from food and rinsed using DI water. Single larvae were briefly dried using a Kimwipe to remove water from the cuticle, and were transferred to a dish containing 3 mL of mineral oil or 25mM AITC in mineral oil. Latency to the onset of nocifensive rolling within 30 seconds was recorded. Trials were recorded using a stereoscope and camera, and the videos were scored for response rate blind to genotype.

Heat Probe

Animals were rinsed in DI water, and Transferred to a moistened 2% agar plate. A heat probe, consisting of a soldering iron, voltage transformer, and thermocouple as touched and held to the lateral side between segments A3 and A6. Latency from stimulus onset was recorded, up to 10 seconds. Temperature was listed temperature ±1°C.

Locomotion

Animals were placed on a 2% agar surface on frustrated total internal reflection (FIM) surface, and imaged for 30 seconds. Crawling was analyzed using FIM together with the FIMTrack software package, and open source package for analyzing locomotion(Risse, Berh, Otto, Klämbt, & Jiang, 2017).

Chemotaxis

Adapted from Larkin et al 2010(Larkin et al., 2010). Animals were washed and transferred to a 9 cm petri dish with about 10 mL of 2% Agar. Each Dish contains 2 plastic caps with filter paper containing 25 uL of H_20 or 10^{-4} dilution of Ethyl Acetate in H_20. Animals were allowed to move freely for 3 minutes, then distribution of animals was recorded and the preference index was calculated. Preference index: (n odor half – n control half)/n total

Light Touch

As described in Kernan et al., 1994(Kernan et al., 1994). Animals were washed and placed on 2% agar. Free crawling animals were touched 4 times on the head segments using an eyelash affixed to a handle with cyanoacrylate glue. Behavior scores are recorded for each trial and summed, giving the Kernan score (from 0-16).

Live Imaging

Larvae were imaged using a Leica SP5 microscope. Images were captured with a 20x .7 NA immersion or 40 x 1.2 NA oil lens. Animals were mounted under Number 1

coverslip in 90% glycerol. Time-lapse animals were recovered in plates containing on standard cornmeal-molasses-agar media.

Immunostaining

Larvae were pinned to Sylguard plates using minuten pins, and dissected up the dorsal or ventral midline. They are then pinned flat, and the viscera, nerve cord, and imaginal discs are removed. They were fixed in 4% PFA for 15-30 minutes, washed 3 x 5 minutes in 0.3% Tx-100 in PBS, and blocked for 1 hour in 5% normal goat serum in PBS-Tx. Antibodies in blocking buffer are incubated at 4°C overnight for primary antibodies and 4 hours at room temperature for secondary.

Morphometric analysis

Scholl analysis of dendrites was carried out using Neurolucida. All other analysis was performed using Fiji with Simple Neurite Tracer.

Acknowledgements:

Fly stocks obtained from the Bloomington Drosophila Stock Center (NIHP40OD018537). Antibodies obtained from the Developmental Studies Hybridoma bank, created by the NICHD of the NIH and maintained at The University of Iowa, were used in this study. We thank Peter Soba for guidance and support in behavior assays.

Bibliography

Ainsley, J. A., Pettus, J. M., Bosenko, D., Gerstein, C. E., Zinkevich, N., Anderson, M. G., … Johnson, W. A. (2003). Enhanced Locomotion Caused by Loss of the Drosophila DEG/ENaC Protein Pickpocket1. *Current Biology*, *13*(17), 1557–1563. https://doi.org/10.1016/S0960-9822(03)00596-7

Babcock, D. T., Landry, C., & Galko, M. J. (2009). Cytokine Signaling Mediates UV-Induced Nociceptive Sensitization in Drosophila Larvae. *Current Biology*, *19*(10), 799–806. https://doi.org/10.1016/j.cub.2009.03.062

Babcock, D. T., Shi, S., Jo, J., Shaw, M., Gutstein, H. B., & Galko, M. J. (2011). Hedgehog Signaling Regulates Nociceptive Sensitization. *Current Biology*, *21*(18), 1525–1533. https://doi.org/10.1016/j.cub.2011.08.020

Baumbauer, K. M., DeBerry, J. J., Adelman, P. C., Miller, R. H., Hachisuka, J., Lee, K. H., … Albers, K. M. (2015). Keratinocytes can modulate and directly initiate nociceptive responses. *ELife*, *4*. https://doi.org/10.7554/eLife.09674

Bejarano, F., Bortolamiol-Becet, D., Dai, Q., Sun, K., Saj, A., Chou, Y.-T., … Lai, E. C. (2012). A genome-wide transgenic resource for conditional expression of Drosophila microRNAs. *Development (Cambridge, England)*, *139*(15), 2821–2831. https://doi.org/10.1242/dev.079939

Bernstein, E., Caudy, A. A., Hammond, S. M., & Hannon, G. J. (2001). Role for a bidentate ribonuclease in the initiation step of RNA interference. *Nature*, *409*(6818), 363–366. https://doi.org/10.1038/35053110

Bishop, T., Hewson, D. W., Yip, P. K., Fahey, M. S., Dawbarn, D., Young, A. R., & McMahon, S. B. (2007). Characterisation of ultraviolet-B-induced inflammation as a model of hyperalgesia in the rat. *Pain*, *131*(1), 70–82. https://doi.org/10.1016/j.pain.2006.12.014

Boiko, N., Medrano, G., Montano, E., Jiang, N., Williams, C. R., Madungwe, N. B., … Eaton, B. A. (2017). TrpA1 activation in peripheral sensory neurons underlies the ionic basis of pain hypersensitivity in response to vinca alkaloids. *PLOS ONE*,

12(10), e0186888. https://doi.org/10.1371/journal.pone.0186888

Boyette-Davis, J. A., Walters, E. T., & Dougherty, P. M. (2015). Mechanisms involved in the development of chemotherapy-induced neuropathy. *Pain Management*, *5*(4), 285–296. https://doi.org/10.2217/pmt.15.19

Chen, Y.-W., Song, S., Weng, R., Verma, P., Kugler, J.-M., Buescher, M., … Cohen, S. M. (2014). Systematic Study of Drosophila MicroRNA Functions Using a Collection of Targeted Knockout Mutations. *Developmental Cell*, *31*(6), 784–800. https://doi.org/10.1016/J.DEVCEL.2014.11.029

Cheng, L. E., Song, W., Looger, L. L., Jan, L. Y., & Jan, Y. N. (2010). The Role of the TRP Channel NompC in Drosophila Larval and Adult Locomotion. *Neuron*, *67*(3), 373–380. https://doi.org/10.1016/J.NEURON.2010.07.004

Fleming, M. S., & Luo, W. (2013). The anatomy, function, and development of mammalian Aβ low-threshold mechanoreceptors. *Frontiers in Biology*, *8*(4). https://doi.org/10.1007/s11515-013-1271-1

Fox, A. N., & Zinn, K. (2005). The Heparan Sulfate Proteoglycan Syndecan Is an In Vivo Ligand for the Drosophila LAR Receptor Tyrosine Phosphatase. *Current Biology*, *15*(19), 1701–1711. https://doi.org/10.1016/j.cub.2005.08.035

Fulga, T. A., McNeill, E. M., Binari, R., Yelick, J., Blanche, A., Booker, M., … Van Vactor, D. (2015). A transgenic resource for conditional competitive inhibition of conserved Drosophila microRNAs. *Nature Communications*, *6*(1), 7279. https://doi.org/10.1038/ncomms8279

Goodman, M. (2006). Mechanosensation. *WormBook*. https://doi.org/10.1895/wormbook.1.62.1

Gorczyca, D. A., Younger, S., Meltzer, S., Kim, S. E., Cheng, L., Song, W., … Jan, Y. N. (2014). Identification of Ppk26, a DEG/ENaC Channel Functioning with Ppk1 in a Mutually Dependent Manner to Guide Locomotion Behavior in Drosophila. *Cell Reports*, *9*(4), 1446–1458. https://doi.org/10.1016/J.CELREP.2014.10.034

Halata, Z., Grim, M., & Baumann, K. I. (2010). Current understanding of Merkel cells,

touch reception and the skin. *Expert Review of Dermatology*, *5*(1), 109–116. https://doi.org/10.1586/edm.09.70

Han, C., Wang, D., Soba, P., Zhu, S., Lin, X., Jan, L. Y., & Jan, Y.-N. (2012). Integrins Regulate Repulsion-Mediated Dendritic Patterning of Drosophila Sensory Neurons by Restricting Dendrites in a 2D Space. *Neuron*, *73*(1), 64–78. https://doi.org/10.1016/J.NEURON.2011.10.036

Hoon, M., Okawa, H., Della Santina, L., & Wong, R. O. L. (2014). Functional architecture of the retina: Development and disease. *Progress in Retinal and Eye Research*, *42*, 44–84. https://doi.org/10.1016/j.preteyeres.2014.06.003

Im, S. H., & Galko, M. J. (2012). Pokes, sunburn, and hot sauce: *Drosophila* as an emerging model for the biology of nociception. *Developmental Dynamics*, *241*(1), 16–26. https://doi.org/10.1002/dvdy.22737

Im, S. H., Takle, K., Jo, J., Babcock, D. T., Ma, Z., Xiang, Y., & Galko, M. J. (2015). Tachykinin acts upstream of autocrine Hedgehog signaling during nociceptive sensitization in Drosophila. *ELife*, *4*. https://doi.org/10.7554/eLife.10735

Jiang, N., Rasmussen, J. P., Clanton, J. A., Rosenberg, M. F., Luedke, K. P., Cronan, M. R., … Parrish, J. Z. (2019). A conserved morphogenetic mechanism for epidermal ensheathment of nociceptive sensory neurites. *ELife*, *8*. https://doi.org/10.7554/eLife.42455

Jiang, N., Soba, P., Parker, E., Kim, C. C., & Parrish, J. Z. (2014). The microRNA bantam regulates a developmental transition in epithelial cells that restricts sensory dendrite growth. *Development (Cambridge, England)*, *141*(13), 2657–2668. https://doi.org/10.1242/dev.107573

Jinushi-Nakao, S., Arvind, R., Amikura, R., Kinameri, E., Liu, A. W., & Moore, A. W. (2007). Knot/Collier and Cut Control Different Aspects of Dendrite Cytoskeleton and Synergize to Define Final Arbor Shape. *Neuron*, *56*(6), 963–978. https://doi.org/10.1016/j.neuron.2007.10.031

Kernan, M., Cowan, D., & Zuker, C. (1994). Genetic dissection of mechanosensory

transduction: mechanoreception-defective mutations of Drosophila. *Neuron*, *12*(6), 1195–1206. Retrieved from http://www.ncbi.nlm.nih.gov/pubmed/8011334

Kim, M. D., Lily, Y. J., & Yuh, N. J. (2006). The bHLH-PAS protein spineless is necessary for the diversification of dendrite morphology of Drosophila dendritic arborization neurons. *Genes and Development*, *20*(20), 2806–2819. https://doi.org/10.1101/gad.1459706

Kim, S. E., Coste, B., Chadha, A., Cook, B., & Patapoutian, A. (2012). The role of Drosophila Piezo in mechanical nociception. *Nature*, *483*(7388), 209–212. https://doi.org/10.1038/nature10801

Knight, S. W., & Bass, B. L. (2001). A role for the RNase III enzyme DCR-1 in RNA interference and germ line development in Caenorhabditis elegans. *Science (New York, N.Y.)*, *293*(5538), 2269–2271. https://doi.org/10.1126/science.1062039

Komendantov, A. O., & Ascoli, G. A. (2009). Dendritic Excitability and Neuronal Morphology as Determinants of Synaptic Efficacy. *Journal of Neurophysiology*, *101*(4), 1847–1866. https://doi.org/10.1152/jn.01235.2007

Krieg, M., Dunn, A. R., & Goodman, M. B. (2015). Mechanical systems biology of *C. elegans* touch sensation. *BioEssays*, *37*(3), 335–344. https://doi.org/10.1002/bies.201400154

Larkin, A., Karak, S., Priya, R., Das, A., Ayyub, C., Ito, K., … Ramaswami, M. (2010). Central synaptic mechanisms underlie short-term olfactory habituation in Drosophila larvae. *Learning & Memory (Cold Spring Harbor, N.Y.)*, *17*(12), 645–653. https://doi.org/10.1101/lm.1839010

Larsson, M. C., Domingos, A. I., Jones, W. D., Chiappe, M. E., Amrein, H., & Vosshall, L. B. (2004). Or83b Encodes a Broadly Expressed Odorant Receptor Essential for Drosophila Olfaction. *Neuron*, *43*(5), 703–714. https://doi.org/10.1016/j.neuron.2004.08.019

Lee, J.-S., von der Hardt, S., Rusch, M. A., Stringer, S. E., Stickney, H. L., Talbot, W. S., … Roehl, H. (2004). Axon Sorting in the Optic Tract Requires HSPG Synthesis

by ext2 (dackel) and extl3 (boxer). *Neuron*, *44*(6), 947–960. https://doi.org/10.1016/j.neuron.2004.11.029

Lehto, S. G., Weyer, A. D., Youngblood, B. D., Zhang, M., Yin, R., Wang, W., … Gavva, N. R. (2016). Selective antagonism of TRPA1 produces limited efficacy in models of inflammatory- and neuropathic-induced mechanical hypersensitivity in rats. *Molecular Pain*, *12*, 174480691667776. https://doi.org/10.1177/1744806916677761

Makara, J. K., & Magee, J. C. (2013). Variable dendritic integration in hippocampal CA3 pyramidal neurons. *Neuron*, *80*(6), 1438–1450. https://doi.org/10.1016/j.neuron.2013.10.033

Maksimovic, S., Nakatani, M., Baba, Y., Nelson, A. M., Marshall, K. L., Wellnitz, S. A., … Lumpkin, E. A. (2014). Epidermal Merkel cells are mechanosensory cells that tune mammalian touch receptors. *Nature*, *509*(7502), 617–621. https://doi.org/10.1038/nature13250

Mandel, S. J., Shoaf, M. L., Braco, J. T., Silver, W. L., & Johnson, E. C. (2018). Behavioral Aversion to AITC Requires Both Painless and dTRPA1 in Drosophila. *Frontiers in Neural Circuits*, *12*. https://doi.org/10.3389/fncir.2018.00045

Moehring, F., Cowie, A. M., Menzel, A. D., Weyer, A. D., Grzybowski, M., Arzua, T., … Stucky, C. L. (2018). Keratinocytes mediate innocuous and noxious touch via ATP-P2X4 signaling. *ELife*, *7*. https://doi.org/10.7554/eLife.31684

Moore, C., Cevikbas, F., Pasolli, H. A., Chen, Y., Kong, W., Kempkes, C., … Liedtke, W. B. (2013). UVB radiation generates sunburn pain and affects skin by activating epidermal TRPV4 ion channels and triggering endothelin-1 signaling. *Proceedings of the National Academy of Sciences of the United States of America*, *110*(34), E3225-34. https://doi.org/10.1073/pnas.1312933110

Morin, X., Daneman, R., Zavortink, M., & Chia, W. (2001). A protein trap strategy to detect GFP-tagged proteins expressed from their endogenous loci in Drosophila. *Proceedings of the National Academy of Sciences of the United States of America*, *98*(26), 15050–15055. https://doi.org/10.1073/pnas.261408198

Neely, G. G., Keene, A. C., Duchek, P., Chang, E. C., Wang, Q.-P., Aksoy, Y. A., … Penninger, J. M. (2011). TrpA1 Regulates Thermal Nociception in Drosophila. *PLoS ONE*, *6*(8), e24343. https://doi.org/10.1371/journal.pone.0024343

O'Brien, G. S., Rieger, S., Wang, F., Smolen, G. A., Gonzalez, R. E., Buchanan, J., & Sagasti, A. (2012). Coordinate development of skin cells and cutaneous sensory axons in zebrafish. *The Journal of Comparative Neurology*, *520*(4), 816–831. https://doi.org/10.1002/cne.22791

Risse, B., Berh, D., Otto, N., Klämbt, C., & Jiang, X. (2017). FIMTrack: An open source tracking and locomotion analysis software for small animals. *PLoS Computational Biology*, *13*(5). https://doi.org/10.1371/journal.pcbi.1005530

Salzberg, Y., Díaz-Balzac, C. A., Ramirez-Suarez, N. J., Attreed, M., Tecle, E., Desbois, M., … Bülow, H. E. (2013). Skin-Derived Cues Control Arborization of Sensory Dendrites in Caenorhabditis elegans. *Cell*, *155*(2), 308–320. https://doi.org/10.1016/j.cell.2013.08.058

Sokabe, T., Tsujiuchi, S., Kadowaki, T., & Tominaga, M. (2008). Drosophila painless is a Ca2+-requiring channel activated by noxious heat. *The Journal of Neuroscience : The Official Journal of the Society for Neuroscience*, *28*(40), 9929–9938. https://doi.org/10.1523/JNEUROSCI.2757-08.2008

Song, W., Onishi, M., Jan, L. Y., & Jan, Y. N. (2007). Peripheral multidendritic sensory neurons are necessary for rhythmic locomotion behavior in Drosophila larvae. *Proceedings of the National Academy of Sciences of the United States of America*, *104*(12), 5199–5204. https://doi.org/10.1073/pnas.0700895104

Takahashi, H., & Magee, J. C. (2009). Pathway Interactions and Synaptic Plasticity in the Dendritic Tuft Regions of CA1 Pyramidal Neurons. *Neuron*, *62*(1), 102–111. https://doi.org/10.1016/j.neuron.2009.03.007

Taniguchi, M., Yuasa, S., Fujisawa, H., Naruse, I., Saga, S., Mishina, M., & Yagi, T. (1997). Disruption of Semaphorin III/D Gene Causes Severe Abnormality in Peripheral Nerve Projection. *Neuron*, *19*(3), 519–530. https://doi.org/10.1016/S0896-6273(00)80368-2

Tapia, R., & Velasco, I. (1997). Ruthenium red as a tool to study calcium channels, neuronal death and the function of neural pathways. *Neurochemistry International*. Elsevier Ltd. https://doi.org/10.1016/S0197-0186(96)00056-3

Terada, S.-I., Matsubara, D., Onodera, K., Matsuzaki, M., Uemura, T., & Usui, T. (2016). Neuronal processing of noxious thermal stimuli mediated by dendritic Ca2+ influx in Drosophila somatosensory neurons. *ELife*, *5*. https://doi.org/10.7554/eLife.12959

Tracey, W. D., Wilson, R. I., Laurent, G., & Benzer, S. (2003). painless, a Drosophila Gene Essential for Nociception. *Cell*, *113*(2), 261–273. https://doi.org/10.1016/S0092-8674(03)00272-1

Varghese, J., Lim, S. F., & Cohen, S. M. (2010). Drosophila miR-14 regulates insulin production and metabolism through its target, sugarbabe. *Genes and Development*, *24*(24), 2748–2753. https://doi.org/10.1101/gad.1995910

Várnai, P., & Balla, T. (1998). Visualization of phosphoinositides that bind pleckstrin homology domains: calcium- and agonist-induced dynamic changes and relationship to myo-[3H]inositol-labeled phosphoinositide pools. *The Journal of Cell Biology*, *143*(2), 501–510. https://doi.org/10.1083/jcb.143.2.501

Wang, F., Wolfson, S. N., Gharib, A., & Sagasti, A. (2012). LAR Receptor Tyrosine Phosphatases and HSPGs Guide Peripheral Sensory Axons to the Skin. *Current Biology*, *22*(5), 373–382. https://doi.org/10.1016/j.cub.2012.01.040

Xiang, Y., Yuan, Q., Vogt, N., Looger, L. L., Jan, L. Y., & Jan, Y. N. (2010). Light-avoidance-mediating photoreceptors tile the Drosophila larval body wall. *Nature*, *468*(7326), 921–926. https://doi.org/10.1038/nature09576

Xu, P., Vernooy, S. Y., Guo, M., & Hay, B. A. (2003). The Drosophila microRNA mir-14 suppresses cell death and is required for normal fat metabolism. *Current Biology*, *13*(9), 790–795. https://doi.org/10.1016/S0960-9822(03)00250-1

Yan, Z., Zhang, W., He, Y., Gorczyca, D., Xiang, Y., Cheng, L. E., … Jan, Y. N. (2013). Drosophila NOMPC is a mechanotransduction channel subunit for gentle-touch

sensation. *Nature*, *493*(7431), 221–225. https://doi.org/10.1038/nature11685

Zajączkowska, R., Kocot-Kępska, M., Leppert, W., Wrzosek, A., Mika, J., & Wordliczek, J. (2019). Mechanisms of Chemotherapy-Induced Peripheral Neuropathy. *International Journal of Molecular Sciences*, *20*(6). https://doi.org/10.3390/ijms20061451

Zhang, W., Yan, Z., Jan, L. Y., & Jan, Y. N. (2013). Sound response mediated by the TRP channels NOMPC, NANCHUNG, and INACTIVE in chordotonal organs of Drosophila larvae. *Proceedings of the National Academy of Sciences of the United States of America*, *110*(33), 13612–13617. https://doi.org/10.1073/pnas.1312477110

Zou, W., Shen, A., Dong, X., Tugizova, M., Xiang, Y. K., & Shen, K. (2016). A multi-protein receptor-ligand complex underlies combinatorial dendrite guidance choices in C. elegans. *ELife*, *5*. https://doi.org/10.7554/eLife.18345

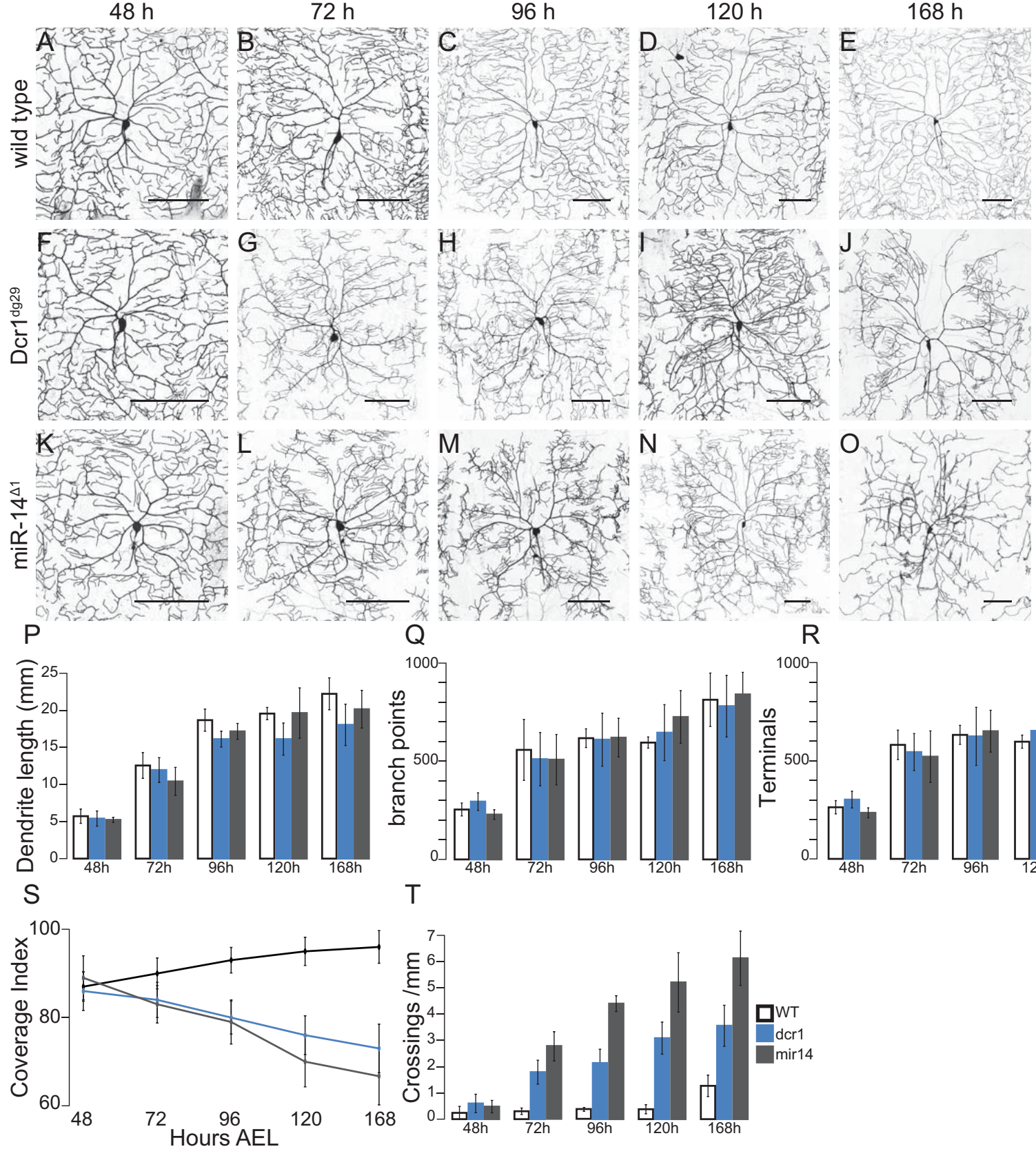
48 h
72 h
96 h
120 h
168 h
wild type
Dcr1dg29
miR-14Δ1
A
B
C
D
E
F
G
H
I
J
K
L
M
N
O
P
Dendrite length (mm)
25
20
15
10
5
0
48h
72h
96h
120h
168h
Q
branch points
1000
500
0
R
Terminals
S
Coverage Index
100
80
60
48
72
96
120
168
Hours AEL
T
Crossings /mm
7
6
5
4
3
2
1
0
WT
dcr1
mir14

Figure 1. Developmental time-course of C4da sensory neurons. (A-E) Wild-type neurons completely tile the epithelial body wall and coordinate growth with the increasing larval body wall. (F-J) Identification of *Dcr1*^{dg29} as a regulator if epithelial-dendrite interactions. Through development, homotypic branch crossing increases and the dendrite fails to maintain body wall coverage. (K-O) The microRNA *miR-14* alone can disrupt proper dendrite morphogenesis. We see similar defects as noted in *dg29*. (P-R) Dendrite length and branching structure are largely unaffected. Bars represent mean count +/- standard deviation (SD). (S) Branches are shifted proximal to the cell body, reducing the percent of body wall covered by C4da neurons. (T) miRNA mutants show increasing homotypic crossings within the C4da arbor through development. Bars represent mean dendrite crossing number per mm of branch length +/- SD.

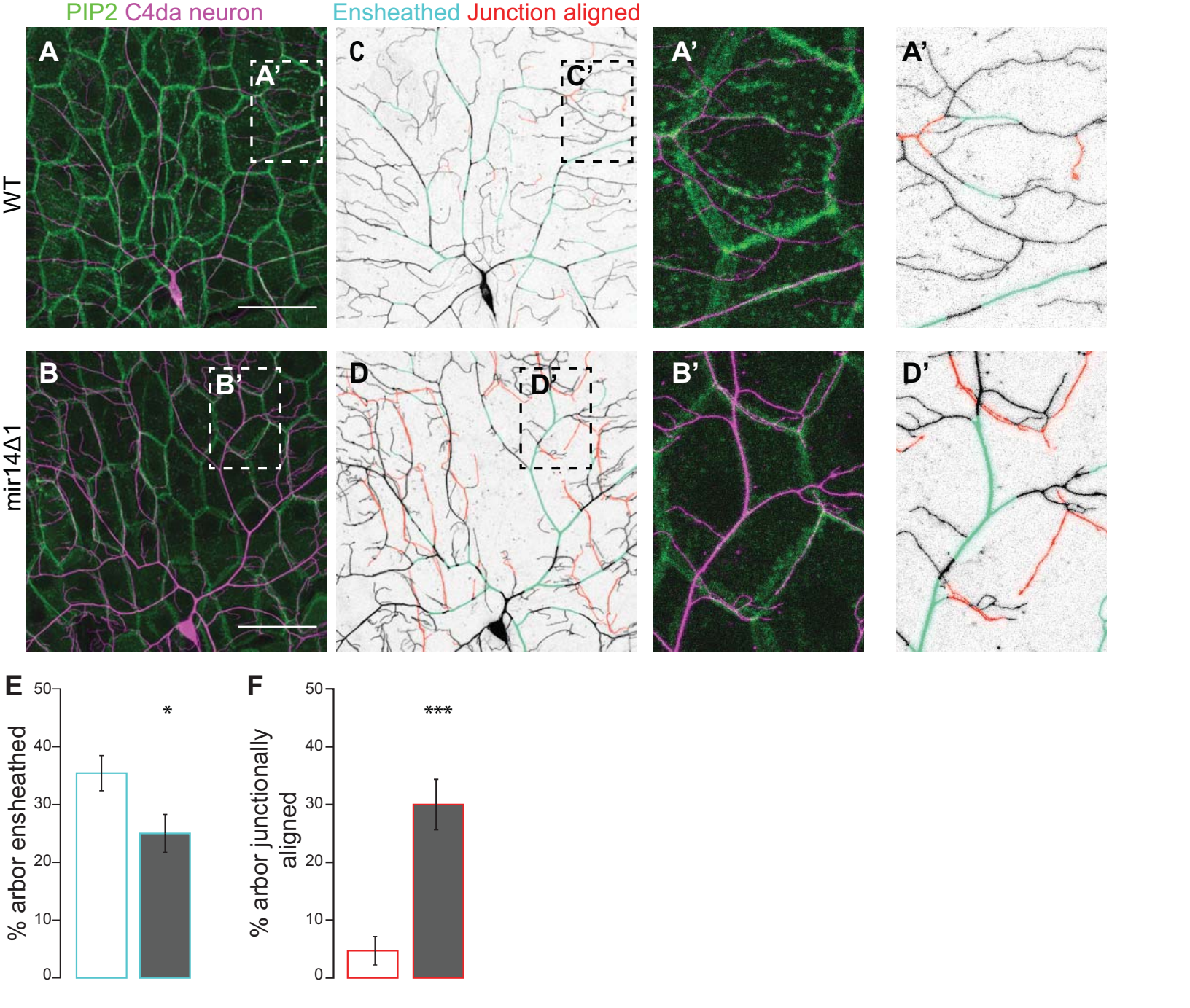

Figure 2. Ensheathment and epithelial junction alignment of dendrites by the Epithelium. (A-B) Confocal images of C4da neurons and epithelial PLC δ-PH-GFP (C-D), Pseudocolored dendrite arbor depicting areas that are ensheathed by the epithelial cell (marked by PIP2, light blue) and areas of alignment along epithelial cell junctions (red). *miR-14* mutants have increased alignment with the epithelial cell junctions. (A'-D') Zoomed region of interest depicting ensheathment and alignment. (E) bars represent the mean +/- SD of percent of total dendrite arbor length ensheathed on the basal surface (as marked by colocalization with epithelial PIP2). (F) bars represent the mean +/- SD of percent of total dendrite arbor length aligned along epithelial cell-cell junctions (as marked by PIP2). *p<0.05, ***p<0.001, Mann-Whitney U-test. n=7 neurons each.

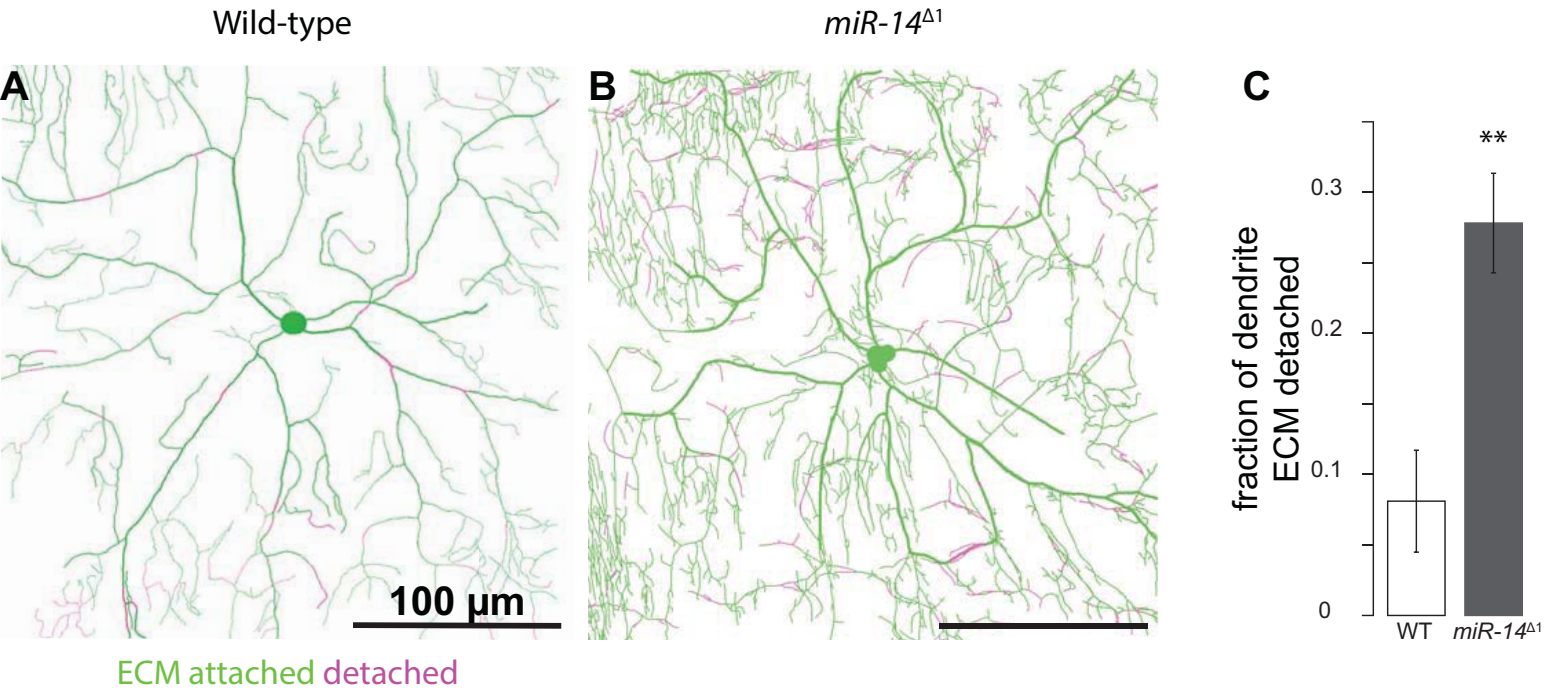

Figure 3. Neuron attachment to ECM is is dysregulated in a domain specific manner in *miR-14* mutants. In late third instar larva, Neuron colocalization with GFP-tagged *trol* was performed as previously described (Han et al., 2012; Jiang et al., 2014). (A) Wild-type animals show detachment from the basement membrane caused by developmentally related ensheathment by the epidermis. (B) Terminal dendrites detached at a much greater rate in *miR-14* mutants. (C) the terminal domain detachment increases the total fraction of the dendrite arbor detached from the ECM. Bars represent mean fraction +/- SD of detached dendrites ([detached length]/ [total length]). **P<0.005 Mann-Whitney U test.

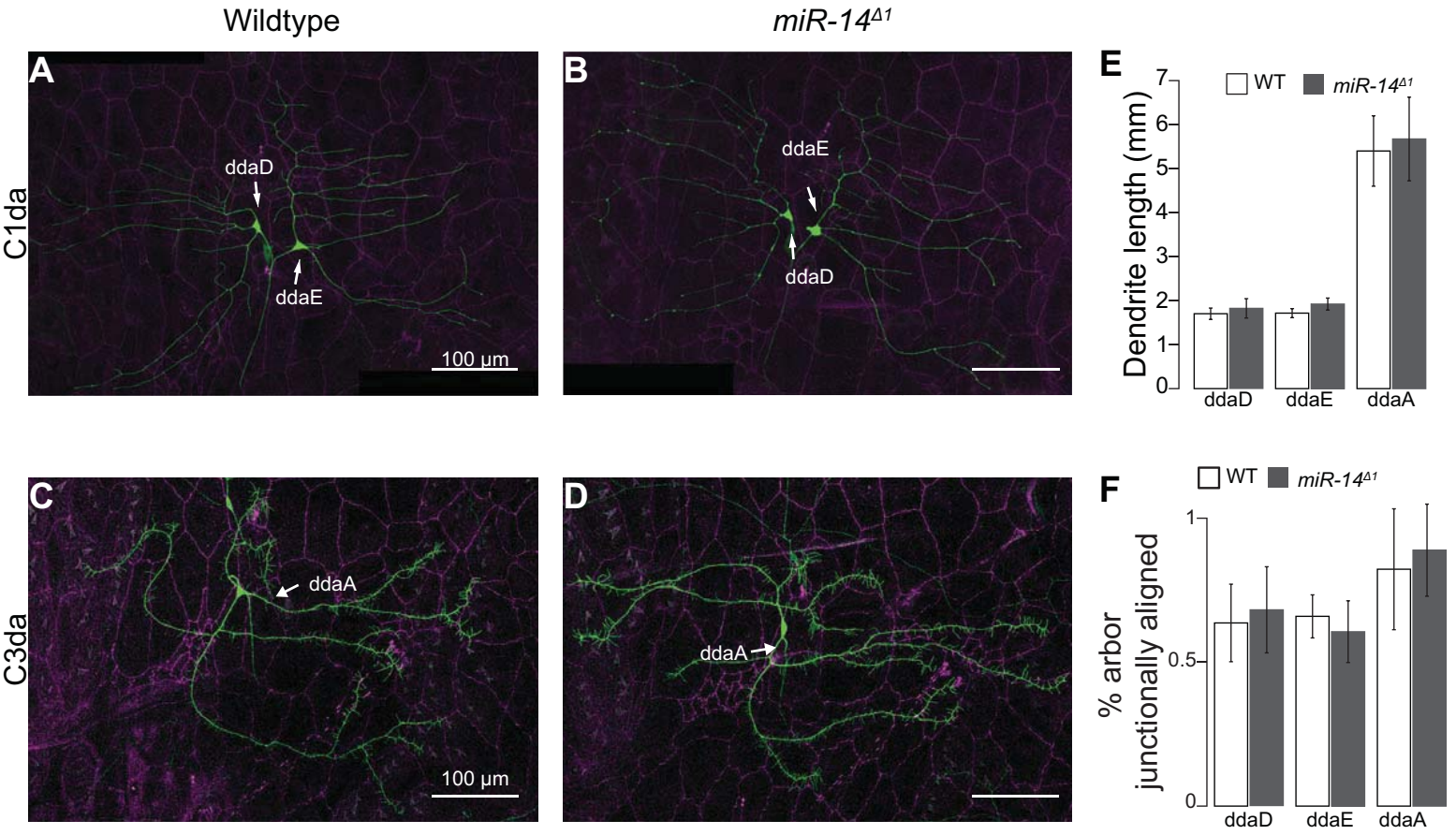

Figure 4. Other classes of peripheral sensory neurons are unaffected by *miR-14* expression. Neurons are labeled with GFP, and cell junctions are labelled with an RFP-tagged shg (Drosophila E-cadherin). (A-B) C1da proprioceptors produce small, fan shaped arbors that project along the anterior-posterior axis. (C-D) C3da neurons have a dendrite of medium complexity, bearing short spike-like protrusions. (E) Dendrite length and structure are unaffected in *miR-14* mutants. (F) A very low percentage (<1%) of the total dendrite arbor length is aligned with epithelial cell junctions, and is unchanged in *miR-14*. p>0.05 Mann-Whitney U-test, n=8 neurons for each condition.

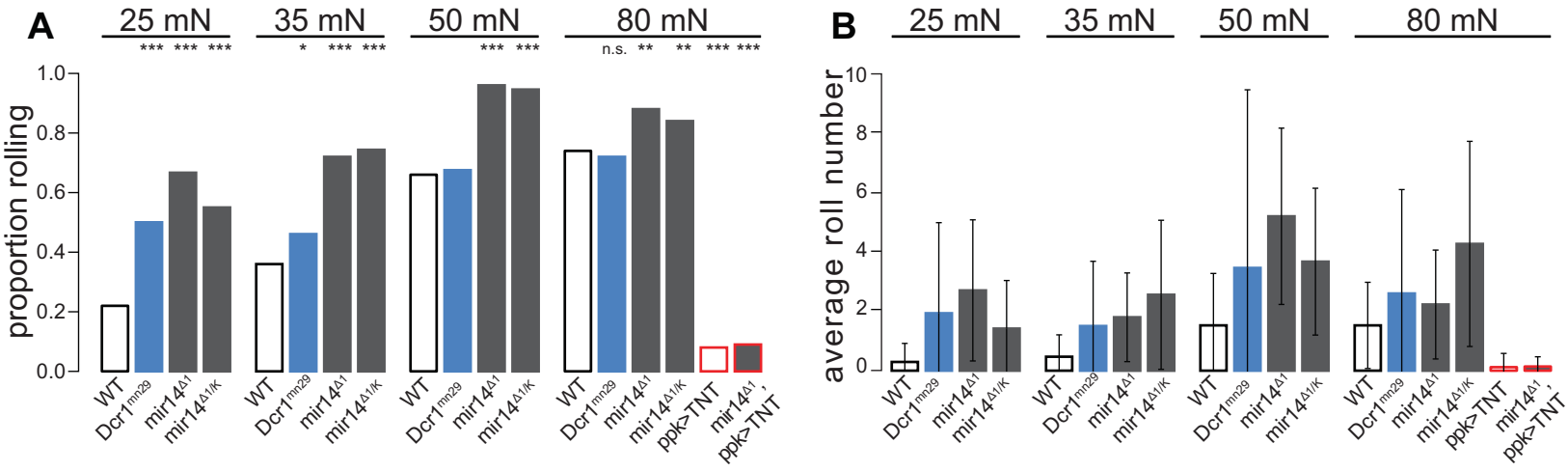

Figure 5. Noxious mechanical stimulus with Von Frey filament of known force. (A) Probability of nocifensive response following single Von Frey stimulation. *Dcr1*^{dg29} and *miR-14* mutants show increased sensitivity to noxious mechanical stimulus. Homoallelic and heteroallelic *miR-14* mutants show similar increases in sensitivity. Behavior is greatly reduced with blockage of synaptic transmission via tetanus toxin in wild-type and miR-14 mutants. (TNT) (red border). (B) Average number of nocifensive rolls in all trials is increased compared to the wild-type control at the same force. n=50 animals per condition.

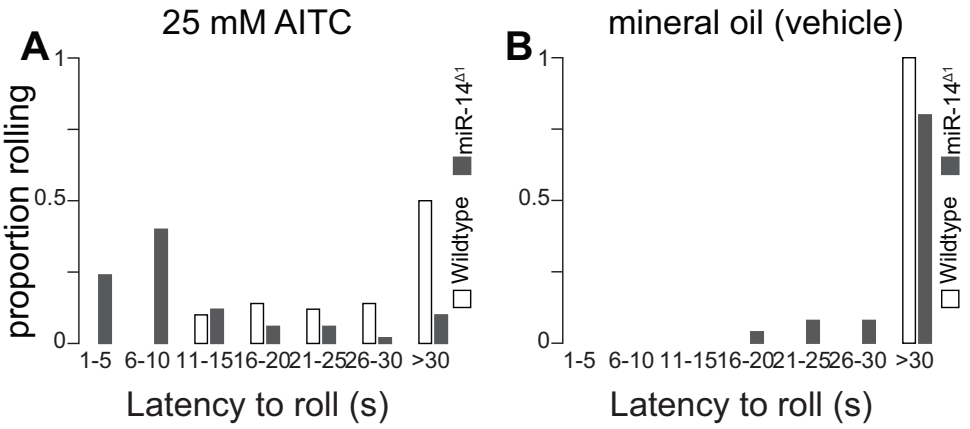

Figure 6. Nocifensive response to the noxious chemical AITC. Animals are placed in 25 mM AITC and mineral oil solution. Latency to initiation of nocifensive rolling is recorded. Animals that do not respond within 30 seconds are grouped. *miR-14* larva exhibit greatly reduced latency.(n=100 animals each) p= 1.463e-9, chi-squared test. (B) mineral oil alone induces low rates of response in *miR-14* (n=35), whereas wild-type animals are agnostic (n=30).

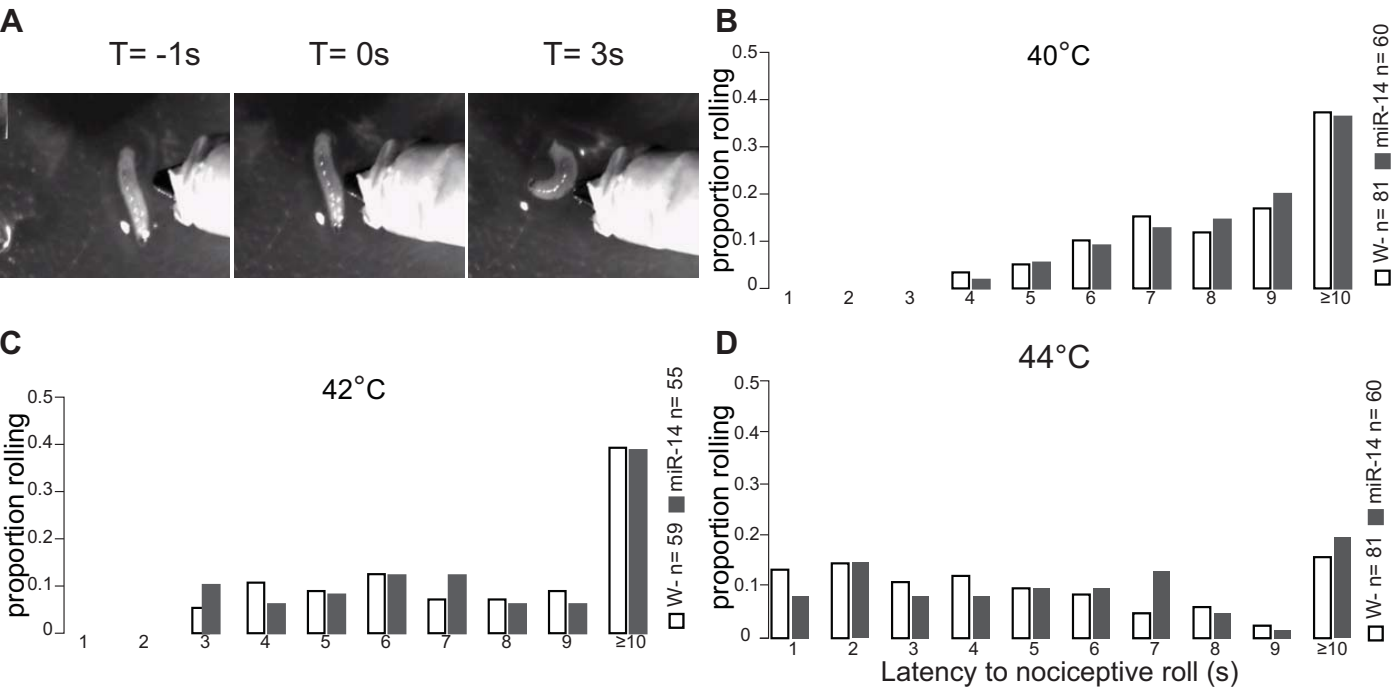

Figure 7. Nocifensive response to heated probe. (A) Representative nocifensive rolling following contact with the thermal probe to the lateral epidermis of a free crawling larva. Latency following contact until initiation of rolling, up to 10 seconds. Animals that do not respond within 10 seconds are grouped. (B) Response to low intensity aversive heat stimulus is unchanged. (C-D) Increasing intensity reduces latency to rolling response. miR-14 mutants do not respond more quickly to noxious thermal stimuli. $p>0.05$, Chi-squared test.

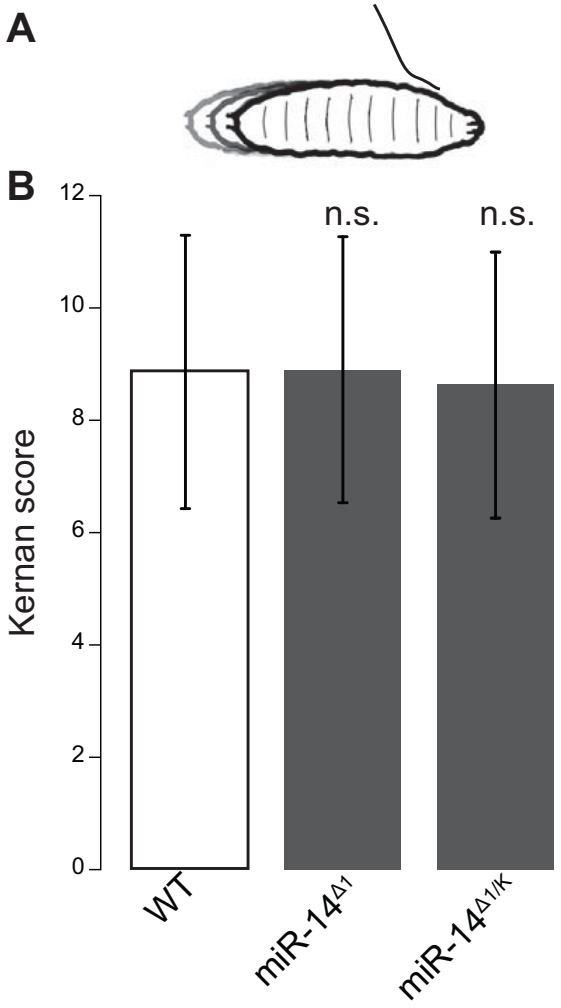

Figure 8. Response to gentle touch. Trials are carried out and scored as described in Kernan et al. 1994. (A) Animals are stimulated by brushing the head with an eyelash and recording the behavior elicited. (B) Animals are stimulated 4 times, and the response index (Kernan score) are totaled, out of a maximum of 16. Bars represent mean Kernan score and standard deviation. (n=50 animals each). Mann-Whitney U test.

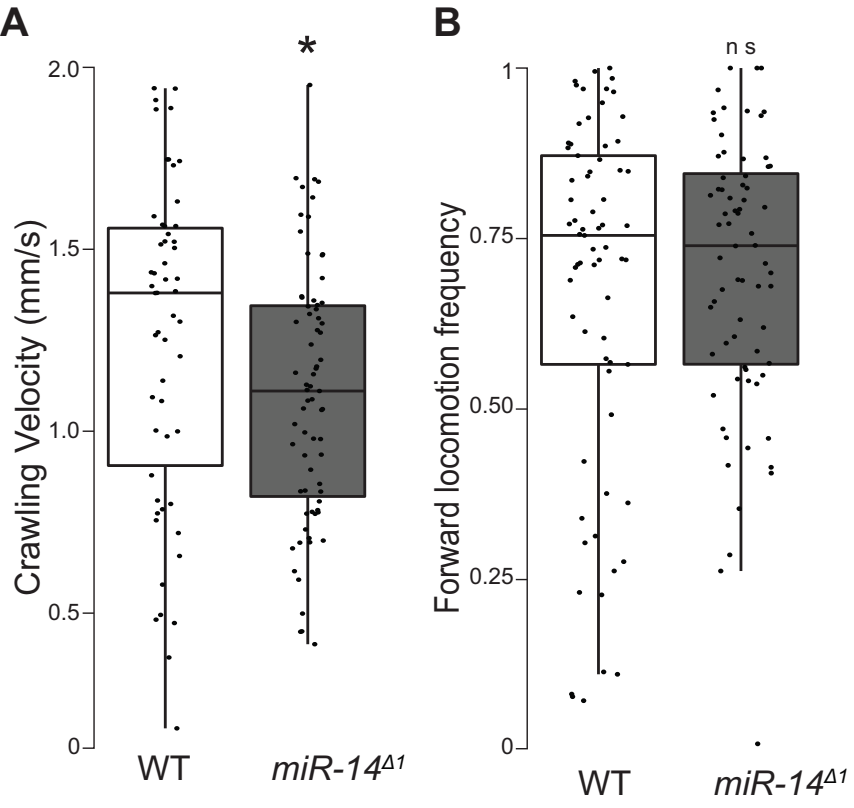

Figure 9. Free locomotion of larvae. Third instar larvae are placed on a moistened 2% agar dish and imaged under infrared light. (A) The average overall speed shows a slight deficit. Box plots depict average crawling velocity, with scatterplot of individual data. (B) The balance between head turning and forward locomotion is unaffected. Box and scatter plots depict the proportion of time forward crawling. *p<0.05, Mann-Whitney U test. WT n=68, *miR-14* n = 70 animals.

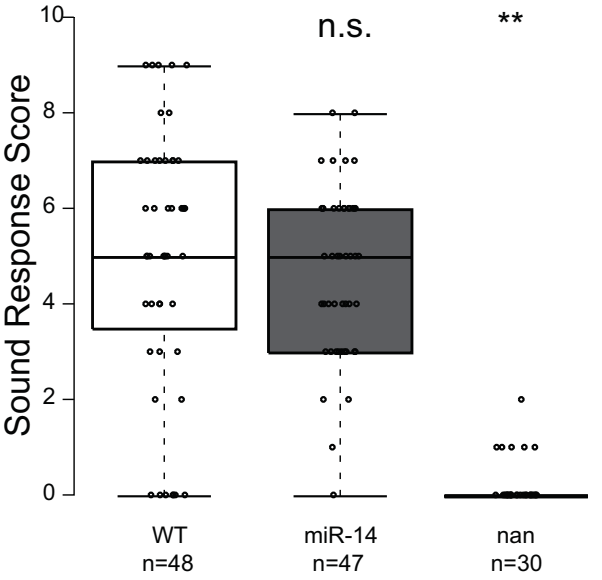

Figure 10. Larval vibration response. 500 Hz pure tones induce pausing and head sweeping in free locomoting larvae. Box and scatterplots represent the number of times out of 10 a one second pulse elicited startle response for each larva as its individual score. miR-14 mutants response is unaffected. Nanchung (nan) mutants are deficient in a key vibration sensitivite mechanoreceptor. **p<.005, Kruskal-Wallis with Bonferroni correction. Animals per condition noted above.

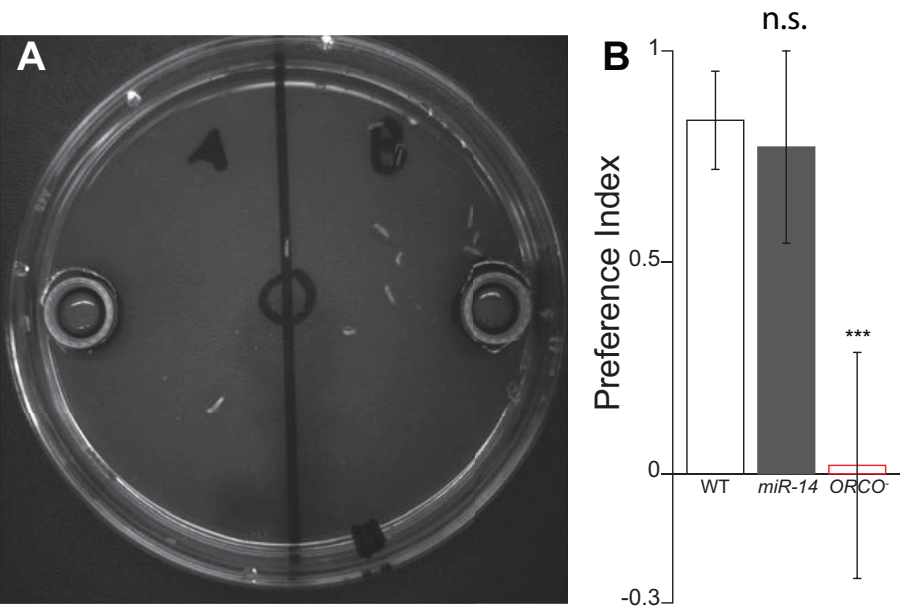

Figure 11. Olfactory chemotaxis preference assay for larvae. (A) Water or 10-4 Ethyl acetate are provided in an 2% agar plate. Animals are placed in the center circle and allowed to freely move for 5 minutes. (B) Preference for the attractive olfactory cue. Preference Index = [(larvae on odor side) – (larvae on water side)]/(total number of larvae)]. WT (W1118) (N=19), Orco- (N=20), *miR-14*$^{\Delta 1}$ (N=19). Each N represents a trial of approximately 20 animals. Bars represent mean + standard deviation. WT and *miR-14* show no difference in olfactory preference. Loss of ORCO, an obligate olfactory co receptor, blocks chemotaxis. ***P<.001 Mann-Whitney U test.

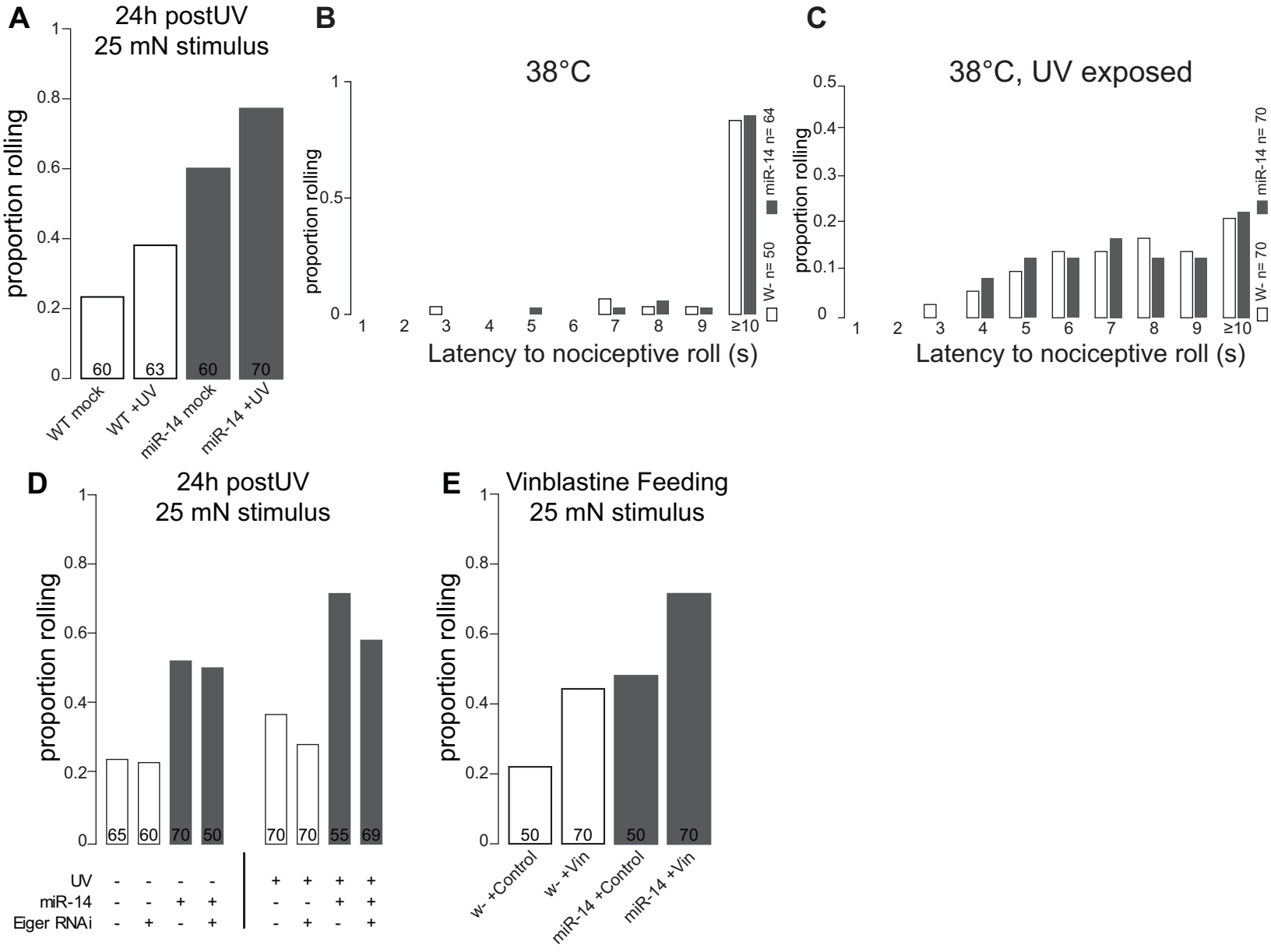

Figure 12. *miR-14* hypersensitivity is not hyperstatic to known modifiers of nociceptive sensitivity. (A) UV sensitization produces an additive effect with *miR-14*, tested 24 hours after exposure. Bars represent probability of nociceptive rolling following mechanical stimulus with of 25 mN. (B). *miR-14* does not respond to sub-threshold thermal stimuli. (C) Wild-type and *miR-14* show similar allodynia following UV exposure. p>0.05, Chi-Squared test. (D) The TNF *Eiger* is required for UV sensitization. *Eiger* knock-down in UV exposure larva reduce the UV-induced mechanosensitivity in both wild-type and *miR-14*. (E) The chemotherapeutic vinblastine activates TRPA1 channels. As above, vinblastine produces an additive hypersensitivity in *miR-14* of similar magnitude to wild-type animals. n tested shown on bars.

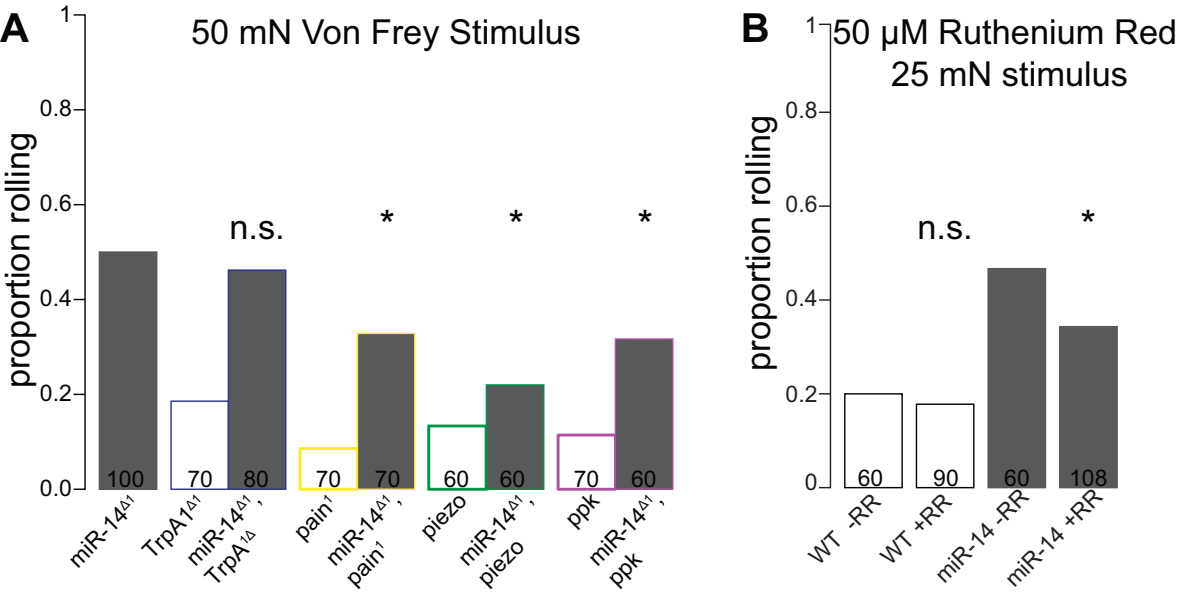

Figure 13. *miR-14* hypersensitivity is epistatic to several mechanosensitive channels, but not TrpA1. (A) Probability of nocifensive rolling following 50 mN Von Frey stimulus. n for each trial is shown on the bars. *p<.05, Kruskal-Wallis with Dunn's post-hoc test with Bonferroni correction. Only comparisons between *miR-14* alone and double mutants are shown. (B) Hypersensitivity is reduced when fed non-specific TRP-family channel blocker ruthenium red (RR), compared to the same genetic background. *p<0.05, Chi-Squared test. n tested shown on bars.

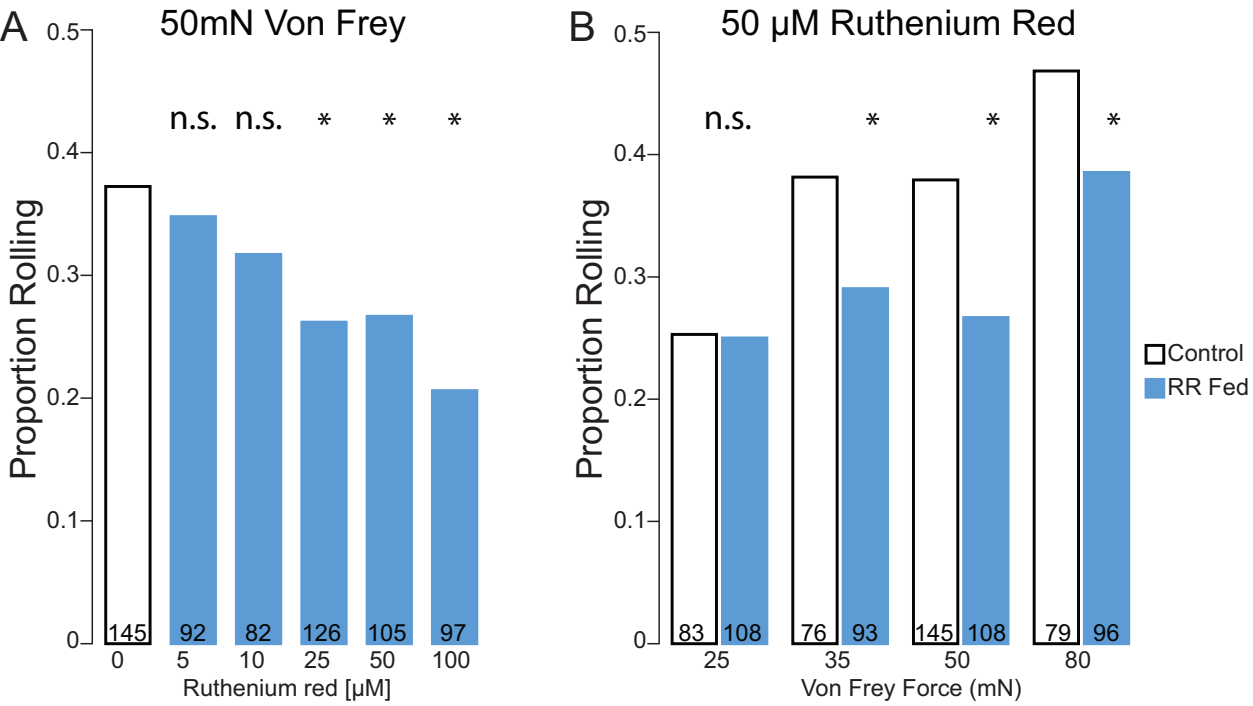

14. Effect of ruthenium red (RR) feeding on larval nocifensive response. Larvae are transferred to standard cornmeal-molasses-agar containing food coloring. RR in water are added to the final concentration noted. (A) Dose response of feeding RR at a constant force. Bars depict the proportion of *w1118* larvae that perform nocifensive rolling in response to 50 mN Von Frey stimulus. Drug Fed animals are compared to no drug control. *p<0.05, Kruskal-Wallis with Bonferroni correction. (B) Force response curve when feeding a constant dose of 50 μM RR. *p<0.05, Chi-Square test. n of animals tested for each condition noted above.

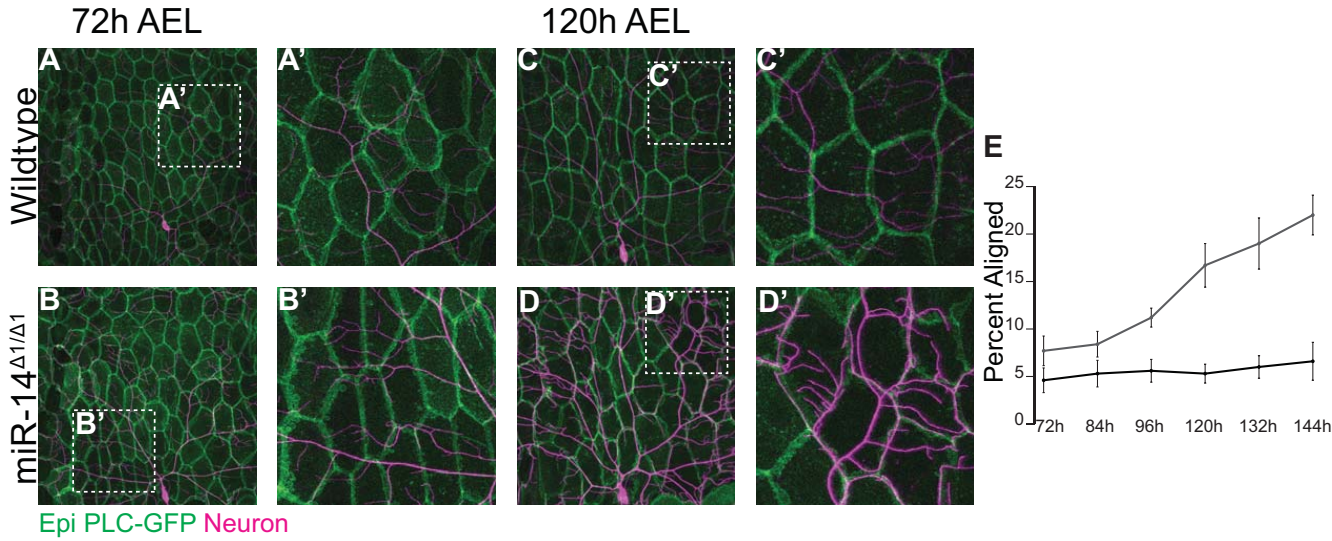
72h AEL
120h AEL
Wildtype
miR-14Δ1/Δ1
A
A'
B
B'
C
C'
D
D'
E
Percent Aligned
25
20
15
10
5
0
72h
84h
96h
120h
132h
144h
Epi PLC-GFP Neuron

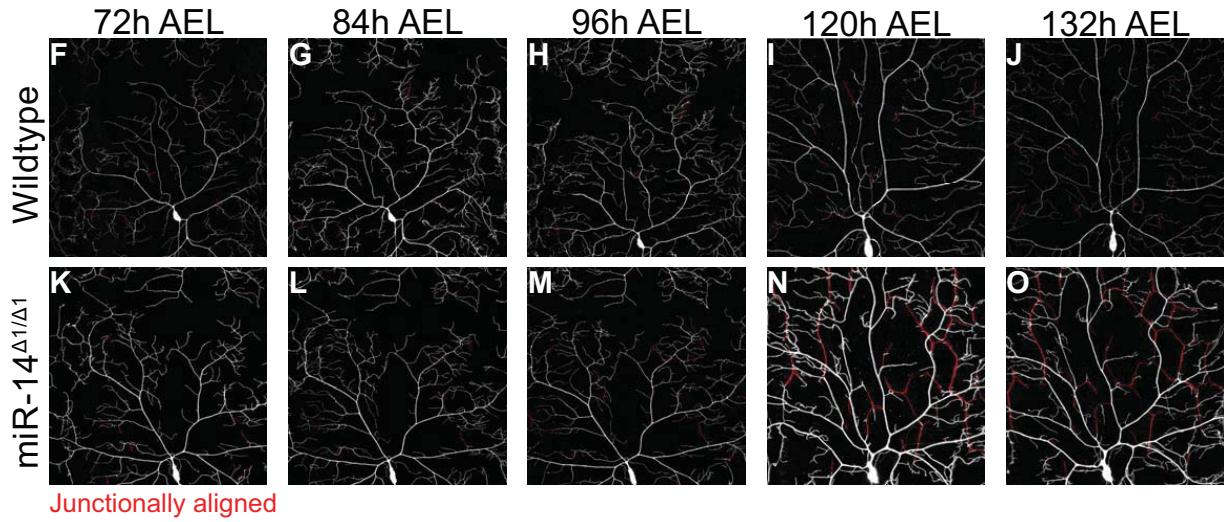
72h AEL
84h AEL
96h AEL
120h AEL
132h AEL
Wildtype
miR-14Δ1/Δ1
F
G
H
I
J
K
L
M
N
O
Junctionally aligned

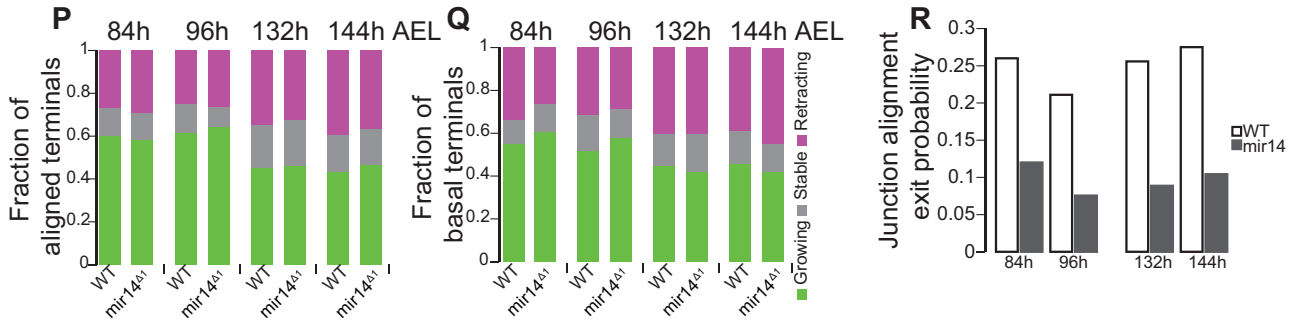
P
84h
96h
132h
144h AEL
Fraction of aligned terminals
1
0.8
0.6
0.4
0.2
0
WT
mir14Δ1
Q
Fraction of basal terminals
Growing
Stable
Retracting
R
Junction alignment exit probability
0.3
0.25
0.2
0.15
0.1
0.05
0
WT
mir14

Figure 15. Timelapse analysis of dendrite growth properties. (A-B') representative neurons at 72h AEL show low levels of alignment. (C-C') Wild-type neurons of late third instar shows low levels of alignment. (D-D') Dendrites of *miR-14* show a progressive increase in the proportion of terminal dendrites that lie along epithelial cell junctions. (E) Junctional alignment quantified across development. Lines represent mean +/- SD of percent of total dendrite arbor aligned. (F-J) A low level of stochastic alignment is present in wild-type neurons. (K-O) *miR-14* terminal branches are particularly likely to aligned. Measures of arbor dynamics suggest that the growth properties of junctionally aligned (P) and non-aligned (Q) dendrite branches do not strongly differ. (R) Probability that an aligned dendrite will exit the junction domain. When present at the epithelial junction, wild-type branches are much more likely to exit. *miR-14* neurons may become trapped within the junction.

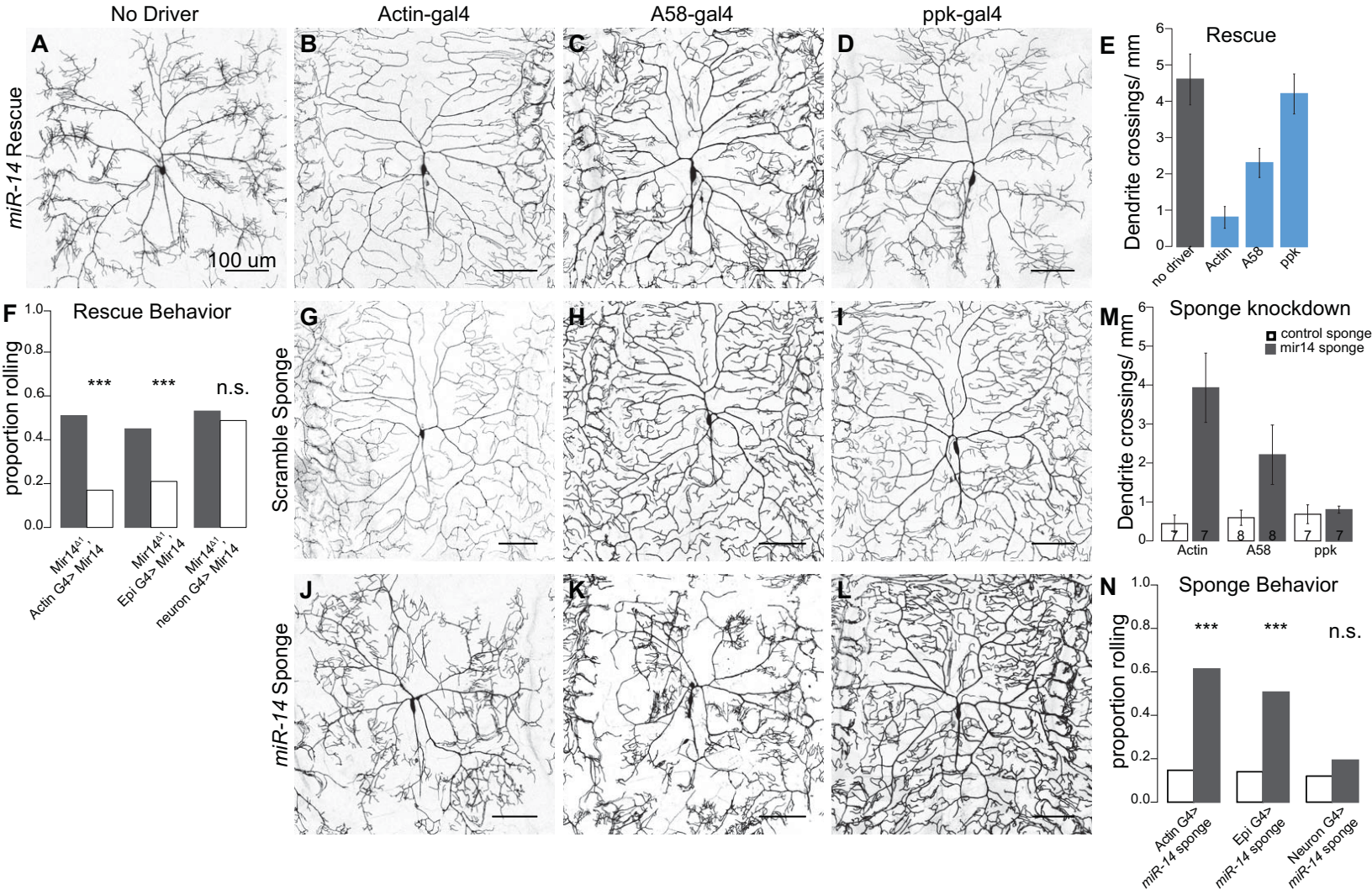
No Driver
Actin-gal4
A58-gal4
ppk-gal4
A
B
C
D
miR-14 Rescue
100 um
E
Rescue
Dendrite crossings/ mm
no driver
Actin
A58
ppk
F
Rescue Behavior
proportion rolling
***
***
n.s.
Mir14Δ1, Actin G4> Mir14
Mir14Δ1, Epi G4> Mir14
Mir14Δ1, neuron G4> Mir14
G
H
I
Scramble Sponge
M
Sponge knockdown
control sponge
mir14 sponge
Dendrite crossings/ mm
Actin
A58
ppk
J
K
L
miR-14 Sponge
N
Sponge Behavior
proportion rolling
***
***
n.s.
Actin G4> miR-14 sponge
Epi G4> miR-14 sponge
Neuron G4> miR-14 sponge

Figure 16. *miR-14* is necessary and sufficient in the epithelium to regulate dendrite morphogenesis. *miR-14* mutants (A) were resupplied with functional *miR-14* in a tissue specific manner. Ubiquitous (B) or epithelial (C) resupply rescues the morphology and behavioral defects, whereas C4da expression (D) does not. (E) Quantification of dendrite crossings per mm of branch length. Bars represent mean +/- SD. (F) Expression of functional *miR-14* in these tissues reduces hypersensitivity. (n=100 animals each) ***p<0.001, Students T test. Expression of a transgenic miRNA sponge carrying scrambled (G-I) or *miR-14* binding sites (J-L). Knockdown of *miR-14* shows a epithelial expression is required for morphogenesis (M). (N) Ubiquitous or epithelial expression of *miR-14* sponge causes nociceptive hypersensitivity. (n=150 animals each). No effect was seen when resupplied in nociceptive neuron alone. ***p<0.001, Students T test, compared to Gal4 control or control sponge.

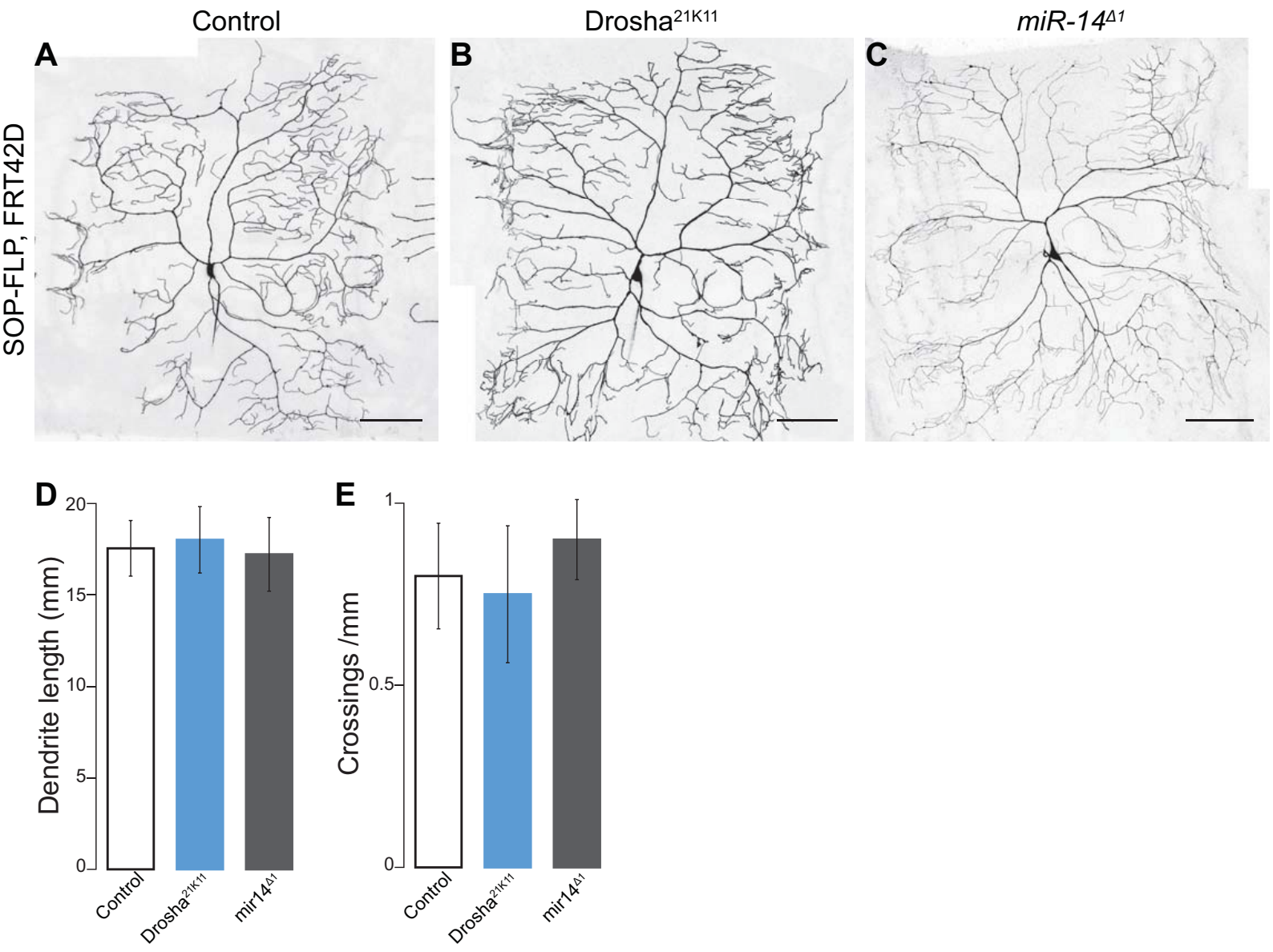

Figure 17. Homozygous single cell clones do not display defects relative to control. Recombination at an FRT site produces positively labeled, single cell clones in a heterozygous background (A). Neither the miRNA processing ribonuclease *Drosha* (B), nor *miR-14* (C), show strong defects in branch pattern (D) or dendrite crossing (E) in neuronal clones. p>0.05 Kruskal-Wallis with Bonferroni correction. n=6 neurons per genotype.

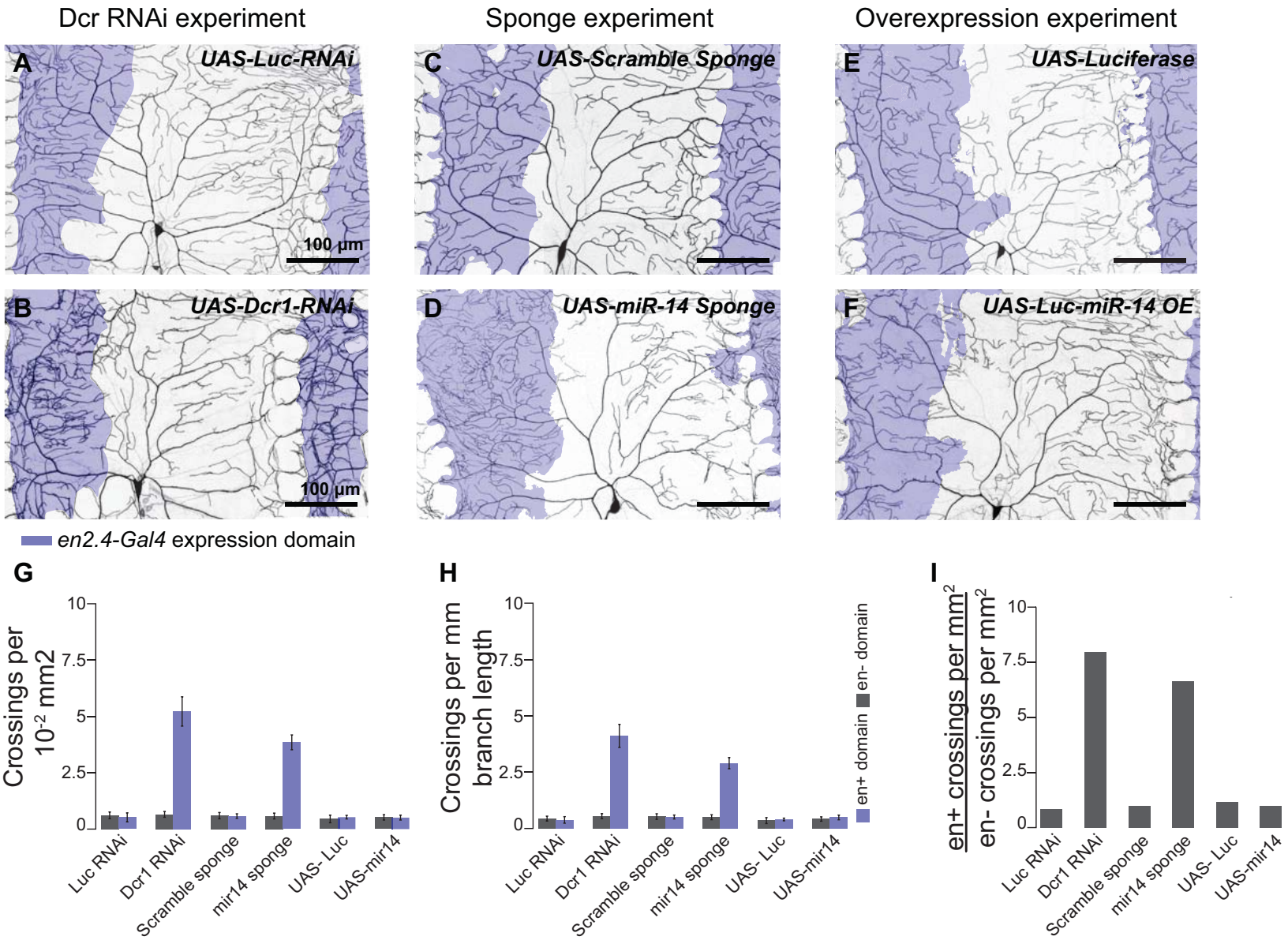

Figure 18. Mosaic expression reveals short range regulation of dendrite-eptihelial regulation. Engrailed-Gal4 is used to express transgenic tools affecting *miR-14* levels in a subdomain of the larval body wall segment. Expression of a control RNAi (A) or *Dcr1* RNAi (B). *Dcr1* knock-down in the epithelium slightly increases branch length in the contacting arbor. (C-D) Expression of *miR-14* sponges increases dendrite crossings without altering branch length. (E-F) Overexpression of *miR-14* does not significantly alter dendrite crossing. (G). Dendrite crossing rates relative to the area of the expression domains. (F) Dendrite crossings normalized to total dendrite branch length within the expression domain. Ratio of dendrite crossing rates within the same dendritic arbor. No difference between en+ and en- domains = 1. n=8 animals per genotype.

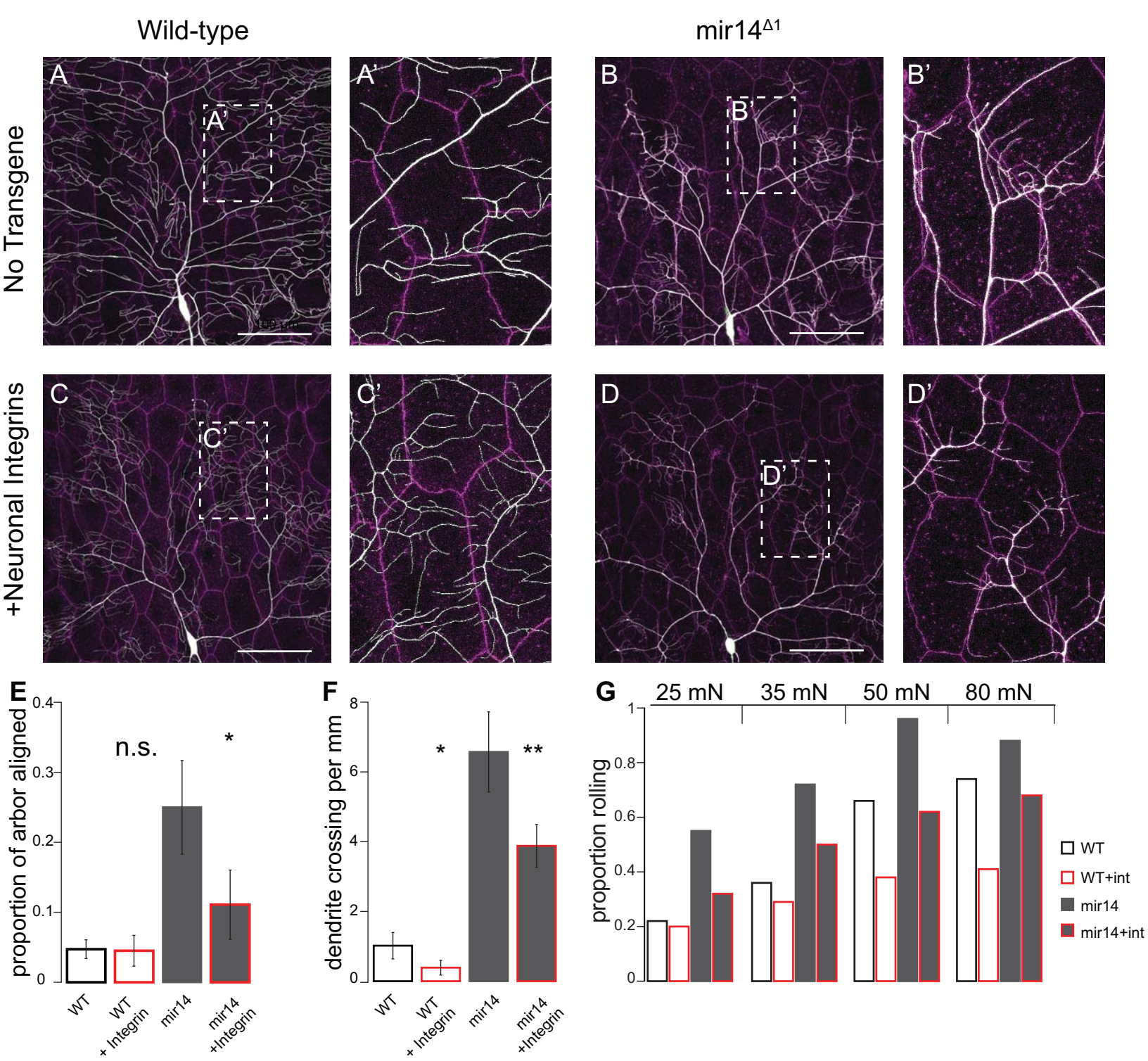

Figure 19. Neuronal integrin overexpression reduces junctional alignment. (A-B') Alignment with epithelial cell junctions marked with RFP-tagged *shg*. (C-C') Integrin overexpression in neurons increases adhesion to the BM. There is little effect on junctional alignment. (D-D') Integrin overexpression is partially epistatic to *miR-14*. It reduces the rate of junction alignment (E). Bars represent mean proportion of arbor aligned +/- SD. (F) Integrin overexpression reduces dendrite crossings in both wild-type and *miR-14*. Bar represents mean +/- SD. Comparison between integrin overexpression and the same genetic background. *p<0.05, **p<0.05, Mann-Whitney U test. (G) Mechanonociceptive sensitivity is reduced by integrin overexpression. Nociceptive response rates were recorded following Von Frey stimulus as noted.

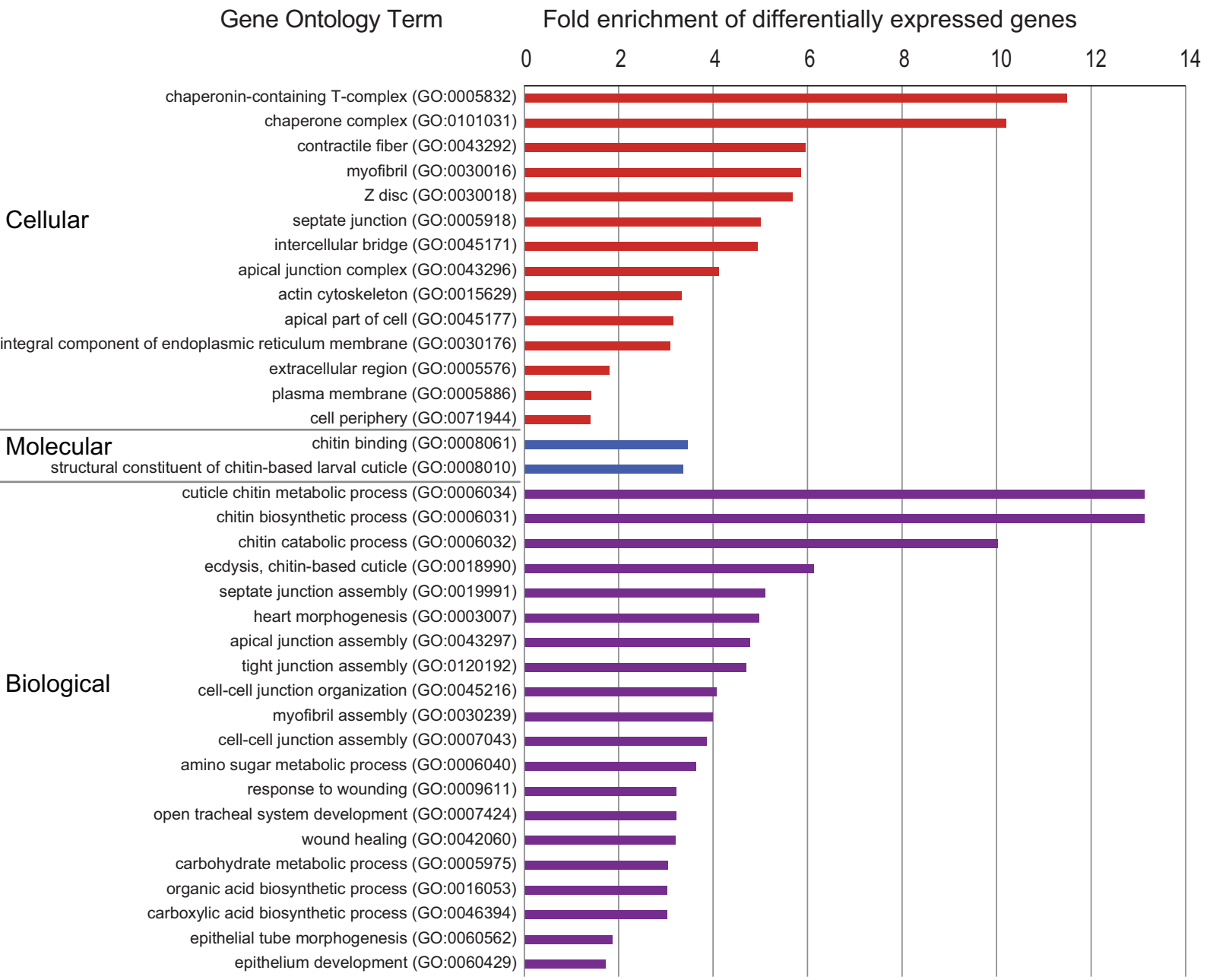

Figure 20. Gene Ontology (GO) enrichment analysis for differentially expressed genes in *miR-14* mutant epithelia. GO terms are grouped based on their classification by cellular, molecular, or biological function. Bars Represent the fold enrichment over the *Drosophila* complete genome for gene ontology terms, Determined by Fischer's Exact test, with a false discovery rate <.05. 801 genes were significantly differentially expressed (2 fold cutoff) in epithlielial samples compared to wildtype. Identified are pathways relating to regulate sugar metabolism and epithelial sheet structure and development.

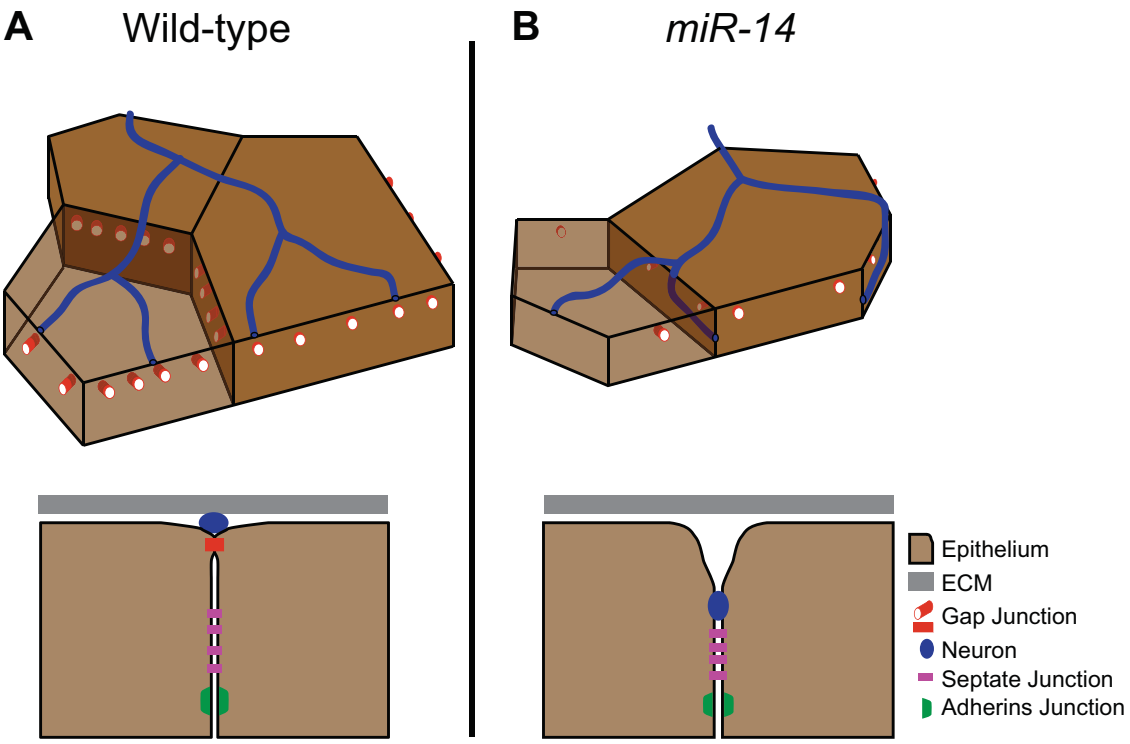

Figure 21. Model of dendrite junctional insertion. (A) Wild-type neurons are prevented from entering the junction by strong adhesion between adjacent cells. (B) *miR-14* dendrite terminals can enter the junction and become apically displaced. We hypothesize reduced gap junction expression allows entrance into the junctional domain.

Appendix The SLC36 transporter Pathetic is required for extreme dendrite growth in *Drosophila* sensory neurons

Lin, W. Y., Williams, C., Yan, C., Koledachkina, T., **Luedke, K**., Dalton, J., … Parrish, J. Z. (2015). The SLC36 transporter pathetic is required for extreme dendrite growth in Drosophila sensory neurons. *Genes and Development*, *29*(11), 1120–1135. https://doi.org/10.1101/gad.259119.115

Abstract

Dendrites exhibit enormous diversity in form and can differ in size by several orders of magnitude even in a single animal. However, whether neurons with large dendrite arbors have specialized mechanisms to support their growth demands is unknown. To address this question, we conducted a genetic screen for mutations that differentially affected growth in neurons with different sized dendrite arbors. From this screen, we identified a mutant that selectively affects dendrite growth in neurons with large dendrite arbors without affecting dendrite growth in neurons with small dendrite arbors or the animal overall. This mutant disrupts a putative amino acid transporter, Pathetic (Path), that localizes to the cell surface and endolysosomal compartments in neurons. Although Path is broadly expressed in neurons and non-neuronal cells, mutation of path impinges on nutrient responses and protein homeostasis specifically in neurons with large dendrite arbors, but not in other cells. Altogether, our results demonstrate that specialized molecular mechanisms exist to support growth demands

in neurons with large dendrite arbors and define Path as a founding member of this growth program.

Results

path regulates protein homeostasis to support dendrite growth

To identify molecular mechanisms of *path*-dependent growth in C4da neurons, we conducted microarray expression profiling of C4da neurons from wild type and *path* mutant larvae (Figure 1A). We identified >2000 transcripts that were significantly deregulated in *path* mutant C4da neurons, indicating that *path* exerts a strong influence on gene expression in these neurons (Supplemental Table S1). Pathway analysis indicated that genes associated with fatty acid metabolism and branched-chain amino acid degradation were significantly over-represented in the set of genes with decreased abundance in *path* mutant C4da neurons (Supplemental Table S2), consistent with *path* mutation eliciting a starvation response in C4da neurons and directly or indirectly regulating these pathways. Indeed, *path* mutant C4da neurons exhibited a striking increase in expression of *Drosophila* 4E-BP (Thor) (Supplemental Table S1), which is elevated in response to starvation (Teleman, Chen, & Cohen, 2005; Tettweiler, Miron, Jenkins, Sonenberg, & Lasko, 2005). Additionally, *path* mutant C4da and to a lesser degree C3da neurons exhibited mitochondrial fusion, which occurs in many cell types after nutrient depletion (Rambold, Kostelecky, Elia, & Lippincott-Schwartz, 2011), whereas C1da neurons and epithelial cells did not (Figure 1B and Supplemental Figure

S1). Thus, mutation of *path* induces an apparent starvation response in neurons with large dendrite arbors but not other cells in the body wall.

We noted that a large number of transcripts associated with translation were deregulated in C4da neurons of *path* mutants, and this was of particular interest for several reasons. First, among deregulated translation factors, translational repressors were, in general, increased in abundance in *path* mutants whereas positive regulators of translation were reduced in abundance (Figure 1C), suggestive of a coherent response to reduce translational activity in C4da neurons. Second, transcription of translational machinery is coupled to nutrient availability (Mayer & Grummt, 2006), thus reduced abundance of factors that promote translation was a further indication of a starvation response. Third, we noted that reporter expression (ppk-CD4-tdTomato) was attenuated in C4da neurons of *path* mutants despite the fact that ppk mRNA levels were apparently not affected (Figure 1D and Supplemental Table S1). Thus, we hypothesized that *path* mutation altered protein homeostasis in C4da neurons via effects on protein synthesis, stability, or both, contributing to growth defects.

To monitor effects of *path* mutation on protein homeostasis *in vivo* we used a collection of GFP protein traps that allows for visualization of proteins expressed from their endogenous loci in *Drosophila* (Morin, Daneman, Zavortink, & Chia, 2001). By comparing levels of these protein traps in wild type and *path* mutant backgrounds we aimed to gain insight into the apparent cellular specificity of growth defects in *path* mutants and to explore the generality of protein accumulation defects in *path* mutant C4da neurons. For these assays, we chose 11 protein traps that displayed a range of expression patterns encompassing the major cell types of the larval body wall (Figure

1E, 1F). Additionally, we predominantly chose gene products whose mRNA expression in C4da neurons was unaffected by *path* (Supplemental Table S1); 3 traps of gene products with increased mRNA accumulation (sm, Gao, and Imp,) and 1 trap of a gene product with reduced mRNA accumulation (CG5174) in *path* mutant C4da neurons were exceptions to this criteria.

Overall, we observed striking concordance between *path*-dependent effects on cell growth and protein trap levels. Each of the 10 protein traps normally expressed in C4da neurons exhibited significantly reduced levels at 96 h AEL in *path* mutants, suggesting that *path* broadly promotes protein accumulation in these neurons. By contrast, these protein traps were expressed at comparable levels in wt and *path* mutant C4da neurons at 36 h AEL, prior to the onset of growth defects (Supplemental Figure S2), after which time protein trap levels were progressively reduced. Therefore, expression of the protein traps closely follows the progression of growth defects in *path* mutant C4da neurons. In C3da neurons, levels of many protein traps were reduced as well, but the effect was less severe. By contrast, levels of protein traps in neurons with small dendrite arbors (C1da neurons, es neurons), peripheral glia, epidermal cells, and muscle were unaffected by *path* mutation, demonstrating remarkable specificity in cell types with *path*-dependent effects on protein accumulation.

In principle, altered protein levels of *path* mutants could be manifest at the level of either synthesis (mRNA translation) or decay (protein stability). To more directly examine the relationship between *path* function and translation in C4da neurons *in vivo*, we turned to celltype specific reporter transgene assays. Similar *in vivo* reporter approaches have been used to dissect tissue-specific functions of other translational

regulators (Schleich et al., 2014). We expressed a UAS-Luciferase reporter specifically in C4da neurons of *path* mutant larvae or WT controls and measured both protein and mRNA expression levels by Luciferase activity assays and qRT-PCR, respectively. This revealed only a modest decrease in mRNA levels in *path* mutants (Figure 1G). In contrast, Luciferase activity decreased to background levels in *path* mutants. These data are consistent with a strong decrease in translational output per mRNA in *path* mutant C4da neurons.

To further assess the cellular specificity of the response to *path* mutation, we monitored effects of *path* mutation on growth of other larval cell types. However, larval cell types other than C4da/C3da neurons exhibited little or no dependence on *path* for growth (Figure 1H). Finally, we used microarray analysis to survey gene expression responses to loss of *path* that were manifest across the larval body wall and observed minimal overlap with *path*-responsive changes in gene expression of C4da neurons (Figure 1I, Supplemental Tables S3 and S4). We conclude that *path* mutation induces a starvation response and alters protein homeostasis specifically in neurons with extreme growth requirements (C4da and C3da neurons).

Our microarray analysis indicated that translational repressors including *pum* were upregulated in *path* mutant C4da neurons whereas core translational machinery was down-regulated, thus we tested whether reducing *pum* function or increasing translational activity abrogated dendrite growth defects of *path* mutants. As previously reported (Ye et al., 2004), we found that *pum* overexpression strongly attenuated terminal dendrite growth in an otherwise wild type background, but *pum* overexpression failed to enhance the growth defect of *path* mutants (Figure 2A), consistent with *pum*

up-regulation contributing to growth defects of *path* mutants. Whereas RNAi knockdown of *pum* in C4da neurons of otherwise wild type larvae caused a modest growth deficit in C4da neurons, *pum*(RNAi) significantly increased dendrite growth in *path* mutant larvae (Figure 2A), demonstrating that *pum* up-regulation is a functionally relevant output of *path*; up-regulation of other translational repressors (*aret, bru-3*, etc; Figure 2C) may similarly contribute to *path* mutant dendrite growth defects.

As with *pum* overexpression, RNAi knockdown of core translational machinery (Rpl22) caused dendrite growth defects comparable to *path* mutants (Figure 2B), but the effects of Rpl22(RNAi) and *path* mutation were not additive, consistent with *path* affecting dendrite growth by modulating translation. If the dendrite growth defects in *path* mutants were due to reduced translational output, we reasoned, then treatments that increase translation should mitigate the dendrite growth defect of *path* mutants. This is what we observed. Overexpression of either eIF4E, which promotes cap-dependent translation (Richter & Sonenberg, 2005) and is downregulated in *path* mutant C4da neurons (Supplemental Figure S3), or a constitutively active form of the Ribosomal protein S6 kinase (CA-S6k), which promotes cell growth by increasing translational activity, increased C4da dendrite growth in *path* mutants (Figure 2B). We note that the efficacy of these treatments in rescuing growth defects of *path* mutant neurons was limited, and this was likely due in part to the growth-inhibitory effect of up-regulated translational repressors (Figure 1C, 2A). Altogether, these results suggest that Path regulates dendrite growth – at least in part – via effects on translation.

The best characterized substrates for SLC36 transporters are amino acids (Thwaites & Anderson, 2011) and SLC36 transporters can modulate TORC1 activity in

cultured cells (Heublein et al., 2010), therefore we hypothesized that Path supports dendrite growth by modulating TORC1 activity in response to amino acids. If Path was functioning as a nutrient sensor for TORC1, we reasoned that TORC1 inactivation should mimic loss of *path* and activation of TORC1 should bypass requirements for *path*. This is not what we observed. First, loss of neuronal TORC1 function (Tor mutation, Tor dominant negative, Raptor mutation, RagA dominant negative) led to a less severe growth defect in C4da neurons than loss of *path* function (Supplemental Figure S4), suggesting that *path* likely engages growth machinery other than just TORC1. Second, overexpression of *Rheb*, which can bypass the nutrient requirement for cell growth (Garami et al., 2003; Saucedo et al., 2003), *Tor*, *raptor*, or a constitutive active version of *Akt*, which can activate TORC2 in response to amino acid starvation under certain conditions (Tato, Bartrons, Ventura, & Rosa, 2011), had no positive effect on dendrite growth of *path* mutants (Supplemental Figure S4). However, co-expression of UAS-*path* and UAS-*Rheb* had a synergistic effect on dendrite growth (Figure 2C), suggesting that *path* can stimulate dendrite growth together with TORC1. We conclude that Path likely functions through TORC1 as well as additional pathways to support the extreme growth requirements of neurons with large dendrite arbors.

Discussion

Neurons exhibit striking diversity in size and shape, but whether large neurons have specialized machinery to support their growth remains largely unknown. Our identification and characterization of Path demonstrates that, at least in *Drosophila*, neurons with large dendrite arbors have additional requirements to meet extreme

growth demands. In neurons with large dendrite arbors, the response to *path* mutation is complex – despite manifesting signs of starvation and defects in protein homeostasis, primary dendrites continue to grow. Thus, dendrite patterning appears to be hierarchical and context dependent: in *path* mutants, neurons lack the ability to generate material for overall arbor expansion, hence material is preferentially allocated to facilitate primary dendrite elongation.

Independent of *path*, dendrites of PNS neurons grow to a maximum of ~3.5 mm, and growth beyond this limit requires *path*. How this limit is determined is currently unknown. One possibility is that the limit may be the result of some cellular commodity being exhausted in the absence of *path* function. If this is the case, *path*-independent and –dependent growth programs could utilize much of the same cellular machinery. Consistent with this scenario, neurons that do not require *path* for normal dendrite growth do require *path* for exuberant growth and hence have the machinery necessary for *path*-dependent growth. By extension, *path* may be broadly engaged in response to extreme growth demands and/or stress in neurons and non-neuronal cells, although *path* is dispensable for growth of most larval cell types under laboratory conditions.

Unexpectedly, the timing and pattern of C4da dendrite growth are remarkably labile. In the absence of *path* activity, dendrites grow to a maximum of ~3.5 mm and persist at that size even as arbors are remodeled to maximize primary dendrite elongation. Resupplying *path* to these neurons, even after several days of growth arrest, completely reversed the growth defects, despite the fact that structural plasticity in C4da dendrites, as in many other systems, is progressively limited (Grueber, Ye, Moore, Jan, & Jan, 2003; Parrish, Xu, Kim, Jan, & Jan, 2009; Ramoa, Campbell, &

Shatz, 1988; Sugimura et al., 2003). Our findings suggest that restriction of structural plasticity in C4da neurons depends on the extent of dendrite growth during early developmental stages; it remains to be seen whether a similar relationship is manifest in other systems. Interestingly, resupplying *path* expression following several days of growth arrest led to more rapid dendrite growth than at any period in wild type development, suggesting that growth-inhibitory cues or other signaling pathways that coordinate dendrite growth and animal growth normally temper dendrite growth at earlier developmental stages.

How might Path regulate dendrite growth? The most straightforward model is that Path is required for transmembrane transport of essential amino acids, which in turn modulate activity of mTORC1 and other amino acid responsive signaling pathways. Path localizes to the cell surface and endolysomal compartments, thus it could be involved in transporting amino acids into the cell or out of the lysosome. Several lines of evidence suggest that either scenario is unlikely. First, although one vertebrate Path counterpart, SLC36A1, promotes amino acid transport out of lysosomes and, as a result, antagonizes mTORC1 activity (Zoncu et al., 2011), Path is most closely related to SLC36A4 (Schiöth, Roshanbin, Hägglund, & Fredriksson, 2013), which has no effect on lysosomal amino acid content. Second, Path is most active at neutral pH (Goberdhan, Meredith, Boyd, & Wilson, 2005), thus it seems unlikely that it is involved in amino acid transport out of lysosomes. Third, although Path displays high affinity for a variety of amino acids, it exhibits minimal processivity in transport assays (Goberdhan et al., 2005), so it seems unlikely that it would substantially contribute to amino acid flux.

While it's possible that Path requires an unidentified co-factor for maximal transport activity, an alternative explanation is that Path may function as a transceptor, a transporter-like protein with a receptor function, to regulate signaling in response to metabolites independent of its transport capacity (Thevelein & Voordeckers, 2009). Examples of transceptors include the System A amino acid transporter SNAT2, which regulates transcription in response to amino acid binding (Hyde, Cwiklinski, MacAulay, Taylor, & Hundal, 2007) and GLUT2, a sugar transporter that has transport-independent functions as a receptor for extracellular glucose (Stolarczyk et al., 2010). Thus, Path could function at the cell surface to report on environmental conditions, gating downstream signaling in response to extracellular amino acid availability. In this model, low levels of extracellular amino acids or absence of Path would signal the cell to marshal its resources and arrest dendrite growth whereas high levels of amino acids would activate signaling that regulates protein homeostasis, supporting extreme dendrite growth. With this in mind, it will be intriguing to further characterize the N-terminal intracellular domain, as the N-terminal domain is a likely site for protein-protein interactions and is required for Path function.

Many degenerative disorders preferentially affect neurons with large axons/dendrites including Purkinje neurons, Betz cells, motoneurons, and sensory neurons. Thus, it's plausible that defects in growth machinery that contribute to extreme neuron growth contribute to pathology in these diseases. Path orthologs are present in vertebrates (Schiöth et al., 2013), but their *in vivo* function remains unknown. Interestingly, two mammalian SLC36 transporters, SLC36A1 and SLC36A4, are highly expressed in the nervous system (Bermingham & Pennington, 2004; Roshanbin et al.,

2014; Sagné et al., 2001). Thus, it will be of great interest to determine whether these SLC36 transporters are required for extreme dendrite growth similar to Path.

Materials and methods

Fly Husbandry

A list of alleles used in this study is available in the supplemental materials. EMS mutagenesis was conducted as previously described (Lee et al. 2015). Transgenic lines were generated using P-element mediated integration.

Live Imaging

Embryos were collected on yeasted grape juice agar and aged at 25°C in a moist chamber. At the appropriate time, a single embryo/larva was mounted in 90% glycerol under coverslips sealed with grease and imaged on Leica SP5 microscope with a 40x 1.25NA lens. For quantitation of dendrite phenotypes, image stacks of dendrites in segments A3-A4 were captured from 8-10 larvae. For time-lapse analysis, larvae were imaged at the indicated time, recovered to yeasted agar plates with vented lids, aged at 25°C, and imaged again.

Measurements

2D projections of Z-stacks were used for computer-assisted dendrite tracing with Neurolucida (MBF Bioscience), and features were measured using the traces. To monitor expression of GFP exon traps, we traced the outline of cells of interest in 2D projections of Z stacks using ImageJ and measured the mean pixel intensity within the

cell. For these experiments, we imaged control and *path* mutant larvae using identical settings, including the same number and thickness of optical sections.

Statistical Analysis

Differences between group means were analyzed via ANOVA with a post hoc Dunnett's test; pairwise comparisons of group means were done with unpaired t-tests with Welch's correction.

Microarray

Class IV neurons were isolated by double sorting via FACS. Microarray analysis of samples as previously described (Parrish et al., 2014).

Accessions

Microarray data is available at the NCBI Gene Expression Omnibus (accession: GSE64477).

Bibliography

Bermingham, J. R., & Pennington, J. (2004). Organization and expression of the SLC36 cluster of amino acid transporter genes. *Mammalian Genome*, *15*(2), 114–125. https://doi.org/10.1007/s00335-003-2319-3

Garami, A., Zwartkruis, F. J. T., Nobukuni, T., Joaquin, M., Roccio, M., Stocker, H., … Thomas, G. (2003). Insulin activation of Rheb, a mediator of mTOR/S6K/4E-BP signaling, is inhibited by TSC1 and 2. *Molecular Cell*, *11*(6), 1457–1466. https://doi.org/10.1016/S1097-2765(03)00220-X

Goberdhan, D. C. I., Meredith, D., Boyd, C. A. R., & Wilson, C. (2005). PAT-related

amino acid transporters regulate growth via a novel mechanism that does not require bulk transport of amino acids. *Development*, *132*(10), 2365–2375. https://doi.org/10.1242/dev.01821

Grueber, W. B., Ye, B., Moore, A. W., Jan, L. Y., & Jan, Y. N. (2003). Dendrites of distinct classes of Drosophila sensory neurons show different capacities for homotypic repulsion. *Current Biology*, *13*(8), 618–626. https://doi.org/10.1016/S0960-9822(03)00207-0

Heublein, S., Kazi, S., Ögmundsdóttir, M. H., Attwood, E. V., Kala, S., Boyd, C. A. R., … Goberdhan, D. C. I. (2010). Proton-assisted amino-acid transporters are conserved regulators of proliferation and amino-acid-dependent mTORC1 activation. *Oncogene*, *29*(28), 4068–4079. https://doi.org/10.1038/onc.2010.177

Hyde, R., Cwiklinski, E. L., MacAulay, K., Taylor, P. M., & Hundal, H. S. (2007). Distinct sensor pathways in the hierarchical control of SNAT2, a putative amino acid transceptor, by amino acid availability. *Journal of Biological Chemistry*, *282*(27), 19788–19798. https://doi.org/10.1074/jbc.M611520200

Lin, W. Y., Williams, C., Yan, C., Koledachkina, T., Luedke, K., Dalton, J., … Parrish, J. Z. (2015). The SLC36 transporter pathetic is required for extreme dendrite growth in Drosophila sensory neurons. *Genes and Development*, *29*(11), 1120–1135. https://doi.org/10.1101/gad.259119.115

Mayer, C., & Grummt, I. (2006, October 16). Ribosome biogenesis and cell growth: mTOR coordinates transcription by all three classes of nuclear RNA polymerases. *Oncogene*. https://doi.org/10.1038/sj.onc.1209883

Morin, X., Daneman, R., Zavortink, M., & Chia, W. (2001). A protein trap strategy to detect GFP-tagged proteins expressed from their endogenous loci in Drosophila. *Proceedings of the National Academy of Sciences of the United States of America*, *98*(26), 15050–15055. https://doi.org/10.1073/pnas.261408198

Parrish, J. Z., Kim, C. C., Tang, L., Bergquist, S., Wang, T., Derisi, J. L., … Davis, G. W. (2014). Krüppel mediates the selective rebalancing of ion channel expression. *Neuron*, *82*(3), 537–544. https://doi.org/10.1016/j.neuron.2014.03.015

Parrish, J. Z., Xu, P., Kim, C. C., Jan, L. Y., & Jan, Y. N. (2009). The microRNA bantam Functions in Epithelial Cells to Regulate Scaling Growth of Dendrite Arbors in Drosophila Sensory Neurons. *Neuron*, *63*(6), 788–802. https://doi.org/10.1016/J.NEURON.2009.08.006

Rambold, A. S., Kostelecky, B., Elia, N., & Lippincott-Schwartz, J. (2011). Tubular network formation protects mitochondria from autophagosomal degradation during

nutrient starvation. *Proceedings of the National Academy of Sciences of the United States of America*, *108*(25), 10190–10195. https://doi.org/10.1073/pnas.1107402108

Ramoa, A. S., Campbell, G., & Shatz, C. J. (1988). Dendritic growth and remodeling of cat retinal ganglion cells during fetal and postnatal development. *Journal of Neuroscience*, *8*(11), 4239–4261. https://doi.org/10.1523/jneurosci.08-11-04239.1988

Richter, J. D., & Sonenberg, N. (2005). Regulation of cap-dependent translation by eIF4E inhibitory proteins. *Nature*, *433*(7025), 477–480. https://doi.org/10.1038/nature03205

Roshanbin, S., Hellsten, S. V., Tafreshiha, A., Zhu, Y., Raine, A., & Fredriksson, R. (2014). PAT4 is abundantly expressed in excitatory and inhibitory neurons as well as epithelial cells. *Brain Research*, *1557*, 12–25. https://doi.org/10.1016/j.brainres.2014.02.014

Sagné, C., Agulhon, C., Ravassard, P., Darmon, M., Hamon, M., El Mestikawy, S., … Giros, B. (2001). Identification and characterization of a lysosomal transporter for small neutral amino acids. *Proceedings of the National Academy of Sciences of the United States of America*, *98*(13), 7206–7211. https://doi.org/10.1073/pnas.121183498

Saucedo, L. J., Gao, X., Chiarelli, D. A., Li, L., Pan, D., & Edgar, B. A. (2003). Rheb promotes cell growth as a component of the insulin/TOR signalling network. *Nature Cell Biology*, *5*(6), 566–571. https://doi.org/10.1038/ncb996

Schiöth, H. B., Roshanbin, S., Hägglund, M. G. A., & Fredriksson, R. (2013, April). Evolutionary origin of amino acid transporter families SLC32, SLC36 and SLC38 and physiological, pathological and therapeutic aspects. *Molecular Aspects of Medicine*. https://doi.org/10.1016/j.mam.2012.07.012

Schleich, S., Strassburger, K., Janiesch, P. C., Koledachkina, T., Miller, K. K., Haneke, K., … Teleman, A. A. (2014). DENR-MCT-1 promotes translation re-initiation downstream of uORFs to control tissue growth. *Nature*, *512*(7513), 208–212. https://doi.org/10.1038/nature13401

Stolarczyk, E., Guissard, C., Michau, A., Even, P. C., Grosfeld, A., Serradas, P., … Gall, M. Le. (2010). Detection of extracellular glucose by GLUT2 contributes to hypothalamic control of food intake. *American Journal of Physiology - Endocrinology and Metabolism*, *298*(5). https://doi.org/10.1152/ajpendo.00737.2009

Sugimura, K., Yamamoto, M., Niwa, R., Satoh, D., Goto, S., Taniguchi, M., … Uemura, T. (2003). Distinct developmental modes and lesion-induced reactions of dendrites of two classes of Drosophila sensory neurons. *Journal of Neuroscience*, *23*(9), 3752–3760. https://doi.org/10.1523/jneurosci.23-09-03752.2003

Tato, I., Bartrons, R., Ventura, F., & Rosa, J. L. (2011). Amino acids activate mammalian target of rapamycin complex 2 (mTORC2) via PI3K/Akt signaling. *Journal of Biological Chemistry*, *286*(8), 6128–6142. https://doi.org/10.1074/jbc.M110.166991

Teleman, A. A., Chen, Y. W., & Cohen, S. M. (2005). 4E-BP functions as a metabolic brake used under stress conditions but not during normal growth. *Genes and Development*, *19*(16), 1844–1848. https://doi.org/10.1101/gad.341505

Tettweiler, G., Miron, M., Jenkins, M., Sonenberg, N., & Lasko, P. F. (2005). Starvation and oxidative stress resistance in Drosophila are mediated through the eIF4E-binding protein, d4E-BP. *Genes and Development*, *19*(16), 1840–1843. https://doi.org/10.1101/gad.1311805

Thevelein, J. M., & Voordeckers, K. (2009, November). Functioning and evolutionary significance of nutrient transceptors. *Molecular Biology and Evolution*. https://doi.org/10.1093/molbev/msp168

Thwaites, D. T., & Anderson, C. M. H. (2011, December). The SLC36 family of proton-coupled amino acid transporters and their potential role in drug transport. *British Journal of Pharmacology*. https://doi.org/10.1111/j.1476-5381.2011.01438.x

Ye, B., Petritsch, C., Clark, I. E., Gavis, E. R., Jan, L. Y., & Jan, Y. N. (2004). nanos and pumilio Are Essential for Dendrite Morphogenesis in Drosophila Peripheral Neurons. *Current Biology*, *14*(4), 314–321. https://doi.org/10.1016/j.cub.2004.01.052

Zoncu, R., Bar-Peled, L., Efeyan, A., Wang, S., Sancak, Y., & Sabatini, D. M. (2011). mTORC1 senses lysosomal amino acids through an inside-out mechanism that requires the vacuolar H+-ATPase. *Science*, *334*(6056), 678–683. https://doi.org/10.1126/science.1207056

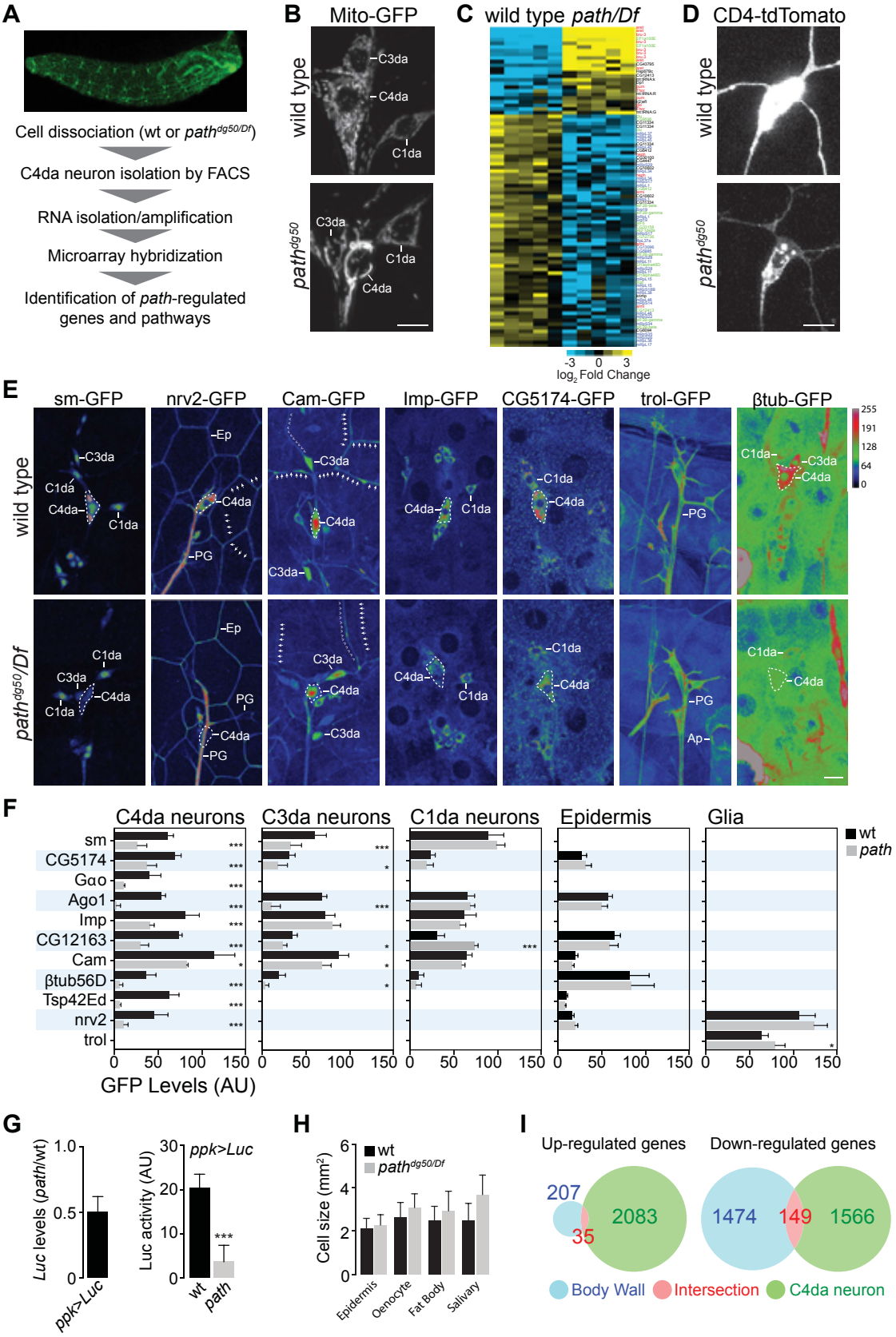
A
Cell dissociation (wt or path^dg50/Df)
C4da neuron isolation by FACS
RNA isolation/amplification
Microarray hybridization
Identification of path-regulated genes and pathways
B
Mito-GFP
wild type
path^dg50
C3da
C4da
C1da
C
wild type path/Df
-3 0 3
log2 Fold Change
D
CD4-tdTomato
wild type
path^dg50
E
sm-GFP
nrv2-GFP
Cam-GFP
Imp-GFP
CG5174-GFP
trol-GFP
βtub-GFP
wild type
path^dg50/Df
Ep
PG
Ap
255
191
128
64
0
F
C4da neurons
C3da neurons
C1da neurons
Epidermis
Glia
wt
path
sm
CG5174
Gαo
Ago1
Imp
CG12163
Cam
βtub56D
Tsp42Ed
nrv2
trol
GFP Levels (AU)
G
Luc levels (path/wt)
ppk>Luc
Luc activity (AU)
wt
path
H
Cell size (mm2)
wt
path^dg50/Df
Epidermis
Oenocyte
Fat Body
Salivary
I
Up-regulated genes
Down-regulated genes
207
2083
35
1474
149
1566
Body Wall
Intersection
C4da neuron

Figure 1. Path affects nutrient signaling and protein homeostasis in C4da neurons.

(A) Workflow for microarray expression profiling of *path* mutant C4da neurons. (B) *path* affects mitochondria morphology in C4da neurons. PNS neurons from wild type control (top) and *path* mutant larvae expressing mitochondrial-targeted GFP (*UAS-mito-GFP*) are shown. Levels of apparent mitochondrial fusion (high, C4da neurons; low, C3da neurons; none, C1da neurons) correlate with severity of dendrite growth defects in *path* mutants. (C) Heat map depicting *path*-regulated transcripts involved in translation. Significantly deregulated transcripts were identified using SAM analysis with a false discovery rate of 0.01 (Tusher et al. 2001). Transcripts are color-coded according to gene function as follows: red, translation inhibitor; green, translation initiation/elongation; blue, core translational machinery; black, unknown. (D-F) *path* affects protein homeostasis in C4da neurons. (D) Levels of the *ppk-CD4-tdTomato* reporter are reduced in *path* mutants, although *ppk* transcription is not affected (Supplemental Table S1). C4da neurons in age-matched wt (top) and *path* mutant (bottom) larvae expressing *ppk-CD4-tdTomato* were imaged under identical conditions. (E) Representative images depicting expression levels of 7 GFP exon trap lines in wt or *path* mutant larvae at 120 h AEL. Images are pseudocolored according to a lookup table (key, top right), C4da cell bodies are outlined with a hatched white line, and cells of interest labeled by each exon trap are indicated (C1da, C3da, and C4da neurons; Ep, epithelial cells; PG, peripheral glia; Ap, apodeme). Arrows mark C4da dendrites and double chevrons mark C3da dendrites. Exon traps were imaged under identical conditions in wt and *path* mutant larvae. (F) Mean expression intensity of exon traps in the indicated cell types. $n \geq 8$ cells for each bar. *$P<0.05$, ***$P<0.001$; ns, not significant compared to wt controls; one-way ANOVA with a post-hoc Dunnett's test. Error bars, standard deviation. Scale bars, 50 mm. (G) Cell size measurements for the indicated cell types in wt or *path* mutant larvae. Cells were

labeled with a membrane reporter (*UAS-mCD8-GFP*) and cell size (2D area) was measured by tracing plasma membranes and measuring area of the resulting polygons. Mean and standard deviation for 100 cells of each genotype are shown. (H) Venn diagram depicting transcriptional changes manifest in the entire body wall (blue) and C4da neurons (green) of *path* mutant larvae; the region of intersection is shown in red.

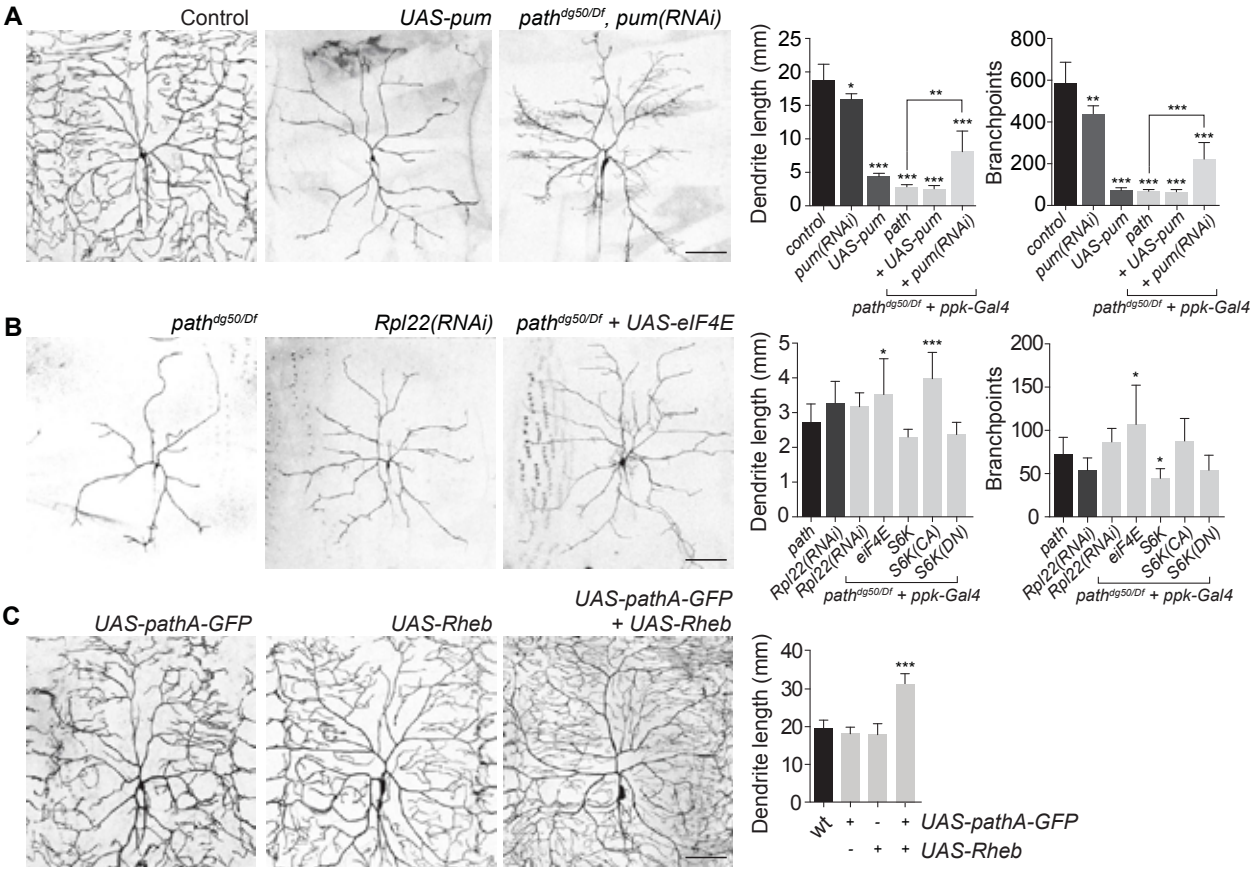

Figure 2. Path regulates dendrite growth via effects on translation.

(A) Increased translational repression contributes to growth defects of *path* mutants. Representative images of C4da dendrites are shown for a wt control, neuronal expression of *UAS-pum* or *UAS-pum(RNAi),* and *path* mutant larvae expressing *UAS-pum(RNAi)* in neurons. Quantification of dendrite growth phenotypes is shown for the indicated genotypes. (B) Reduced translational capacity likely contributes to dendrite growth defects in *path* mutants. RNAi of core translational machinery such as *Rpl22* causes growth defects similar to *path*, whereas overexpression of *eIF4e* partially mitigates *path* mutant growth defects. Quantification of dendrite growth phenotypes is shown for the indicated genotypes. (C) *path* can cooperate with TORC1 to promote dendrite growth. *Left*, representative C4da neurons expressing *UAS-pathA-GFP*, *UAS-Rheb*, or both are shown. Right, quantification of effects of *UAS-pathA-GFP* and/or

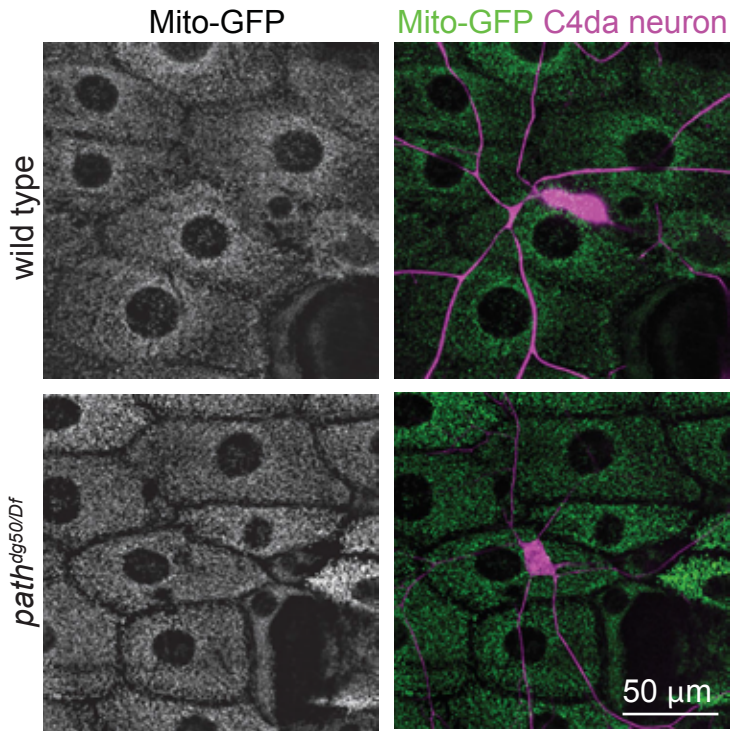

Figure S1. Supplement to Figure 1.

Images of wild type or *path* mutant larvae expressing mitochondrial-targeted GFP in epithelial cells (*A58-Gal4, UAS-mitoGFP*) and Tomato in C4da neurons (*ppk-CD4tdTomato*). Whereas *path* mutant C4da neurons exhibit striking alterations in mitochondrial morphology (Fig. 1), wild type and *path* mutant larvae exhibit comparable epithelial mitochondria morphology.

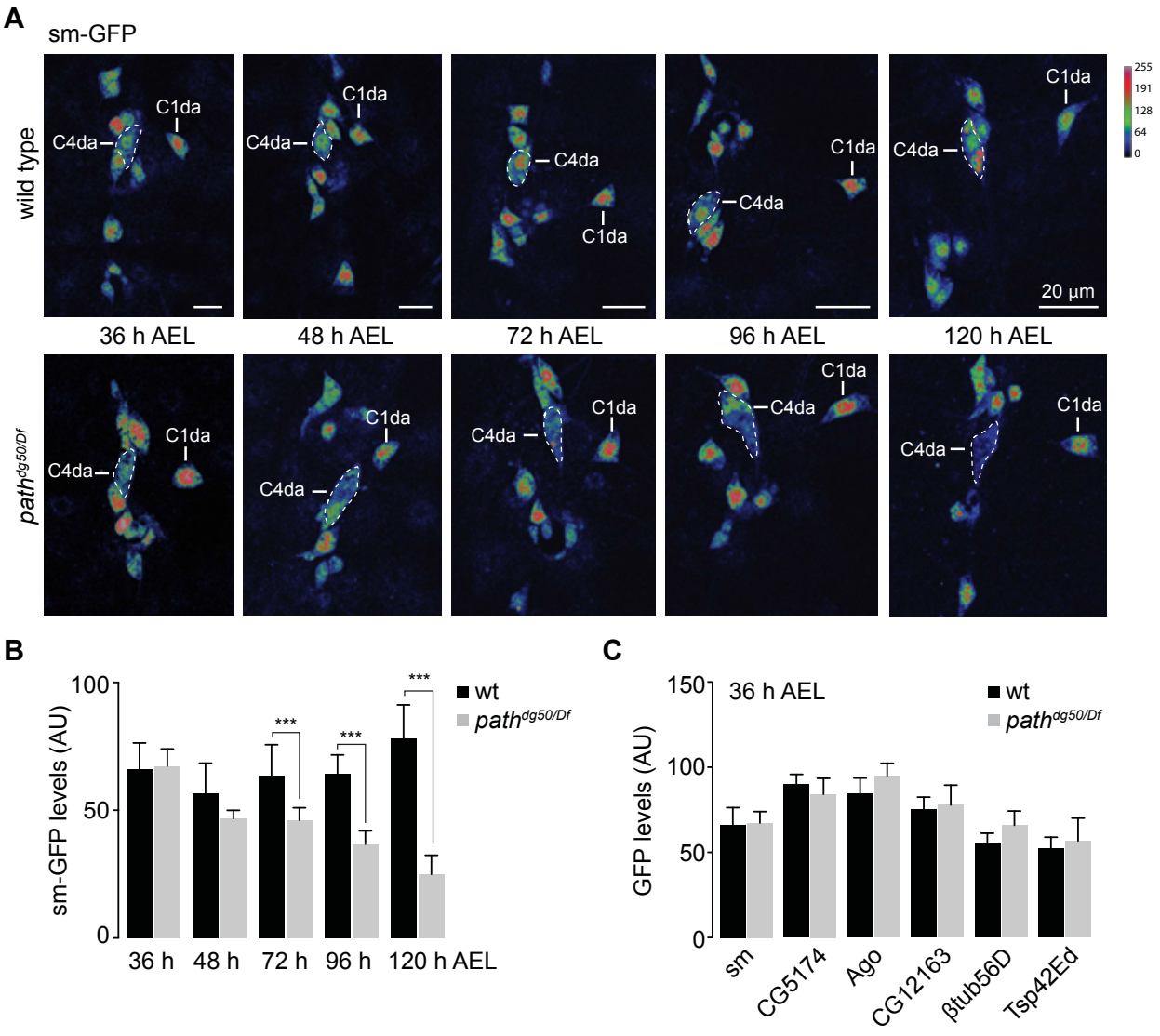

Figure S2. Supplement to Figure 1.

(A) Time-course of sm-GFP expression in wild type control and *path* mutant larvae. C4da and C1da neurons are marked in each image and C4da neuron cell bodies are outlined with a white hatched line. All images were captured using live confocal microscopy and levels were assessed by measuring mean pixel intensity in cells of interest. Images are pseudocolored according to a lookup table (key, top right). (B) Plot depicting sm-GFP levels in C4da neurons over a developmental time-course in wt control and *path* mutant larvae. $n>10$ cells for each bar. ***$P<.001$ relative to time-matched wt control, one-way ANOVA with a post-hoc Tukey's test.

(C) Plot depicting GFP levels for the indicated exon traps at 36 h AEL in wt control and *path* mutant larvae. $n>10$ cells for each bar. GFP levels for each of the exon traps did not significantly differ between wt control and *path* mutant larvae at 36 h AEL, unpaired t-test with Welch's correction.

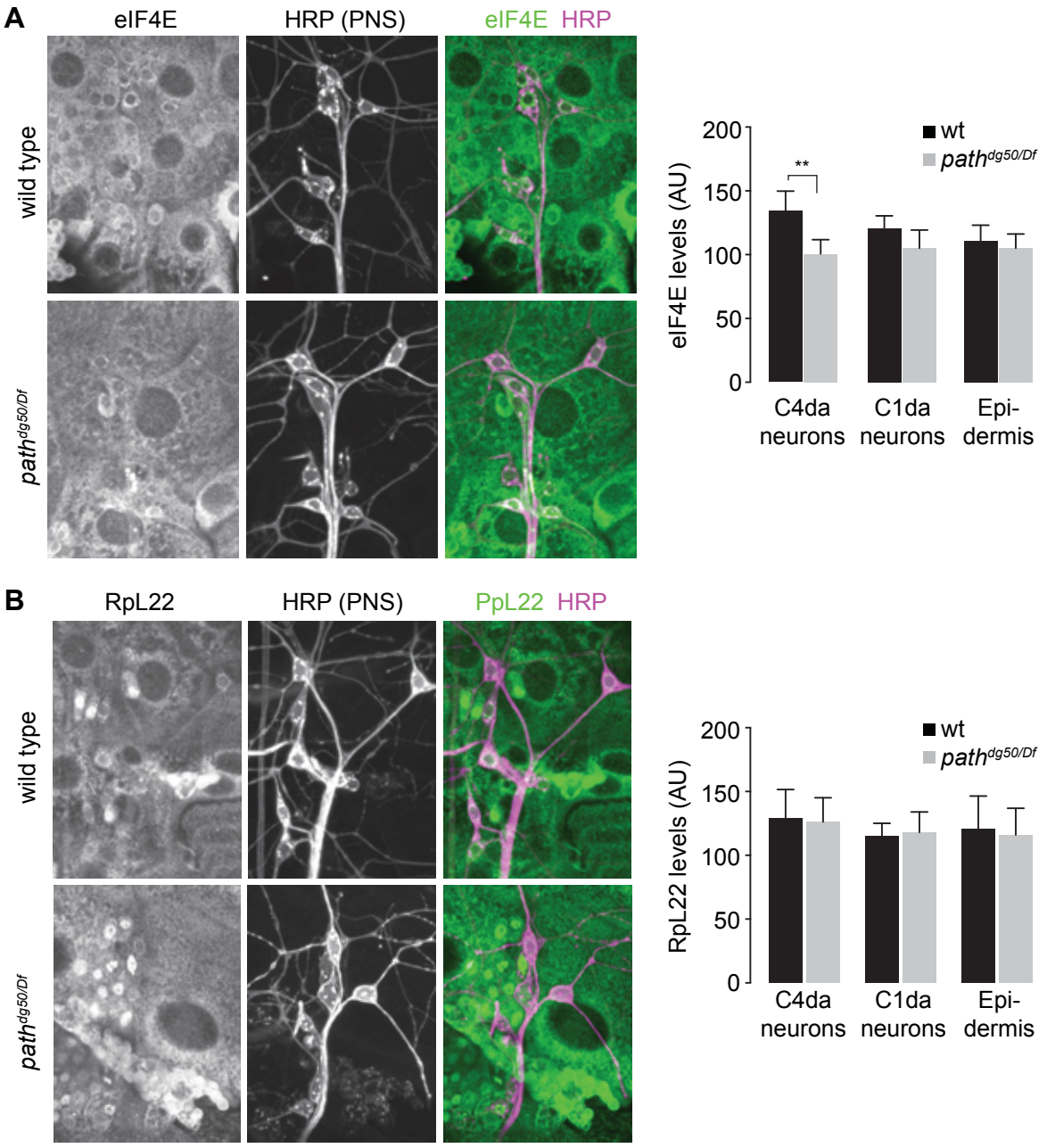

Figure S3. Supplement to Figure 2.

(A) eIF4E and (B) Rpl22 levels in wild type control and *path*$^{dg50/Df}$ mutant larvae. Third instar larvae (96 h AEL) were stained with antibodies to eIF4E (A) or RpL22 (B) and HRP (to label PNS neurons). eIF4E (A) and Rpl22 (B) signal intensities were measured in 2D projections of confocal stacks. Control and *path* mutant fillets were processed identically (stained in the same

tube, imaged using identical settings). Mean values and standard deviation for intensity measurements of 10 cells for each cell type/genotype combination shown. ***$P<.001$, one-way ANOVA with a post-hoc Tukey's test.

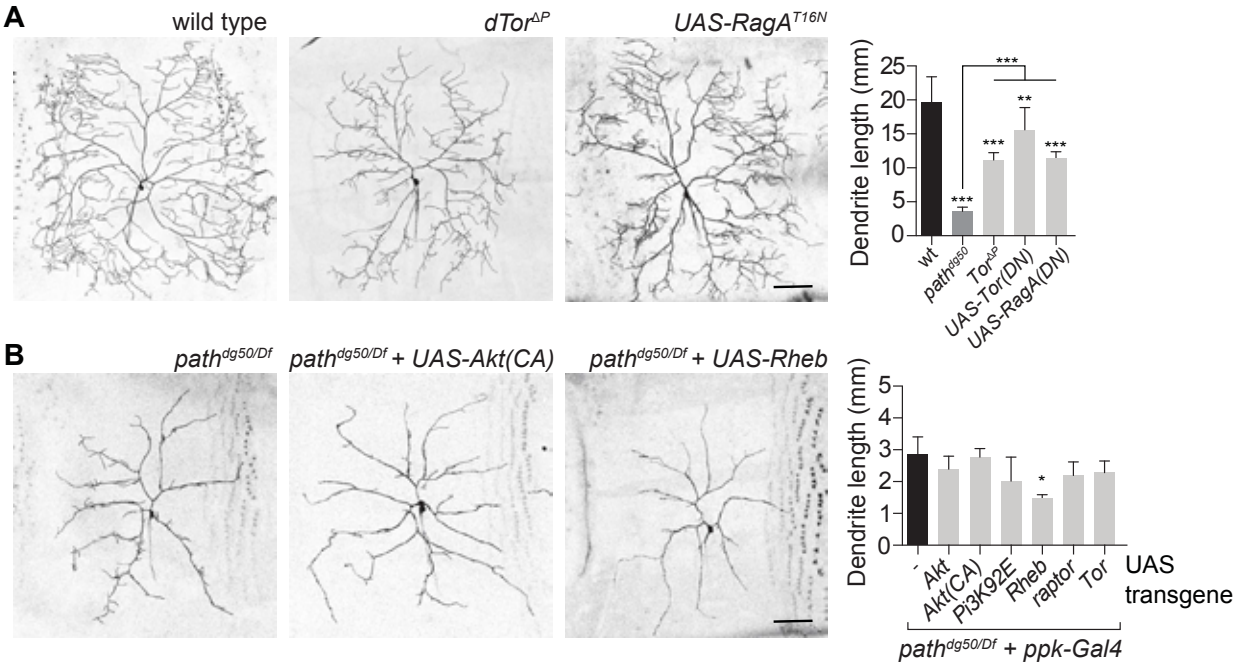

Figure S4. Relationship between Path and TORC1 in dendrite growth.

(A) Effect of TORC1 inactivation on C4da dendrite growth. Representative images of wild type control, *dTor* mutant, or RagA dominant-negative expressing C4da MARCM clones are shown. Quantification depicts mean total dendrite length for the indicated genotypes ($n > 6$ neurons for each). (B) Assaying rescue activity of TORC1 activation on C4da growth defects in *path* mutants. The indicated transgenes were expressed in C4da neurons of *path* mutants. Quantification depicts mean total dendrite length for the indicated genotypes ($n > 8$ neurons for each). *$P<0.05$; **$P<0.01$; ***$P<0.001$; ns, not significant; one-way ANOVA with a post-hoc Dunnett's test. Scale bars, 50μm.